The PHILOSOPHICAL MAGAZINE

FIRST PUBLISHED IN 1798

OL. 42 SEVENTH SERIES No. 334 November, 1951

A Journal of Theoretical Experimental and Applied Physics

PRICE 12s. 0d.
Annual Subscription £6 0s. 0d. payable in advance

D AND PUBLISHED BY TAYLOR & FRANCIS LTD., RED LION COURT, FLEET ST., LONDON, E.C.4

A New Publication added to

THE PHILOSOPHICAL MAGAZINE

(A Journal of Theoretical, Experimental and Applied Physics)

QUARTERLY SUPPLEMENT

ADVANCES IN PHYSICS

VOLUME 1 **JANUARY 1952** **NUMBER 1**

CONTENTS

PRICE per annum **£2 15s. 0d.** post free

CXX. *The Interaction in the Theory of Beta Decay.*

By D. L. Pursey*,
Department of Natural Philosophy, Glasgow University†.

[Received July 5, 1951.]

Abstract.

The cross terms occurring in the expression for the theoretical nth forbidden beta spectrum are given for an arbitrary mixture of interactions. Relations are derived between the six first forbidden vector nuclear matrix elements. Comparison with experiment is made for first forbidden transitions with allowed shape beta spectra. The results are discussed in relation to other recent work in the theory of beta decay. It is concluded that the interaction is most probably tensor with little or no admixture of other interactions.

§ 1. Introduction.

The Fermi type theory of beta decay postulates an interaction between heavy and light particle fields proportional to a linear combination of the five Lorentz invariant expressions:

$$\left.\begin{aligned} \mathrm{S} &= (\Psi^*\beta\Phi)(\psi^*\beta\phi), \\ \mathrm{V} &= (\Psi^*\Phi)(\psi^*\phi)-(\Psi^*\boldsymbol{\alpha}\Phi)(\psi^*\boldsymbol{\alpha}\phi), \\ \mathrm{T} &= (\Psi^*\beta\boldsymbol{\sigma}\Phi)(\psi^*\beta\boldsymbol{\sigma}\phi)+(\Psi^*\beta\boldsymbol{\alpha}\Phi)(\psi^*\beta\boldsymbol{\alpha}\phi), \\ \mathrm{A} &= (\Psi^*\boldsymbol{\sigma}\Phi)(\psi^*\boldsymbol{\sigma}\phi)-(\Psi^*\gamma_5\Phi)(\psi^*\gamma_5\phi), \\ \mathrm{P} &= (\Psi^*\beta\gamma_5\Phi)(\phi^*\beta\gamma_5\phi), \end{aligned}\right\} \qquad (1)$$

where Ψ, Φ, ψ and ϕ are the proton, neutron, electron and neutrino fields respectively, and $\boldsymbol{\alpha}$, $\boldsymbol{\sigma}$, β and γ_5 are the usual Dirac matrices. There is no good theoretical reason for preferring any particular linear combination of these interactions over any other, and consequently the interaction is free to be fitted with experiment. The large amount of accurate experimental information which has become available during the past few years not only has firmly established this type of theory for allowed and certain forbidden transitions, but helps considerably towards the experimental determination of the interaction.

Because of the arguments favouring the Gamow–Teller selection rules (summarized by Konopinski 1943), the interaction has long been thought to contain at least a proportion of either T or A. The most

* Now at Physics Department, King's College, London.
† Communicated by Professor J. C. Gunn.

convincing evidence for this now available, however, is the experimental discovery of several beta spectra having the characteristic shape, predicted only by T and A, for first forbidden transitions with an angular momentum change of two units and parity change. An excellent survey of recent experimental work, including the results just mentioned, has been given by Wu (1950).

With a mixture of interactions, cross terms may occur which affect the predicted spectrum shape. For allowed transitions, such cross terms occur only for mixtures of S with V or of A with T, and have the effect of multiplying the allowed spectrum by a factor $(1+a/W)$, where W is the beta particle energy in units of mc^2. These cross terms have been calculated by Fierz (1937), who neglected the Coulomb field of the nucleus, and more recently by De Groot and Tolhoek (1950). The latter authors give an upper limit of $\frac{1}{10}$ for a, and conclude that mixing of S with V or of A with T, if it occurs at all, must be very slight.

It is clear from the foregoing that to be consistent with recent experimental evidence on forbidden transitions the interaction must contain either T or A, while evidence on allowed spectra forbids interactions containing both T and A, or both S and V. There remain unconsidered, however, a fair number of transitions which, although forbidden according to the semi-empirical *ft* classification, nevertheless have allowed shape beta spectra. Some of these transitions may be interpreted as first forbidden with an angular momentum change of 0 or 1 unit and change of parity, and they will be used here to gain further information about the beta decay interaction.

§ 2. Correction Factors.

Greuling (1942, equations (11)–(16)) has given the correction factors by which the allowed spectrum must be multiplied to give the theoretical nth forbidden spectrum for each of the five interactions. For this paper, however, the correction factors associated with cross terms are also required. To obtain these, the nth forbidden correction factor for an arbitrary mixture of interactions was calculated by the method given by Konopinski and Uhlenbeck (1941). The correction factors for the cross terms are rather cumbersome, and to avoid interrupting the argument, they are given in an appendix. These cross terms when used in conjunction with Greuling's formulæ give the complete nth forbidden correction factor for an arbitrary mixture of interactions, except for a few terms unimportant except for J=0 to J=0 transitions, and a few terms which can be regarded as small corrections to the $(n-1)$th forbidden correction factor. As an example, the nth forbidden correction factor for the mixture $A+yS$ is $C_{n\mathrm{A}}+y^2C_{n\mathrm{S}}+yC_n(\mathrm{S, A})$, where $C_{n\mathrm{A}}$ and $C_{n\mathrm{S}}$ are the correction factors given by Greuling for the pure axial vector and pure scalar interactions respectively, and $C_n(\mathrm{S, A})$ is the cross term given in the appendix.

§ 3. The Pseudoscalar Interaction.

By convention, P in this paper is regarded as having no allowed transitions. It is then seen from Greuling's formulæ, and from the cross terms given in the appendix, that the selection rules for an nth forbidden transition according to the interaction P are the same as those for an $(n-2)$th forbidden transition according to the interactions T and A. Hence the correction factors will be almost independent of the amount of P in the interaction unless this is great enough to overcome the extra forbiddenness. If this were the case, one would expect the first forbidden pseudoscalar matrix element of P to give apparently superallowed transitions; all the observed superallowed transitions, however, with the exception of B^{12}, are already well explained by Wigner's theory of supermultiplets (see, for example, Konopinski 1943), and for none of them does a parity change seem reasonable. Furthermore, if the third forbidden P matrix element were strong enough to affect first forbidden transitions with unit angular momentum change, it would certainly dominate the much weaker transitions with angular momentum change of two units, and this does not appear to be the case. For these reasons, it is concluded that, while the amount of P in the interaction may be quite large, it is not sufficient to affect the correction factors for first forbidden transitions with unit angular momentum change. The correction factor for first forbidden transitions with no angular momentum change, however, may well be modified or even dominated by the presence of P in the interaction.

§ 4. Nuclear Matrix Elements.

In the first forbidden correction factor, terms occur involving twelve different matrix elements. Of these, two are the second order tensors responsible for the transitions with angular momentum change of two units; their contribution to other first forbidden transitions is small, and will be ignored. Four of the matrix elements are pseudoscalars, and therefore cannot contribute to transitions involving an angular momentum change. In this section, relations will be found between the remaining six matrix elements, all of which are vectors.

The notation $(f|\mathbf{a}|i)$ will be used for these matrix elements, instead of the notation $\int\mathbf{a}$ used by Konopinski and Uhlenbeck (1941); by this is to be understood (for electron emission)

$$(f|\mathbf{a}|i)=\int d\mathbf{r}^1 \ldots \int d\mathbf{r}^A \Psi_f^* \sum_{j=1}^{A} \tfrac{1}{2}(\tau_1^j - i\tau_2^j)\mathbf{a}^j \Psi_i, \quad \ldots \quad (2)$$

where Ψ_i and Ψ_f are respectively the nuclear wave functions for the initial and final states, $\mathbf{a}$ is a charge independent vector operator, τ_1 and τ_2 are the usual isotopic operators, the superscripts refer to the particles in the nucleus, and the integration includes summation over spin and isotopic spin states. As is usual in the theory of beta decay,

that representation of the Dirac matrices is chosen in which β and $\boldsymbol{\alpha}$ become in non-relativistic approximation -1 and $-\mathbf{v}/\mathbf{c}$ respectively, while the units of action, velocity and mass are chosen to be $\hbar$, $\boldsymbol{c}$ and $\boldsymbol{m_e}$.

In the absence of any relativistic model of the nucleus the results of this section must be regarded as essentially non-relativistic, although relativistic notation will be used for the sake of convenience. It is therefore permissible to replace β by its non-relativistic approximation -1, provided it commutes with the other operators appearing in the matrix element, and hence

$$(f|\beta\mathbf{r}|i)=-(f|\mathbf{r}|i)\,;\quad (f|\beta\boldsymbol{\sigma}\wedge\mathbf{r}|i)=-(f|\boldsymbol{\sigma}\wedge\mathbf{r}|i). \quad . \quad . \quad . \quad (3)$$

Further relations can be derived using the Hartree type of single particle model. A sufficient condition that the single particle states should be eigenstates of the operator $k=\beta[(\boldsymbol{\sigma}\,.\,\mathbf{m})+1]$, where $\mathbf{m}$ is the orbital angular momentum, is that the magnitudes l and j of the orbital and total angular momentum of the states should both be good quantum numbers. This condition is certainly satisfied by the shell model of Mayer (1949, 1950) and of Haxel, Jensen and Süss (1949, 1950). The operator k is the well-known angular momentum operator of relativistic theory (see, for example, Dirac 1947), and has eigenvalues

$$k=\begin{cases} -(j+\frac{1}{2}), & j=l+\frac{1}{2} \\ +(j+\frac{1}{2}), & j=l-\frac{1}{2} \end{cases} \quad . \quad . \quad . \quad . \quad . \quad . \quad . \quad (4)$$

The following relations, in which [] and {} denote commutators and anti-commutators respectively, are easily verified:

$$\left.\begin{aligned} [k,\mathbf{r}] &=-i\beta\boldsymbol{\sigma}\wedge\mathbf{r}, \\ [k^2,\boldsymbol{\alpha}]&=\{k,\beta\boldsymbol{\alpha}\}, \end{aligned}\right\} \quad . \quad . \quad . \quad . \quad . \quad . \quad (5)$$

$$\left.\begin{aligned} [k,[k^2,\mathbf{r}]]&=\{k,\mathbf{r}\}, \\ [k,[k^2,\boldsymbol{\alpha}]]&=\{k,\boldsymbol{\alpha}\}, \end{aligned}\right\} \quad . \quad . \quad . \quad . \quad . \quad . \quad (6)$$

(6) expresses the selection rules $k_i+k_f=0$ or $k_i-k_f=\pm 1$ for the matrix elements of $\mathbf{r}$ and $\boldsymbol{\alpha}$; from (4) they are seen to be equivalent to $\Delta j=0,\pm 1$, yes. (5) gives the relations

$$(f|\beta\boldsymbol{\sigma}\wedge\mathbf{r}|i)=-i\epsilon(f|\mathbf{r}|i)\,;\quad (f|\beta\boldsymbol{\alpha}|i)=-\epsilon(f|\boldsymbol{\alpha}|i), \quad . \quad . \quad . \quad (7)$$

where $\epsilon=k_i-k_f$. If $k_i+k_f=0$, the second of these relations is true only in non-relativistic approximation. These relations, together with (3), enable the six vector matrix elements to be reduced to two, namely $(f|\mathbf{r}|i)$ and $(f|\boldsymbol{\alpha}|i)$.

The selection rules for $(f|\boldsymbol{\sigma}|i)$ are found similarly to be $k_i=k_f$ or $k_i+k_f=\pm 1$, while, provided $k_i\neq k_f$,

$$(f|\beta\boldsymbol{\sigma}|i)=(k_i+k_f)(f|\boldsymbol{\sigma}|i). \quad . \quad . \quad . \quad . \quad . \quad . \quad (8)$$

Since β commutes with $\boldsymbol{\sigma}$, it may be replaced in non-relativistic approximation by -1. Consequently the matrix element for transitions with $k_i+k_f=+1$ must vanish in non-relativistic approximation, and must therefore be of order $(v/\mathbf{c})^2$; indeed, it is clear that (8) is self-consistent for such transitions only if the large components of the wave functions do not contribute to the matrix element. Obviously, transitions of this type will appear to be forbidden, and they must not be confused with genuinely first forbidden transitions, all of which involve a parity change. From (4) it is seen that the selection rule $k_i+k_f=+1$ is equivalent to $\Delta j=\pm 1$, $\Delta l=\pm 2$; for the allowed transitions with $k_i+k_f=-1$ or $k_i=k_f$, $\Delta l=0$.

To obtain a relation between $(f|\boldsymbol{\alpha}|i)$ and $(f|\mathbf{r}|i)$, the nuclear Hamiltonian is assumed to be

$$\begin{aligned}\mathrm{H}=&-\sum_{j=1}^{\mathrm{A}}\{(\boldsymbol{\alpha}^j\,.\,\mathbf{p}^j)+\tfrac{1}{2}\beta^j[(1+\tau_3^j)\mathrm{M}_n+(1-\tau_3^j)\mathrm{M}_p]\}\\&+\frac{1}{2}\sum_{j=1}^{\mathrm{A}}\sum_{k\neq j}^{\mathrm{A}}\{\mathrm{V}_0(jk)+(\boldsymbol{\tau}^j\,.\,\boldsymbol{\tau}^k)\mathrm{V}_e(jk)-(\boldsymbol{\sigma}^j+\boldsymbol{\sigma}^k)\,.\,(\mathbf{r}^j-\mathbf{r}^k)\wedge(\mathbf{p}^j-\mathbf{p}^k)\mathrm{V}_s(jk)\\&+\tfrac{1}{4}(1-\tau_3^j)(1-\tau_3^k)\mathrm{V}_c(jk)\},\qquad\qquad(9)\end{aligned}$$

where V_0, V_e, V_s and V_c are the ordinary, charge exchange, spin–orbit and Coulomb potentials between two nucleons respectively, and M_n and M_p are the neutron and proton masses. As before, the use of relativistic notation is for convenience only, and this Hamiltonian is to be considered valid only in non-relativistic approximation. For the sake of simplicity, and in the absence of any evidence to the contrary, the spin–orbit coupling is supposed not to be of charge exchange type.

By calculating the commutator of $\frac{1}{2}\sum_{j=1}^{\mathrm{A}}(\tau_1^j-i\tau_2^j)\mathbf{r}^j$ with H, it is found that

$$\begin{aligned}(f|\boldsymbol{\alpha}|i)=&\,i(\mathrm{W}_i-\mathrm{W}_f)(f|\mathbf{r}|i)+i(\mathrm{M}_n-\mathrm{M}_p)(f|\beta\mathbf{r}|i)\\&-\tfrac{1}{2}i\sum_{j=1}^{\mathrm{A}}\sum_{k\neq j}^{\mathrm{A}}\int d\mathbf{r}^1\ldots\int d\mathbf{r}^{\mathrm{A}}\Psi_f^*(\tau_1^j-i\tau_2^j)\{\tau_3^k(\mathbf{r}^j-\mathbf{r}^k)\mathrm{V}_e(jk)\\&-i(\boldsymbol{\sigma}^j+\boldsymbol{\sigma}^k)\wedge(\mathbf{r}^j-\mathbf{r}^k)\mathrm{V}_s(jk)-\tfrac{1}{2}(1-\tau_3^k)\mathbf{r}^j\mathrm{V}_c(jk)\}\Psi_i.\qquad(10)\end{aligned}$$

The last term in this expression will be averaged over the particles k, assuming they form a spin saturated spherical core of uniform density and radius ρ equal to the nuclear radius.

For both the exchange force and spin–orbit coupling contributions to (10), the problem is essentially that of averaging $(\mathbf{r}^j-\mathbf{r}^k)\mathrm{V}(r)$, where $r=|\mathbf{r}^j-\mathbf{r}^k|$, over the core formed by the particles k. If $\mathrm{V}(r)$ is expanded in a series of Legendre polynomials of the cosine of the angle between $\mathbf{r}^j$ and $\mathbf{r}^k$ and the spherical symmetry of the core is used, this averaging becomes elementary, and gives

$$\overline{(\mathbf{r}^j-\mathbf{r}^k)\mathrm{V}(r)}=\mathbf{r}^j(3/16r_j^3\rho^3)\int_{|\varrho-r_j|}^{\varrho+r_j}\mathrm{V}(r)[(\rho+r_j)^2-r^2][r^2-(\rho-r_j)^2]r\,dr,\qquad(11)$$

where $r_j = |\mathbf{r}^j|$. Since the transforming particle is presumably in an outer shell, r_j may be taken approximately equal to ρ. For a Yukawa well of depth v and range $1/k$, the averaging then gives

$$\mathbf{r}^j v(3A/2k^3\rho^3)\{(k\rho)^{-1}-3(k\rho)^{-3}+\exp(-2k\rho)[2+5(k\rho)^{-1}+6(k\rho)^{-2}+3(k\rho)^{-3}]\} \quad . \quad . \quad . \quad (12\,a)$$

(Hughes and Le Couteur (1950) have also found this result, using a rather different method), while for a square well of depth v and range $1/k$, one obtains

$$\mathbf{r}^j v(3A/16k^4\rho^4)[1-\tfrac{1}{6}(k\rho)^{-2}]. \quad . \quad . \quad . \quad . \quad . \quad (12\,b)$$

In the charge exchange contribution to $(f|\boldsymbol{\alpha}|i)$, the factor τ_3^k gives on averaging a factor (N−Z)/A where N is the neutron number of the initial nucleus and Z the proton number of the product nucleus. V_e is assumed to be of the form $[a_1+a_2(\boldsymbol{\sigma}^j \cdot \boldsymbol{\sigma}^k)]V(jk)$ but because of the spin saturation of the core, only the term with coefficient a_1 will contribute; for the same reason, any tensor forces of the usual type will vanish. Using the value given by Rosenfeld (1948) for a_1, based on the ratio of the triplet and singlet s potentials and the requirement of saturation for heavy nuclei, the effective V_e is found to be $-(1/10)V(^3s)$ where $V(^3s)$ is the triplet s potential. Taking the nuclear radius ρ to be $r_0A^{1/3}$, and using both a Yukawa well of depth $100\boldsymbol{mc}^2$ and range r_0 and a square well of depth $40\boldsymbol{mc}^2$ and range $2r_0$ for $V(^3s)$, the exchange force contribution to $(f|\boldsymbol{\alpha}|i)$ is found to be

$$\text{Yukawa well}: \quad -15iA^{-4/3}(N-Z)(1-3A^{-2/3})(f|\mathbf{r}|i). \quad . \quad . \quad (13\,a)$$

$$\text{Square well}: \quad -12iA^{-4/3}(N-Z)(1-\tfrac{2}{3}A^{-2/3})(f|\mathbf{r}|i). \quad . \quad . \quad (13\,b)$$

The two wells give results in fair agreement. This exchange contribution is so small in any case that the use of more accurate well parameters is unnecessary.

Hughes and Le Couteur (1950) estimate that for V_s a Yukawa well of range r_0 and depth 1 MeV. is consistent both with the probable spin–orbit separation in He^5 and with the separation necessary according to the spin–orbit coupling shell model to account for the apparent level order in heavy nuclei. (The factor 2 difference in the depth given above from that given by Hughes and Le Couteur is due to a different definition of $\boldsymbol{\sigma}$; in this paper the spin angular momentum is $\frac{1}{2}\boldsymbol{\sigma}$). On averaging, the contribution to $(f|\boldsymbol{\alpha}|i)$ from the spin–orbit coupling is found to be

$$-3A^{-1/3}(1-3A^{-2/3})(f|\boldsymbol{\sigma}\wedge\mathbf{r}|i)=-3i\epsilon A^{-1/3}(1-3A^{-2/3})(f|\mathbf{r}|i) \quad . \quad (14)$$

on using (7).

The Coulomb contribution to $(f|\boldsymbol{\alpha}|i)$ can be estimated by a similar averaging procedure, and is found to be $i(Z\alpha/\rho)(f|\mathbf{r}|i)$. Collecting these results, one obtains

$$(f|\boldsymbol{\alpha}|i)=ix(f|\mathbf{r}|i)$$

where

$$\left.\begin{aligned} x=(W_i-W_f)-(M_n-M_p)+(Z\alpha/\rho)-15A^{-4/3}(N-Z)(1-3A^{-2/3}) \\ -3\epsilon A^{-1/3}(1-3A^{-2/3}). \end{aligned}\right\} \quad . \quad . \quad (15)$$

For most first forbidden transitions, the first two terms in x approximately cancel, while the exchange force and spin–orbit terms are small compared to the Coulomb term. For positron emitters, the second, third and fourth terms in x change sign.

§ 5. Comparison with Experiment.

It was pointed out in the introduction that the interaction cannot contain both S and V, or both T and A, while the pseudoscalar interaction P was discussed in § 3 and found not to contribute to first forbidden transitions involving an angular momentum change. To avoid consideration of P, attention will be confined to transitions in which an angular momentum change of one unit for the transforming single particle state seems plausible according to the shell model of Mayer and of Haxel, Jensen and Süss. Consequently the only mixtures that need be discussed are those of S with T, A with V, V with T and S with A. The first two of these have almost identical correction factors, and therefore only the first of them will be considered. The correction factors for these mixtures and the type of transition under consideration may be found from the general formulæ of Greuling together with the cross terms given in the appendix, and may be further simplified using the relations between matrix elements found in the last section. In low Z approximation, they are

$$\begin{aligned}\mathrm{T}+y\mathrm{S}:\ C=&\{\xi^2+(2\xi/3\mathrm{W})+(\eta/18)+\tfrac{1}{9}\}\\&-2y\epsilon\{\xi[(Z\alpha/2\rho)+(\zeta/3)]+(\mathrm{W}_0\zeta/9)+(Z\alpha/\rho)/(6\mathrm{W})\}\\&+y^2\{(Z\alpha/2\rho)^2+(Z\alpha/\rho)(\zeta/3)+(\eta/3)-\tfrac{2}{9}(\mathrm{W}_0-\mathrm{W})(\mathrm{W}-1/\mathrm{W})\}.\end{aligned} \quad . \ . \ . \quad (16\,a)$$

$$\begin{aligned}\mathrm{T}+y\mathrm{V}:\ C=&(1+y^2)\{\xi^2+(2\xi/3\mathrm{W})+(\eta/18)+\tfrac{1}{9}\}+y^2(\eta/6)\\&-2y\epsilon\{(\xi^2/\mathrm{W})+(2\xi/3)+(\mathrm{W}_0/9)(2-\mathrm{W}_0/\mathrm{W})\}.\end{aligned} \quad . \ . \ . \quad (16\,b)$$

$$\begin{aligned}\mathrm{A}+y\mathrm{S}:\ C=&(1+y^2)\{(Z\alpha/2\rho)^2+(Z\alpha/\rho)(\zeta/3)+(\eta/6)-\tfrac{2}{9}(\mathrm{W}_0-\mathrm{W})(\mathrm{W}-1/\mathrm{W})\}\\&+y^2(\eta/6)-2y\epsilon\{[(Z\alpha/2\rho)^2-(Z\alpha/\rho)(\mathrm{W}_0/3)](1/\mathrm{W})+(Z\alpha/3\rho)\},\end{aligned} \quad . \ . \ . \quad (16\,c)$$

where

$$\left.\begin{aligned}\xi&=x-(Z\alpha/2\rho)-\mathrm{W}_0/3,\\ \eta&=\mathrm{W}_0^2-1-2\mathrm{W}_0\mathrm{W}+2\mathrm{W}^2,\\ \zeta&=2\mathrm{W}-\mathrm{W}_0-1/\mathrm{W},\end{aligned}\right\} \quad . \ . \ . \ . \ . \quad (17)$$

x is the ratio of $(f|\boldsymbol{\alpha}|i)$ to $i(f|\mathbf{r}|i)$, and $\epsilon=k_i-k_f=\pm 1$, depending on the transition. A factor $|(f|\mathbf{r}|i)|^2$ has been omitted from all of these correction factors. For positron emitters, the sign of Z must be changed throughout, and the sign of the cross term (proportional to y) changed in the mixture $\mathrm{T}+y\mathrm{S}$.

Only transitions with an ft value greater than 10^6 and whose experimental Kurie plot is straight to within 5 per cent for a reasonable energy range will be regarded as sufficiently forbidden and sufficiently accurately investigated to warrant detailed comparison with theory.

A search in the literature for such transitions has yielded the following: Na^{22} (Good, Peaslee and Deutsch 1946), Na^{24} (Siegbahn 1946), Sc^{46} (Peacock and Wilkinson 1948), V^{48} (Peacock and Deutsch 1946), Pr^{146} (Feldman, Lidofsky, Macklin and Wu 1949), Pm^{147} (Agnew 1950, Langer, Motz and Price 1950, Lidofsky, Macklin and Wu 1949), Hf^{181} (Chu and Wiedenbeck 1949), Re^{186} (Beach, Peacock and Wilkinson 1949, Langer and Price 1949), W^{187} (Peacock and Wilkinson 1948), Au^{198} (Langer and Price 1949, Saxon 1948, Steffen, Huber and Humbel 1949). P^{32}, Ga^{66} and Cs^{134} are more probably of the $\Delta j=1$, $\Delta l=2$ type of transition mentioned in the last section, while Mo^{99} and I^{131} are not easily interpreted on the shell model picture; these five interactions are therefore not considered.

The sign of ϵ is obtained from the shell model interpretation of the transition. The level scheme given by Haxel, Jensen and Süss (1950) is used in conjunction with the measured spins of neighbouring odd nuclei to suggest the initial state, and, if the transition is between ground states, also the final state, of the transforming nucleon. If the transition is to an excited level of the product nucleus, a reasonable transition involving parity change must be postulated. In this case, for heavy nuclei with a large neutron excess the transforming neutron need not belong to the outermost occupied neutron shell, and several interpretations may be possible.

For Na^{22} and Na^{24}, the shell model interpretation is complicated by the anomalous filling of the $d_{5/2}$ shell; however, for Na^{22} the most probable transition seems to be $p_{3/2}\rightarrow s_{1/2}$, for which $\epsilon=-1$, while for Na^{24} the transition is probably $d_{5/2}\rightarrow f_{7/2}$ with $\epsilon=+1$. For both Sc^{46} and V^{48}, the only reasonable transition is $f_{7/2}\rightarrow d_{5/2}$, with $\epsilon=-1$. Pr^{143} and Pm^{147} undergo ground state to ground state transitions, and are almost certainly of the type $h_{9/2}\rightarrow g_{7/2}$ with $\epsilon=+1$. For Hf^{181}, Re^{186} and W^{187} the transition may be any of $i_{13/2}\rightarrow h_{11/2}$, $f_{5/2}\rightarrow g_{7/2}$, $p_{1/2}\rightarrow d_{3/2}$, $f_{7/2}\rightarrow d_{5/2}$, all with $\epsilon=-1$, or $h_{9/2}\rightarrow g_{7/2}$ with $\epsilon=+1$, or $f_{7/2}\rightarrow g_{7/2}$ in which case the transition is not of the required type; for these transitions ϵ was assumed to be -1. For Au^{198}, the transition is probably $f_{5/2}\rightarrow d_{3/2}$ with $\epsilon=+1$.

The correction factors (16 *a*) and (16 *b*) are not very sensitive to the value of x unless ξ is small. This is the case for Na^{22}, and fig. 1 shows theoretical Kurie plots for this transition according to the tensor interaction for different values of x. (15) gives for x the value $-2{\cdot}5$, and this gives an almost straight Kurie plot in fair agreement with experiment. The possibility of error, however, cannot be denied, and in particular if ϵ is $+1$ instead of -1 as assumed, (15) gives $x=-3{\cdot}9$ and a Kurie plot far from straight. It seems unlikely, therefore, that any reliance can be put on conclusions about mixtures involving T or V based on this transition. It is also found that for the positron emitters Na^{22} and V^{48} the Kurie plots for all mixtures of the type $A+y$S are reasonably straight in the experimentally measured region. Consequently, no

reliable information about any mixtures of interactions can be obtained from the available evidence on Na^{22}, and this transition will no longer be considered. For all the other transitions, the theoretical spectrum shapes are not very sensitive to the value of x, and the estimate of § 4 should give fairly reliable results.

For heavy nuclei with fairly low end points, the spectrum shapes predicted by all the pure interactions are indistinguishable from the allowed shape. For mixtures, however, if the cross term is negative there may be a large cancellation causing the theoretical spectrum to deviate strongly from the allowed shape. This is illustrated for

Fig. 1.

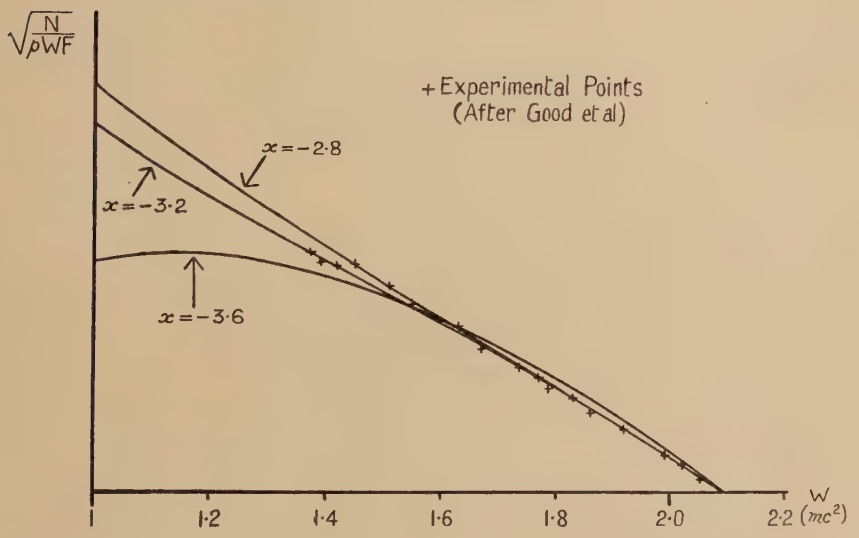

Theoretical Kurie plots for Na^{22} according to the tensor interaction, with different values for the ratio x of $-i(f|\boldsymbol{\alpha}|i)$ to $(f|\mathbf{r}|i)$. The estimate of §4 gives $x=-2{\cdot}5$.

Pr^{143} in fig. 2. For all mixtures, if $y\epsilon=-1$ the theoretical Kurie plot is similar to that shown for the mixture A+S, while if y increases or decreases, the Kurie plot approaches a straight line. The mixtures T+yS and V+yA are remarkable in that the theoretical Kurie plot changes from " concave down " through an S-shape to " concave up " before becoming straight ; this change is very rapid, and for Pr^{143} it is complete when $y=0{\cdot}8$. Frequently the experimental Kurie plot shows an excess of low energy electrons which may be due to experimental difficulties such as source thickness effects, or to a second low energy transition, or it may be genuine. As a precaution which should be more than adequate to prevent false conclusions being drawn, only that part of the Kurie plot which is experimentally straight is compared with

theory. Theoretical and experimental Kurie plots are regarded as consistent with each other if the discrepancy between them is not more than 5 per cent at the low energy end and 10 per cent at the high energy end of the straight portion. For Pr^{143}, only that part of the Kurie plot above $1{\cdot}4\ mc^2$ is used, and the Kurie plots for the mixtures $A-\frac{1}{3}S$ and $T+\frac{1}{2}S$ both show the maximum allowed discrepancy. Since the sign of the cross term depends on ϵ and therefore on the transition, it is clear that by considering different transitions both lower and upper limits can be obtained for the ratio y of the interaction constants in any mixture.

For lighter nuclei such as Na^{24}, the picture is very similar, except that the predicted spectrum shapes for pure A and S are no longer

Fig. 2.

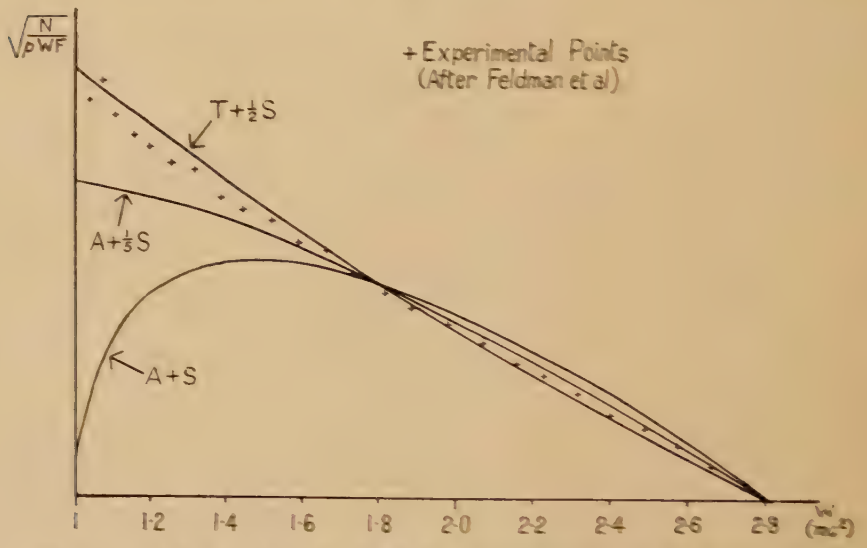

Theoretical Kurie plots for Pr^{143} for various mixtures of interactions.

allowed, and indeed for Na^{24} no mixture whatsoever of S with A gives an allowed shape spectrum. Fig. 3 gives theoretical Kurie plots for Na^{24} for the interactions A, A—S and T, of which only the last is consistent with experiment. It was pointed out in the introduction that the interaction must contain either T or A, but not both: the spectrum of Na^{24} seems to favour T, but A with a large admixture of V cannot be ruled out. Of the nine transitions under consideration, Na^{24} is the only one capable of distinguishing between T and A in this way, and it should be kept in mind that the Na^{24} result is valid only if the transition is genuinely first forbidden and not a highly unfavoured allowed transition, and if the first forbidden pseudoscalar matrix elements do not contribute. This will be the case whatever the angular momentum change of the nucleus as a whole, provided, as was assumed

above, the single particle transition is of the type $d_{5/2} \rightarrow f_{7/2}$; if, however, the transition is, for example, $d_{5/2} \rightarrow f_{5/2}$, the result will be valid only if the nucleus as a whole changes its angular momentum.

The limits to the amount of mixing found from each of the nine transitions considered are given in Table I. The first-named interaction in each mixture is assumed to predominate, so that y is numerically less than one; since, however, the mixtures S$-y$A and V$-y$T are almost identical with the mixtures A$-y$S and T$-y$V respectively, and since the limits are given for both T$-y$S and S$-y$T, this means no loss of generality. The mixtures V$-y$A and A$-y$V are almost identical to the mixtures T$+y$S and S$+y$T respectively.

Fig. 3.

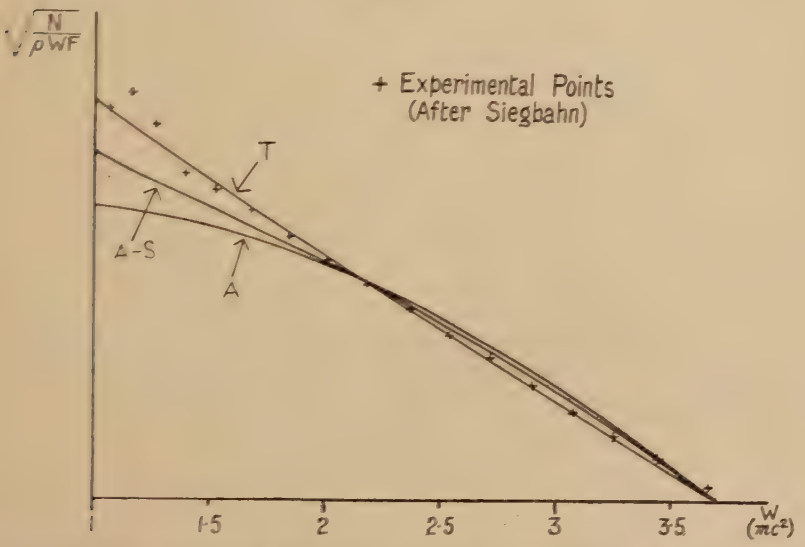

Theoretical Kurie plots for Na^{24} for various interactions. No mixture of the type A$+y$S is consistent with experiment.

From Table I. it is seen that very little admixture of S with A, and little admixture of V with T is permissible. Mixtures of T and S, or of V and A, are possible, but one or other of the two interactions must predominate. If the evidence of Na^{24} is accepted, then the only permissible interactions are T with perhaps a small admixture of either V or S, and a mixture of A and V with V predominating. The tensor interaction T is the only pure interaction consistent both with the interpretation given for Na^{24} and with all the other experimental data on beta spectrum shapes.

The validity of these results, of course, depends on the accuracy of the estimates used for the ratios of the nuclear matrix elements, and on the correctness of the shell model interpretations of the transitions. An error in the relations between the matrix elements will cause a proportionate error in some or all of the limits given in Table I.; such an

error, however, would have to be very large before it would alter the main features of the table. An error in the shell model interpretation may cause the adoption of the wrong sign for ϵ; in this case, the limits given will be true for $-y$ instead of for y.

TABLE I.

Upper and Lower Limits for the Mixture Parameter y.

Mixture	Na^{24}	Sc^{46}	V^{48}	Pr^{143}	Pm^{147}	Hf^{181}	Re^{186*}	W^{187}	Au^{198}
A+yS	X	−0·5		0·2	0·2	−0·33	− 0·1	−0·7	0·1
T+yV	0·2	−0·5	−0·5	0·33	0·33	−0·5	−0·33		0·33
T+yS	0·35 −0·7	−0·65	0·25	0·5	0·7	−0·7	−0·5	−0·65	0·5
S+yT	X	−0·75	0·7	0·5	0·9		−0·5	−0·75	0·6

The first-named interaction is assumed to predominate. The upper and lower rows of figures for each mixture are respectively upper and lower limits for y, while the columns indicate the transitions from which the limits are derived. X denotes that no values of y are consistent with experiment.

* See note added in proof.

§ 6. Conclusion.

In the introduction, it was pointed out that because of the arguments in favour of the Gamow–Teller selection rules, and because of the discovery of spectra having the characteristic first forbidden spin change of two shape, the interaction must contain either T or A. From the allowed spectrum shapes, it was seen that the interaction cannot contain both S and V, or both T and A. Taken in conjunction with these results, the work of this paper shows that the interaction must either be mainly T with possibly a small admixture of S or V, or mainly V with an admixture of A. If the evidence of Na^{24} is not accepted a predominantly axial vector interaction is also possible. The decays of RaE of Cs^{137} are almost certainly second forbidden, and their spectrum shapes appear to demand an interaction in which either T or V predominates (Konopinski and Uhlenbeck 1941, Langer and Moffat 1951), though not all possible mixtures have been considered. By considering the lifetimes of superallowed transitions, and assuming Wigner's theory of supermultiplets, Moszkowski (1951) has concluded that the interaction is either almost entirely T or almost entirely A. Marshak (1942) and Greuling (1942) have calculated theoretical half-lives for various forbidden

transitions using the tensor interaction, and found reasonable agreement with experiment. It appears therefore that the experimental evidence strongly favours the pure tensor interaction, although none of the above evidence precludes an admixture of P.

Tiomno Wheeler and Rau (1949) and Tiomno and Wheeler (1949) have shown that the beta decay and the capture by protons of μ-mesons can both be explained by quadrilinear interactions with the same interaction constant as in nuclear beta decay, and this has led to the idea of a universal quadrilinear interaction. For such an interaction, symmetry properties with respect to the interchange of fields having similar physical properties may have physical significance. The best known interaction having such properties is the Critchfield interaction S–A–P (Critchfield 1943), which, if the fields are quantized so that any two anti-commute, is symmetric with respect to the interchange of any pair of fields. Apart from the pure interactions, all of which are either symmetrical or antisymmetrical with respect to the interchange of the light particle or the heavy particle fields, the only two other interactions having special symmetry properties which are consistent with allowed beta spectra are S−T−P and 3S−T−3P, which are respectively symmetrical and antisymmetrical with respect to the interchange of the two neutral or the two charged fields. Of these three interactions, only the last is consistent with the results of Table I., and it is inconsistent with Moszkowski's results, and probably also with the RaE and Cs^{137} spectra. On changing the order of the charged and neutral fields in the interaction to that used by Michel (1950) in calculating the theoretical beta spectrum from μ-meson decay, 3S−T−3P becomes pure tensor, which predicts a spectrum in complete disagreement with experiment. Consequently a universal interaction, if one exists, can have no special symmetry properties, and the ordering of the fields in the interaction must therefore be uniquely determined by their physical properties such as charge, or sign of magnetic moment of a neutral particle. This need not preclude the hypothesis of a Majorana neutrino, provided there are some neutral particles which are not of Majorana type; this is, however, the case, since, both because of its magnetic moment and because of the stability of nuclei, the neutron cannot be a Majorana particle. By comparing either with Michel's results or with the figures given by Tiomno, Wheeler and Rau, it is seen that the tensor interaction with the ordering of the fields usual in the theory of nuclear beta decay is consistent with the beta spectrum from μ-meson decay, whether the neutrino is a Dirac or a Majorana neutral particle.

Acknowledgments

The author is indebted to Professor J. C. Gunn and Dr. B. F. X. Touschek for suggesting this problem and for many stimulating discussions, and to the Department of Scientific and Industrial Research for a maintenance grant during the tenure of which this work was performed.

APPENDIX.

The correction factors for the cross terms occurring in the expression for the theoretical nth forbidden beta spectrum for an arbitrary mixture of interactions are given below, using Greuling's (1942) notation except that $Q_n(\mathbf{a})$ is written for Greuling's $Q_n(\mathbf{a}, \mathbf{r})/(n\,!)$. The units of action, velocity and mass are chosen to be $\hbar$, $\mathbf{c}$ and $\mathbf{m}_e$ respectively. The method of using these correction factors was explained in § 2.

$$C_n(\mathrm{S,\,V}) = -[Q_n(\beta\mathbf{r})Q_n^*(\mathbf{r}) + \mathrm{c.c.}] \sum_{\nu=0}^{n} \{A_{n\nu}Q_\nu q^{2(n-\nu)-2} + D_{n\nu}P_\nu q^{2(n-\nu)}\}$$

$$+ i[Q_n(\beta\mathbf{r})Q_n^*(\boldsymbol{\alpha}) - \mathrm{c.c.}] \sum_{\nu=0}^{n} \{A_{n\nu}R_\nu q^{2(n-\nu)-2} + C_{n\nu}P_\nu q^{2(n-\nu)-1}\},$$

$$C_n(\mathrm{S,\,T}) = i[Q_n(\beta\mathbf{r})Q_n^*(\beta\boldsymbol{\alpha}) - \mathrm{c.c.}] \sum_{\nu=0}^{n} \{A_{n\nu}N_\nu q^{2(n-\nu)-2} + C_{n\nu}L_\nu q^{2(n-\nu)-1}\}$$

$$+ i[Q_n(\beta\mathbf{r})Q_n^*(\beta\boldsymbol{\sigma}\wedge\mathbf{r}) - \mathrm{c.c.}] \sum_{\nu=0}^{n} \{A_{n\nu}M_\nu q^{2(n-\nu)-2}$$

$$+ (D_{n\nu} - B_{n\nu})L_\nu q^{2(n-\nu)}\},$$

$$C_n(\mathrm{S,\,A}) = -i[Q_n(\beta\mathbf{r})Q_n^*(\boldsymbol{\sigma}\wedge\mathbf{r}) - \mathrm{c.c.}] \sum_{\nu=0}^{n} \{A_{n\nu}Q_\nu q^{2(n-\nu)-2} - 2C_{n\nu}R_\nu q^{2(n-\nu)-1}$$

$$+ (D_{n\nu} - B_{n\nu})P_\nu q^{2(n-\nu)}\},$$

$$C_n(\mathrm{V,\,T}) = [Q_n(\boldsymbol{\alpha})Q_n^*(\beta\boldsymbol{\alpha}) + \mathrm{c.c.}] \sum_{\nu=0}^{n} A_{n\nu}P_\nu q^{2(n-\nu)-2}$$

$$- i[Q_n(\mathbf{r})Q_n^*(\beta\boldsymbol{\alpha}) - \mathrm{c.c.}] \sum_{\nu=0}^{n} \{-A_{n\nu}R_\nu q^{2(n-\nu)-2} + C_{n\nu}P_\nu q^{2(n-\nu)-1}\}$$

$$- i[Q_n(\mathbf{r})Q_n^*(\beta\boldsymbol{\sigma}\wedge\mathbf{r}) - \mathrm{c.c.}] \sum_{\nu=0}^{n} \{A_{n\nu}Q_\nu q^{2(n-\nu)-2} + 2C_{n\nu}R_\nu q^{2(n-\nu)-1}$$

$$+ (D_{n\nu} - B_{n\nu})P_\nu q^{2(n-\nu)}\}$$

$$- [Q_n(\boldsymbol{\alpha})Q_n^*(\beta\boldsymbol{\sigma}\wedge\mathbf{r}) + \mathrm{c.c.}] \sum_{\nu=0}^{n} \{-A_{n\nu}R_\nu q^{2(n-\nu)-2} + C_{n\nu}P_\nu q^{2(n-\nu)-1}\},$$

$$C_n(\mathrm{V,\,A}) = [Q_n(\boldsymbol{\alpha})Q_n^*(\boldsymbol{\sigma}\wedge\mathbf{r}) + \mathrm{c.c.}] \sum_{\nu=0}^{n} \{A_{n\nu}N_\nu q^{2(n-\nu)-2} + C_{n\nu}L_\nu q^{2(n-\nu)-1}\}$$

$$+ i[Q_n(\mathbf{r})Q_n^*(\boldsymbol{\sigma}\wedge\mathbf{r}) - \mathrm{c.c.}] \sum_{\nu=0}^{n} \{A_{n\nu}M_\nu q^{2(n-\nu)-2}$$

$$+ (D_{n\nu} - B_{n\nu})L_\nu q^{2(n-\nu)}\},$$

$$C_n(\mathrm{V,\,P}) = -i[Q_{n-1}(\boldsymbol{\alpha}\wedge\mathbf{r})Q_{n-1}^*(\beta\gamma_5\mathbf{r}) - \mathrm{c.c.}] \sum_{\nu=0}^{n-1} \{A_{n-1,\,\nu}Q_\nu q^{2(n-\nu-1)-2}$$

$$- 2C_{n-1,\,\nu}R_\nu q^{2(n-\nu-1)-1} + (D_{n-1,\,\nu} - B_{n-1,\,\nu})P_\nu q^{2(n-\nu-1)}\},$$

$$C_n(\mathrm{T,\,A})=-[Q_{n+1}(\beta\boldsymbol{\sigma})Q^*_{n+1}(\boldsymbol{\sigma})+\mathrm{c.c.}]\sum_{\nu=0}^{n} B_{n\nu}P_\nu q^{2(n-\nu)}$$

$$-[Q_n(\beta\boldsymbol{\sigma}\wedge\mathbf{r})Q^*_n(\boldsymbol{\sigma}\wedge\mathbf{r})+\mathrm{c.c.}]\sum_{\nu=0}^{n}\{A_{n\nu}Q_\nu q^{2(n-\nu)-2}$$

$$+\left(D_{n\nu}-\frac{1}{n+1}B_{n\nu}\right)P_\nu q^{2(n-\nu)}\}$$

$$+[Q_n(\beta\boldsymbol{\alpha})Q^*_n(\boldsymbol{\sigma}\wedge\mathbf{r})+\mathrm{c.c.}]\sum_{\nu=0}^{n}\{A_{n\nu}R_\nu q^{2(n-\nu)-2}+C_{n\nu}P_\nu q^{2(n-\nu)-1}\},$$

$$C_n(\mathrm{T,\,P})=-i[Q_n(\beta\boldsymbol{\sigma})Q^*_n(\beta\gamma_5\mathbf{r})-\mathrm{c.c.}]\sum_{\nu=0}^{n}\{A_{n\nu}N_\nu q^{2(n-\nu)-2}+C_{n\nu}L_\nu q^{2(n-\nu)-1}\},$$

$$C_n(\mathrm{A,\,P})=i[Q_n(\boldsymbol{\sigma})Q^*_n(\beta\gamma_5\mathbf{r})-\mathrm{c.c.}]\sum_{\nu=0}^{n}\{A_{n\nu}R_\nu q^{2(n-\nu)-2}+C_{n\nu}P_\nu q^{2(n-\nu)-1}\}.$$

These last two correction factors represent a mixing of the $(n+1)$th forbidden P spectrum with the $(n-1)$th forbidden T and A spectra respectively.

The quantities P_ν, Q_ν and R_ν are defined analogously to L_ν, M_ν and N_ν by

$$P_\nu=(2p^2F_0)^{-1}[g^2_\nu-f^2_{-(\nu+2)}]\rho^{-2\nu},$$

$$Q_\nu=(2p^2F_0)^{-1}[g^2_{-(\nu+2)}-f^2_\nu]\rho^{-2(\nu+1)},$$

$$R_\nu=(2p^2F_0)^{-1}[f_\nu g_\nu+f_{-(\nu+2)}g_{-(\nu+2)}]\rho^{-2\nu-1}.$$

By expanding the radial functions g and f in powers of ρ and neglecting the first and higher powers, one obtains

$$P_\nu=(F_\nu/F_0)\left(\frac{2^\nu\nu!}{(2\nu+1)!}p^\nu\right)^2\left(\frac{s_\nu(\nu+1+s_\nu)}{2(\nu+1)^2}\right)\frac{1}{W},$$

$$Q_\nu=(F_\nu/F_0)\left(\frac{2^{\nu+1}\nu!}{(2\nu+2)!}p^\nu\right)^2\left\{-\frac{2s_\nu}{\nu+1+s_\nu}\left(\frac{Z\alpha}{2\rho}\right)^2\frac{1}{W}+\frac{(Z\alpha)^2}{\nu+1+s_\nu}\left(\frac{Z\alpha}{\rho}\right)\right.$$

$$+\frac{s_\nu(\nu+1)}{(2s_\nu+1)^2}\left[1+\frac{s_\nu(Z\alpha)^2}{(\nu+1)(\nu+1+s_\nu)}\right]\frac{p^2}{W^2}$$

$$\left.+\left[1-\frac{(4s+3)(Z\alpha)^2}{\nu+1+s_\nu}\right]\left(\frac{Z\alpha}{2s_\nu+1}\right)^2 W\right\},$$

$$R_\nu=(F_\nu/F_0)\left(\frac{2^{\nu+1}\nu!}{(2\nu+2)!}p^\nu\right)^2\left\{-\frac{s_\nu}{W}\left(\frac{Z\alpha}{2\rho}\right)+(Z\alpha)^2\right\}.$$

For low Z, s_ν may be put equal to $\nu+1$, $F_\nu=F_0$, and $(Z\alpha)^2=0$ to give the simpler expressions

$$P_\nu=\left(\frac{2^\nu\nu!}{(2\nu+1)!}p^\nu\right)^2\frac{1}{W};\quad Q_\nu=\left(\frac{2^{\nu+1}\nu!}{(2\nu+2)!}p^\nu\right)^2\left\{-\frac{1}{W}\left(\frac{Z\alpha}{2\rho}\right)^2+\left(\frac{\nu+1}{2\nu+3}\right)^2\frac{p^2}{W}\right\},$$

$$R_\nu=-\left(\frac{2^\nu\nu!}{(2\nu+1)!}p^\nu\right)^2\frac{1}{\nu+1}\left(\frac{Z\alpha}{2\rho}\right)\frac{1}{W}.$$

For positron emitters, the sign of Z and, as De Groot and Tolhoek (1950) have shown, the signs of C_n(S, V), C_n(S, T), C_n(V, A), C_n(T, A), C_n(V, P) and C_n(T, P) should be changed.

Note added in proof.—Since this paper was written, papers by Metzger and Hill (1951) and Steffen (1951) have been received confirming the result of Grant and Richmond (1949) that the spectrum of Re^{186} is complex. In calculating Table I., this spectrum was assumed to be simple: consequently the limits in Table I. derived from the Re^{186} transition are narrower than experiment now warrants.

References.

Agnew, H. M., 1950, *Phys. Rev.* [2], **77,** 655.

Beach, L. A., Peacock, C. L., and Wilkinson, R. G., 1949, *Phys. Rev.* [2], **76,** 1585.

Chu, K. Y., and Wiedenbeck, M. L., 1949, *Phys. Rev.* [2], **75,** 226.

Critchfield, C. L., 1943, *Phys. Rev.* [2], **63,** 417.

De Groot, S. R., and Tolhoek, H. A., 1950, *Physica*, **16,** 456.

Dirac, P. A. M., 1947, *Quantum Mechanics*, 3rd. Ed., p. 266 (Oxford: The University Press).

Feldman, L., Lidofsky, L., Macklin, P., and Wu, C. S., 1949, *Phys. Rev.* [2], **75,** 1888.

Fierz, M., 1937, *Zeits. f. Phys.*, **104,** 553.

Good, W. M., Peaslee, D., and Deutsch, M., 1946, *Phys. Rev.* [2], **69,** 313.

Grant, P. J., and Richmond, R., 1949, *Proc. Phys. Soc.*, A., **62,** 573.

Greuling, E., 1942, *Phys. Rev.* [2], **61,** 568.

Haxel, O., Jensen, J. H. D., and Suss, H. E., 1949, *Phys. Rev.* [2], **75,** 1766; 1950, *Zeits. f. Phys.*, **128,** 294.

Hughes, J., and Le Couteur, K. J., 1950, *Proc. Phys. Soc.* A, **63,** 1219.

Konopinski, E. J., 1943, *Rev. Mod. Phys.*, **15,** 209.

Konopinski, E. J., and Uhlenbeck, G. E., 1941, *Phys. Rev.* [2], **77,**798.

Langer, L. M., and Moffat, R. J. D., 1951, *Phys. Rev.* [2], **82,** 635.

Langer, L. M., Motz, J. W., and Price, H. C. Jr., 1950, *Phys. Rev.* [2], **77,** 798.

Langer, L. M., and Price, H. C. Jr., 1949, *Phys. Rev.* [2], **76,** 641.

Lidofsky, L., Macklin, P., and Wu, C. S., 1949, *Phys. Rev.* [2], **76,** 1888.

Marshak, R. E., 1942, *Phys. Rev.* [2], **61,** 431.

Mayer, M. G., 1949, *Phys. Rev.* [2], **75,** 1969; 1950, *Phys. Rev.* [2], **78,** 16, 22.

Metzger, F. R., and Hill, R. D., 1951, *Phys. Rev.* [2], **82,** 646.

Michel, L., 1950, *Proc. Phys. Soc.* A, **63,** 514, 1371.

Moszkowski, S. A., 1951, *Phys. Rev.* [2], **82,** 118.

Peacock, W. C., and Deutsch, M., 1946, *Phys. Rev.* [2], **69,** 306.

Peacock, C. L., and Wilkinson, R. G., 1948, *Phys. Rev.* [2], **74,** 297.

Rosenfeld, L., 1948, *Nuclear Forces*, Chap. XI. (Amsterdam: North-Holland Publishing Company).

Saxon, D., 1948, *Phys. Rev.* [2], **70,** 127.

Steffen, R. M., 1951, *Phys. Rev.* [2], **82,** 827.

Steffen, R. M., Huber, O., and Humbel, F., 1949, *Helvetica physica Acta*, **22,** 167.

Tiomno, J., and Wheeler, J. A., 1949, *Rev. Mod. Phys.*, **21,** 153.

Tiomno, J., Wheeler, J. A., and Rau, R. R., 1949, *Rev. Mod. Phys.*, **21,** 144.

Wu, C. S., 1950, *Rev. Mod. Phys.*, **22,** 386.

CXXI. *Ultrasonic Propagation in Liquid Helium near the Lambda-Point.*

By A. B. Pippard,
The Royal Society Mond Laboratory, Cambridge *.

[Received June 27, 1951.]

Abstract.

It is suggested that the sharp minimum in velocity and maximum in attenuation of ultrasonic waves in liquid helium in the region of the λ-point is a consequence of fluctuations which lead to the production of inclusions of He II in He I above the λ-point, and of He I in He II below the λ-point. Expressions are derived for the velocity and attenuation in an inhomogeneous fluid, and are applied, with some modifications, to liquid helium. It is found that the shape of the velocity curve may be accounted for satisfactorily, and that the observed attenuation just above the λ-point requires the inclusions of He II to consist of about 850 atoms. It is shown that fluctuation theory predicts the presence of inclusions of this size in the concentration required to explain the experimental results.

§ 1. Introduction.

Experiments on the propagation of ultrasonic waves in liquid helium have revealed peculiarities of behaviour at temperatures near the λ-point (2·18° K.); the velocity drops to a sharp minimum at the λ-point, and at the same time the attenuation rises rapidly to a peak. The effect which culminates at the λ-point begins to be apparent not far below 3° K., at which temperature the specific heat also displays the first symptoms of its rise to a sharp maximum, so that it is probable the two effects are intimately related. Naturally the specific heat variation is reflected in a corresponding variation of γ, the ratio of the principal specific heats, which drops to a value near unity at the λ-point, and this provides a satisfactory phenomenological explanation of the shape of the velocity curve. It does not, however, in itself suggest a mechanism for the rapid increase in attenuation, for which a number of tentative proposals have been made, none of which has been worked out fully enough to carry conviction. The present paper is intended as a crude analysis of a model of liquid helium above the λ-point which provides a qualitative explanation of the observed attenuation. A complete theoretical investigation would be of far too great a complexity to be practicable at present.

It has been suggested by Keesom and Keesom (1935) that the increase in the specific heat of He I between 3·0° K. and 2·18° K. is to be attributed to thermodynamical fluctuations of sufficient magnitude to

* Communicated by the Author.

lead to the formation of inclusions of He II in the liquid, and, although their analysis is not sufficiently refined to give more than a rough estimate of the importance of this effect, there can be little doubt of its essential correctness. As a starting-point, therefore, we shall assume that in this temperature range the liquid is inhomogeneous in the sense that it contains small inclusions whose thermodynamical properties, if not exactly the same as those of He II in bulk, are at least markedly different from those of He I. Their influence on γ may be readily understood by considering the reduction which they bring about in the temperature rise during adiabatic compression. For the present purpose it is convenient to think of the effect of adiabatic compression as equivalent, so far as temperature changes are concerned, to the injection of heat at constant pressure. The inclusions are now seen to exert a two-fold influence. In the first place they reduce the temperature rise by increasing the mean specific heat of the liquid, and in the second place they actually reduce the equivalent heat input ; for while in order to simulate the temperature changes accompanying adiabatic compression heat must be injected into He I, it must be removed from He II on account of the negative expansion coefficient of the latter. The net result is that the temperature rise of the liquid is less than it would be in the absence of inclusions, and correspondingly γ and the velocity of sound are reduced.

As mentioned above, a detailed analysis of the processes taking place in a real liquid subject to fluctuations during passage of a sound wave would be a very difficult matter to treat rigorously, and we shall therefore in the next section consider a model of an inhomogeneous liquid from which the major theoretical obstacles have been eliminated. We shall then be enabled to discuss qualitatively the extent to which the behaviour of this model parallels that of liquid helium, and hence to demonstrate that the fluctuation theory is capable of accounting for the general features observed experimentally.

§2. Propagation of Sound in an Inhomogeneous Medium.

Consider a medium consisting of a number of spherical inclusions of uniform size embedded at random in a matrix of different properties, and initially at the same temperature. In order to determine the propagation characteristics for a compressional wave of angular frequency ω in this medium it is necessary to calculate the adiabatic compressibility. It is clear from the previous section that if the temperature rise of the inclusions during compression is less than that of the matrix, and if there is thermal equilibrium between the two, the compressibility of the medium as a whole will be affected by the presence of the inclusions. Moreover, if ω is so high that thermal equilibrium is not perfect, the volume oscillations of the medium will lag behind the pressure oscillations, and there will be a continuous conversion of the mechanical energy of the wave into heat.

If a fraction x of the medium is in the form of inclusions, whose compressibility under the conditions of the experiment is k_2, while the compressibility of the matrix is k_1, the mean compressibility will be given by the expression :

$$\bar{k}=(1-x)k_1+xk_2. \quad . \quad . \quad . \quad . \quad . \quad . \quad . \quad (1)$$

The actual compressibility of the matrix, k_1, is related to its adiabatic compressibility, k_{1a}, by the expression :

$$k_1=\gamma_1 k_{1a}-\beta_1 \frac{d\mathrm{T}_1}{dp}, \quad . \quad . \quad . \quad . \quad . \quad . \quad . \quad (2)$$

where β_1 is the expansion coefficient, $1/\mathrm{V}\ (\partial \mathrm{V}/\partial \mathrm{T})_p$, of the matrix, and $d\mathrm{T}_1/dp$ is the rise of temperature of the matrix as a result of compression under the conditions of the experiment. Since for adiabatic compression of the matrix,

$$\left(\frac{\partial \mathrm{T}_1}{\partial p}\right)_{\mathrm{S}}=\frac{\gamma_1-1}{\beta_1}k_{1a},$$

we may rewrite (2) in the form,

$$k_1/k_{1a}=\gamma_1-(\gamma_1-1)h_1, \quad . \quad . \quad . \quad . \quad . \quad . \quad (3)$$

where $h_1=\{d\mathrm{T}_1/dp\}/(\partial \mathrm{T}_1/\partial p)_{\mathrm{S}}$. Similarly for the inclusions

$$k_2/k_{2a}=\gamma_2-(\gamma_2-1)h_2. \quad . \quad . \quad . \quad . \quad . \quad . \quad (4)$$

If h_1 and h_2 vary from point to point they must be replaced by their average values $\bar{h}_1$ and $\bar{h}_2$. Thus the determination of $\bar{k}$ is resolved into the problem of determining $\bar{h}_1$ and $\bar{h}_2$.

As explained earlier, we may simulate the effects of adiabatic compression by injecting heat ; for a given rate of change of pressure let the appropriate rate of injection of heat be q_1 per unit volume of matrix and q_2 per unit volume of inclusions. It is a simple matter to show thermodynamically that

$$q_2/q_1=\beta_2/\beta_1=\lambda \text{ (say)}.$$

If the heat is injected and withdrawn periodically with frequency ω, the resulting temperature oscillations of the matrix and inclusions would be represented, in the absence of thermal contact, by the equations

$$i\omega \mathrm{C}_1\mathrm{T}_1=q_1 \quad \text{and} \quad i\omega \mathrm{C}_2\mathrm{T}_2=q_2,$$

in which T_1 and T_2 are the departures from the mean of the temperatures of matrix and inclusions respectively, and C_1 and C_2 are specific heats per unit volume. As is common in the solution of periodic problems, $\partial/\partial t$ is replaced by $i\omega$.

In order to calculate the effects of thermal transfer it is convenient to divide the heat sources into two parts, which may be superposed to give the complete solution. Let us first supply heat at a rate q_1 per unit volume of matrix and μq_1 per unit volume of inclusion, where $\mu=\mathrm{C}_2/\mathrm{C}_1$.

This we shall refer to as the standard state, in which the temperature oscillation is the same, $q_1/i\omega C_1$, for both matrix and inclusions, without the necessity of heat exchange between the two. To represent the actual state of affairs we must in addition supply heat to the inclusions at a rate $q_1(\lambda-\mu)$ per unit volume. We may first consider one inclusion only to be supplied with this additional heat, the rest being in the standard state, and solve the resulting conduction problem. Afterwards the result may be summed over all inclusions, since all the effects are additive.

If the material outside the one inclusion considered be smoothed out into a uniform material of specific heat $C\,(=(1-x)C_1+xC_2)$, the conduction problem is straightforward. The equation of heat conduction in the material surrounding the inclusion takes the form, for spherical symmetry,

$$\frac{d^2T}{dr^2}+\frac{2}{r}\frac{dT}{dr}-\frac{i\omega C}{\kappa}T=0,$$

where κ is the thermal conductivity; and the appropriate solution, in which T tends to zero as r tends to infinity, may be written:

$$T=\frac{u}{r}\exp(-\zeta r), \quad \text{where} \quad \zeta=\sqrt{(i\omega C/\kappa)}.$$

The integration constant, u, is determined by the boundary condition at the surface of the inclusion, where $r=a$. For simplicity we shall suppose the inclusion to be at a uniform temperature at all times, the same as that of the matrix immediately surrounding it, that is $[T]_a$. Then since heat is supplied to the inclusion at a rate $\frac{4}{3}\pi a^3 q_1(\lambda-\mu)$ from the exterior source, and at a rate $4\pi a^2\kappa[dT/dr]_a$ by conduction from the matrix, the rate of rise of temperature of the inclusion, $i\omega[T]_a$, is governed by the equation

$$\frac{3\kappa}{a}[dT/dr]_a-i\omega C_2[T]_a+q_1(\lambda-\mu)=0.$$

From this equation u may be determined, and the amplitude of the temperature oscillation of the inclusion is found to be given by the expression

$$[T]_a=\frac{a^2}{3\kappa}\cdot\frac{q_1(\lambda-\mu)}{1+a\zeta+i\omega\tau}, \quad \text{where} \quad \tau=C_2a^2/3\kappa. \quad . \quad . \quad . \quad (5)$$

Thus of the heat $q_1(\lambda-\mu)$ supplied to unit volume of the inclusion, the amount which remains within it is given by $i\omega C_2[T]_a$, *i. e.*

$$i\omega\tau\cdot\frac{q_1(\lambda-\mu)}{1+a\zeta-i\omega\tau}, \quad . \quad . \quad . \quad . \quad . \quad . \quad . \quad . \quad (6)$$

and the rest, which is conducted to the surrounding material is given by $q_1(\lambda-\mu)-i\omega C_2[T]_a$, *i. e.*

$$(1+a\zeta)\cdot\frac{q_1(\lambda-\mu)}{1+a\zeta+i\omega\tau}. \quad . \quad . \quad . \quad . \quad . \quad . \quad . \quad (7)$$

Now the surrounding material is made up of matrix and inclusions in the standard state, and the heat (7) will be divided among them in the proportions :

$$\frac{1-x}{1+(\mu-1)x} \text{ to the matrix,} \quad \frac{\mu x}{1+(\mu-1)x} \text{ to the inclusions.*} \quad . \quad (8)$$

Let us now add together the effects of all the inclusions, acting in the same way. In unit volume of material there will be a volume x occupied by inclusions, so that, combining (7) and (8), we see that the heat supplied to the matrix by all the inclusions amounts to

$$(1+a\zeta)\frac{q_1(\lambda-\mu)}{1+a\zeta+i\omega\tau}\frac{x(1-x)}{1+(\mu-1)x},$$

or, since the total volume of matrix is $(1-x)$,

$$(1+a\zeta)\frac{q_1(\lambda-\mu)}{1+a\zeta+i\omega\tau}\frac{x}{1+(\mu-1)x}$$

per unit volume of matrix. To this we must add the heat supplied to unit volume of matrix in the standard state, which is just q_1, to give for the resultant total rate of heat supplied per unit volume to the matrix

$$q_1'=q_1\left\{1-\frac{x(1+a\zeta)(\mu-\lambda)}{(1+a\zeta+i\omega\tau)[1+(\mu-1)x]}\right\}.$$

Similarly we may calculate the resultant total rate of heat supply per unit volume to the inclusions

$$q_2'=q_2\left\{1+\frac{1}{\lambda}\cdot\frac{(1-x)(1+a\zeta)(\mu-\lambda)}{(1+a\zeta+i\omega\tau)[1+(\mu-1)x]}\right\}.$$

Now $q_1'/q_1=\bar{h}_1$ and $q_2'/q_2=\bar{h}_2$; hence from (1), (3) and (4),

$$\begin{aligned}\bar{k}&=(1-x)k_{1a}+xk_{2a}\\&\quad+\frac{x(1-x)(\mu-\lambda)(1+a\zeta)}{(1+a\zeta+i\omega\tau)[1+(\mu-1)x]}[k_{1a}(\gamma_1-1)-k_{2a}(\gamma_2-1)/\lambda],\\&=(1-x)k_{1a}+xk_{2a}+\frac{x(1-x)(\mu-\lambda)^2(1+a\zeta)(\gamma_1-1)k_{1a}}{\mu(1+a\zeta+i\omega\tau)[1+(\mu-1)x]}, \quad . \quad . \quad (9)\end{aligned}$$

since, by a well-known thermodynamical formula, $\gamma-1=\beta^2T/Ck$.

From this expression for the mean compressibility it will be seen that at sufficiently high frequencies only the first two terms are important, and this clearly corresponds to such rapid oscillations of pressure that no heat is exchanged between the inclusions and the matrix. The last term expresses the modification brought about by heat exchange at

* This is true only if there is thermal equilibrium between the matrix and inclusions, *i. e.* at low frequencies, but the error involved at higher frequencies should not be great, provided that x is not too large.

lower frequencies. When $\omega=0$, $a\zeta$ and $\omega\tau$ vanish, and for frequencies low enough for $a\zeta$ and $\omega\tau$ to be much smaller than unity, (9) may be rewritten in a slightly simpler, approximate form:

$$\bar{k}\doteqdot(1-x)k_{1a}+xk_{2a}+\frac{x(1-x)(\mu-\lambda)^2(\gamma_1-1)k_{1a}}{\mu[1+(\mu-1)x]}(1-i\omega\tau). \quad . \quad (10)$$

Since the velocity of sound, $v=1/\sqrt{(k\rho)}$, where ρ is the density, the velocity and attenuation of a sound wave may be immediately deduced from (9) or (10). If v_0 is the limiting velocity at high frequencies, corresponding to a compressibility given by the first two terms of (10), and Δv is written for v_0-v, then from (10),

$$\frac{\Delta v}{v_0}\doteqdot\frac{x(1-x)(\mu-\lambda)^2(\gamma_1-1)k_{1a}}{2\mu[1+(\mu-1)x][(1-x)k_{1a}+xk_{2a}]}, \quad . \quad . \quad . \quad . \quad (11)$$

and the attenuation per unit distance,

$$\alpha\doteqdot\frac{x(1-x)(\mu-\lambda)^2(\gamma_1-1)\omega^2\tau}{2\mu v_0[1+(\mu-1)x]}. \quad . \quad . \quad . \quad . \quad . \quad . \quad (12)$$

This expression for α is, of course, valid only when $\omega\tau\ll1$; as the frequency is increased α rises as ω^2 at first, but more slowly as $\omega\tau$ approaches unity, and finally, when $\omega\tau\gg1$, it increases only as $\sqrt{\omega}$ so that the attenuation per wavelength actually decreases. If k_{1a} and k_{2a} are not greatly different, equations (11) and (12) may be combined to yield a simple expression for α at frequencies for which $\omega\tau\ll1$,

$$\alpha\doteqdot\frac{\omega^2\tau\Delta v}{v_0^2}=\frac{\omega^2C_2a^2\Delta v}{3\kappa v_0^2}. \quad . \quad . \quad . \quad . \quad . \quad . \quad . \quad (13)$$

Before discussing the relation between the model we have analysed and the actual state of affairs in liquid helium, we may take the argument one stage further. Up to now we have assumed that the medium contains permanent inclusions, but it would more nearly approximate to a fluctuating liquid if we considered the inclusions as transient, appearing and disappearing in a random manner at all points in the medium. As will appear below, this transience of the inclusions does not modify equation (11) for the velocity, but it may reduce the attenuation. In order to understand the effect let us return to an early stage in the previous calculation, and consider one inclusion surrounded by the material in the standard state. The inclusion oscillates in temperature with an amplitude $[T]_a$ given by (5), in addition to the oscillation of the standard state. Thus the actual amplitude under these conditions is

$$\frac{q_1}{i\omega C_1}(1-i\omega\tau'), \text{ if } \omega\tau'\ll1, \text{ where } \tau'=\tau(1-\lambda/\mu).$$

The oscillation of the inclusion is thus of very nearly the same amplitude as that of the rest of the material, but with a time-lag of τ'.

Now consider a small region of the material, which, if the inclusions are transient, will spend a fraction x of the time as part of an inclusion, and the rest $(1-x)$, as part of the matrix. So long as it is part of the matrix its temperature will stay in phase with that of the standard state, but as soon as it becomes part of an inclusion it will tend to lag behind the standard state, and if it remains part of an inclusion for a time long compared with τ' it will assume the time-lag τ' corresponding to dynamical equilibrium. When, with the disappearance of the inclusion, it becomes once more part of the matrix, the time-lag will revert to zero with a time constant approximately equal to τ'. Thus if the time of persistence of the inclusions is much greater than τ', the mean time-lag of the inclusions will be the same as if they were permanent, and the results of the previous calculation will apply. On the other hand, if the inclusions persist only for a time shorter than τ' they will not take up the full time-lag before they disappear, their mean time-lag will be less than τ' and the attenuation will be correspondingly reduced. For any given time of persistence of the inclusions, their mean time-lag, $f\tau'$ (say), where $f<1$, may in principle be calculated, and the previous arguments may be carried through exactly as before, with τ everywhere replaced by $f\tau$. Clearly equation (11) for the velocity will be unaltered, since it does not involve τ, but (12) and (13), expressing the attenuation, will be modified, and a new approximation to the attenuation coefficient may be written :

$$\alpha \doteqdot \frac{\omega^2 f C_2 a^2 \Delta v}{3\kappa v_0^2}. \quad \ldots\ldots\ldots \quad (14)$$

We shall return later to a discussion of the value to be assigned to f.

§ 3. Application to Liquid Helium.

The model which we have analysed in some detail resembles the actual state of affairs in liquid helium only superficially, and the analysis has been given mainly in order to make clear the nature of the processes which may affect the velocity and attenuation in an inhomogeneous fluid. The major difference between a fluctuating liquid and the model lies in the fact that in the former the inclusions exist essentially as a result of temperature fluctuations, so that it is not possible to consider the initial state of the material, before the passage of a sound wave, as one of uniform temperature. In spite of this difference, however, a close analogy may be drawn between the two systems, and to a large extent the fluctuations may be disregarded except in so far as they are the mechanism responsible for the appearance of inclusions. This may be understood by reference to a new model which more closely resembles a real fluctuating liquid. Let us suppose that the liquid is initially entirely free from spontaneous fluctuations and is uniform in temperature and in all other properties ; now let heat be injected into and withdrawn from the liquid from point to point in a random manner, in such a way that the total internal energy remains constant. The temperature of the

liquid will now fluctuate randomly, and the energy flow resulting from its thermal conductivity will be similar to that which occurs spontaneously in a real liquid. If the mean temperature is not too much higher than the λ-point the local withdrawals of heat may be sufficient to produce transient inclusions of He II. Now let us superimpose on this random heat injection an orderly injection which will simulate the effect produced by adiabatic compression; that is, we inject heat at a uniform rate into every region of the matrix (He I), and at a different, but uniform, rate into every inclusion (He II). If the amount of heat injected in this way is very much smaller than the random injections its influence on the distribution of the inclusions will not be very great, though, as we shall see below, it cannot be entirely neglected. Since the equation of heat conduction is linear the energy flow due to each cause is independent, so that the ordered heat flow is the same as if matrix and inclusions were initially at the same temperature. Moreover, the effect of each type of energy flow on the volume of the liquid is independent, so that each contributes independently to the compressibility. The random fluctuations, however, do not affect the volume, so that they may be disregarded. To this degree of approximation, therefore, the real liquid may be treated as exactly analogous to the model which we have studied, and the expressions for the velocity and attenuation of a sound wave may be taken over directly.

There is, however, one assumption in the preceding argument which is not strictly valid, namely that the passage of a sound wave does not affect the distribution of the inclusions. In fact the heating of the material by compression shortens the lifetime of each inclusion in such a way as to decrease appropriately the number of inclusions present at a higher temperature. If this effect were negligible it would be possible, as in the model, to express the specific heat, C, in the form $(1-x)C_1+xC_2$; but, in fact, there will be an important contribution arising from $dx/d\mathrm{T}$. Any attempt to calculate the specific heat of liquid helium above the λ-point would involve a complete statistical description of the assembly, and would be at least as difficult as an exact calculation of the specific heat arising from an order–disorder transition. Since, therefore, we cannot justify the analogy between the actual liquid and our model so far as the specific heat is concerned, we shall modify the argument so as to incorporate experimental values of the specific heat. The calculation may be simplified without serious error by taking as zero the expansion coefficient, β_2, of He II. This assumption is equivalent to neglecting λ in comparison with μ in the model already analysed, and is justified by the fact that the relative change in specific heat at the λ-point is much greater than the relative change in expansion coefficient. At the same time we must for consistency put $\gamma_2=1$ and hence $k_2=k_{2a}$. A short calculation now leads to an expression for the real part of the mean compressibility at frequencies such that $\omega\tau\ll 1$, which, as may be seen from equation (10), may be obtained by assuming thermal equilibrium between matrix and

inclusions. The rate of input of heat per unit volume is $q_1(1-x)$, since $q_2=\beta_2 q_1/\beta_1=0$, and thus the rate of rise of temperature of the matrix is $q_1(1-x)/C$. Since for the pure matrix the corresponding rate would be q_1/C_1, we have immediately that $\bar{h}_1=C_1(1-x)/C$. Hence, from (1) and (3),

$$\bar{k}/k_{1a}=1+x\Delta k/k_{1a}+(\gamma_1-1)(1-x)[1-b(1-x)],$$

where $$\Delta k=k_{2a}-k_{1a} \text{ and } b=C_1/C.$$

If now we write v_1 for $1/\sqrt{(\rho_1 k_{1a})}$, the velocity of a sound wave in an extended volume of the pure matrix (He I), and v_2 for $1/\sqrt{(\rho_2 k_{2a})}$, the velocity in an extended volume of the material of the inclusions (He II), and further introduce the definitions :

$$\Delta v_0=v_1-v_2,$$
$$\Delta v'=v_1-v,$$

where v is the velocity in the actual material, we have that

$$\Delta v'=x\Delta v_0+\tfrac{1}{2}v_1(\gamma_1-1)(1-x)[1-b(1-x)]. \quad . \quad . \quad . \quad (15)$$

It is worth emphasizing that γ_1 in (15) is not the experimentally determined value of γ in actual He I, but the value which would be observed if there were no inclusions of He II. This " ideal γ ", as we shall show later when comparing theory and experiment, can be fairly precisely estimated by extrapolation from higher temperatures.

So far as the attenuation coefficient is concerned, it seems likely that the expression (14) derived from the model, for values of $\omega\tau$ much less than unity, needs little modification when applied to the real liquid ; the attenuation arises from the lag of the temperature oscillation of the inclusions behind the pressure oscillation, which should not be influenced to any great extent by the variations in the mean lifetime of the inclusions brought about by the temperature oscillation, provided that the amplitude of the temperature oscillation is small. We shall therefore use (14) in comparing theory and experiment, choosing some plausible value for C_2, the specific heat of the material which composes the inclusions. It is also necessary to ascribe a value to f, which can only be done by guessing the mean life-time of the inclusions. It will be remembered that $f=1$ if this life-time is much greater than τ' and decreases to zero as the life-time becomes much smaller than τ'. Now since τ' is the relaxation time for heat transfer between the matrix and the inclusions it is reasonable to suppose that the life-time of the inclusions will be of the order of τ', under which conditions f will be approximately $\frac{1}{3}$. Probably at temperatures well above the λ-point, at which inclusions are only rarely formed as a result of an unusually large fluctuation, the life-time of such inclusions will be rather shorter than τ' and f will be correspondingly smaller ; conversely, near the λ-point the inclusions will be readily formed, and may persist for times

longer than τ'. In the absence of any detailed theory of the fluctuations the best that can be done is to take $\frac{1}{3}$ as a compromise value of f with reasonable assurance that except very near and very far from the λ-point it will not be wrong by more than a factor 2. We shall therefore write for the attenuation coefficient:

$$\alpha \doteqdot \frac{\omega^2 C_2 a^2 \Delta v}{9\kappa v_0^2}, \qquad \ldots\ldots\ldots \quad (16)$$

where, as in the model, v_0 is the limiting velocity at high frequencies, corresponding to a compressibility $(1-x)k_{1a}+xk_{2a}$, and $\Delta v = v_0 - v$.

§ 4. Comparison of Theory and Experiment.

In order to compare the predictions of (15) and (16) with experiment it is necessary to choose values for the physical quantities entering into these expressions. The two which particularly need discussion are C_1 and γ_1 the specific heat and ratio of principal specific heats of "ideal He I" containing no inclusions of He II. These must be estimated by extrapolation from higher temperatures, and, since the properties of helium in the range from 2·18° to nearly 3° K. are to varying extents influenced by the presence of inclusions, the required extrapolation is considerable. Fortunately, however, a few plausible assumptions enable the extrapolation to be carried out without too much uncertainty. The data which will be used are to be found most conveniently exhibited in Keesom's (1942) book, and the references in the following paragraphs are to diagrams therein.

We consider first the "ideal specific heat" of helium I, C_1. It is clear from diagram 4.17 that between 4° and 3° K. the specific heat falls almost linearly, that is, much more slowly than might be expected for a normal liquid, and this trend is exhibited in an even more striking fashion by the entropy diagram 4.40. From the latter diagram it is clear that the entropy of solid He and He II at 0° K. takes a value about −0·85 (the entropy of liquid He I at the normal boiling point is taken as zero), and it is very nearly to this value that the entropy curve of He I above 3° K. extrapolates. It is likely, therefore, that the λ-transition in helium is in this respect analogous to that in superconductors rather than to order–disorder transitions; that is to say, even if the phase-transition did not occur there would be still no excess entropy at 0° K.* In parenthesis it may be remarked that if liquid He_3 is similar to He_4 I, then there need be no cause, on thermodynamical grounds, for surprise that no transition occurs. All that is necessary to eliminate the entropy by the time the liquid has cooled to 0° K. is that the specific heat shall vary roughly as T, as apparently occurs in He I. To return to the immediate problem, we shall assume that the entropy curve 4.40 can be extrapolated almost linearly to a value −0·85 at 0° K., and hence derive an almost linear ideal specific heat curve for He I.

* *Note added in proof.*—This behaviour has already been noted by Daunt and Mendelssohn (1946).

In fig. 1 are exhibited the experimental curve of C and the assumed curve for C_1, from which the ratio $b(=C_1/C)$ may be determined as a function of temperature. In this diagram C and C_1 are referred to unit mass rather than unit volume, and are measured at the vapour pressure of the liquid.

The ideal ratio of the principal specific heats, γ_1, may be derived from the thermodynamic relation :

$$\frac{\gamma-1}{\gamma} = -\frac{T}{\rho^2 C_p}\left(\frac{\partial p}{\partial T}\right)_\varrho \left(\frac{\partial \rho}{\partial T}\right)_p,$$

where C_p is the specific heat per unit mass at constant pressure.

We have already considered the extrapolated curve for C_1, which is measured at the vapour pressure, and a small correction for the variation of vapour pressure with temperature must be applied to convert it into

Fig. 1.

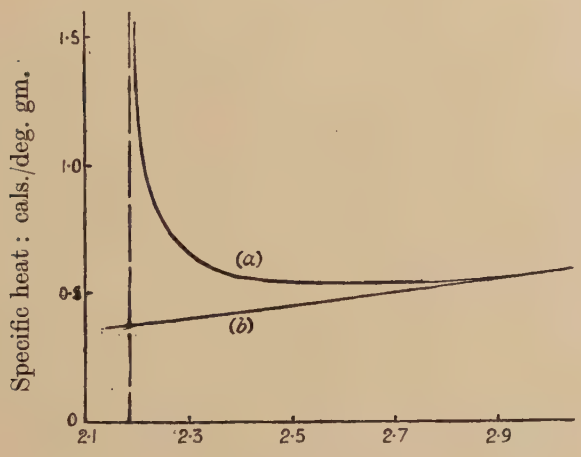

Specific heat of HeI : (*a*) Experimental curve.
(*b*) Assumed curve for "ideal HeI".

a curve for C_p. The density, ρ, changes so slowly with temperature that there is no need to correct the measured values, but the two differential coefficients in the expression are affected by the approach to the λ-point and require correction. Keesom's curves 4.38 for $(\partial p/\partial T)_\varrho$ at various densities give a clear indication of how the extrapolation should be made, since they lie close together and run parallel above 2·7° K., only diverging as each approaches its discontinuity at the λ-point. Now the λ-point for helium of density 0·18 gm./cm.^{3} lies 0·3° K. lower than that of helium under its vapour pressure, so that at 2·2° K. it will hardly be affected by the approaching discontinuity. The ideal curve for $(\partial p/\partial T)_\varrho$ of helium under its vapour pressure may therefore be constructed by

continuing the curve above 3° K. parallel to the curve corresponding to a density of 0·18 gm./cm.^{3}. No similar method is available for $(\partial\rho/\partial T)_p$ which is exhibited in 4.39, but the extrapolation presents no difficulties. Values of $(\partial\rho/\partial T)_p$ were plotted against T for temperatures above 3·0° K. and the curve was extrapolated by eye to 2·1° K., bearing in mind that it must tend to zero, according to Nernst's theorem, as T tends to zero. From these extrapolated curves a curve for (γ_1-1) was constructed, and the result is shown in fig. 2.

We are now in a position to see whether the expression (15) provides a satisfactory explanation of the variation of the velocity with temperature, of which the experimental curve (Atkins and Chase 1951) is shown in

Fig. 2.

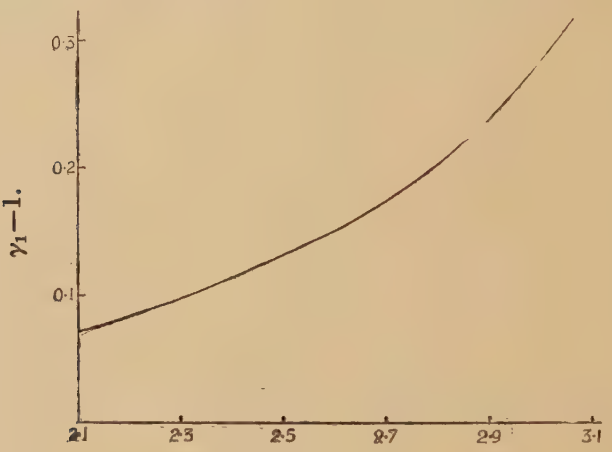

Ratio of principal specific heats of " ideal HeI".

fig. 3 (*a*). One might tackle this problem by guessing a reasonable form of the curve for v_1 (which should join smoothly on to the experimental curve at about 3° K.): the difference between this curve and the experimental curve would give values of $\Delta v'$, which could then be compared with the predictions of equation (15). We prefer, however, to work in the reverse order, estimating $\Delta v'$ from (15) and hence constructing a curve for v_1. The aim is now to see whether a curve may be thus obtained which behaves in the expected way, becoming steadily flatter as the temperature is lowered, and tending to a zero gradient at 0° K. in accordance with Nernst's theorem. Since the major contribution to $\Delta v'$ arises from b rather than x, especially at the higher temperatures, we may as a first approximation to $\Delta v'$ put $x=0$ in equation (15), obtaining the simpler expression

$$\Delta v' \doteqdot \tfrac{1}{2}v_1(\gamma_1-1)(1-b).$$

Values of $\Delta v'$ calculated in this way for different temperatures and added to the experimental values of v give a first approximation to the curve of v_1 versus T, which is shown as curve (b) in fig. 3. It is encouraging that this curve joins smoothly to the experimental curve above 3° K. Below 2·5° K., however, it takes a less satisfactory shape, and it is in this region that non-zero values of x must be assumed in order to smooth out the curve. It is now necessary to use values of Δv_0 in (15), and therefore to estimate v_2, the velocity of sound in the material of the inclusions. Since it is not possible without a detailed theory to determine the extent to which the inclusions resemble small regions of He II, there must obviously be considerable latitude in the choice of v_2. For the present comparison a value of 217·5 m./sec. has been chosen, corresponding approximately to the velocity just below the λ-point, but other values

Fig. 3.

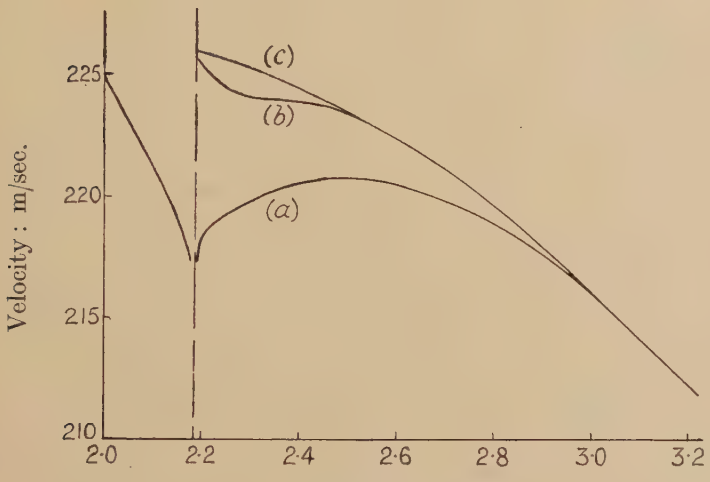

Velocity of sound in helium :

(a) Experimental curve.

(b) First approximation to curve for "ideal HeI".

(c) Final curve for "ideal HeI".

are equally likely, and the calculations which follow could readily be modified to suit them. It is now a matter only of finding such values of x that a smooth curve for v_1 may be drawn, using the complete expression (15) for $\Delta v'$. One possible variation of x with T is shown in fig. 4, and the corresponding curve for v_1 as curve (c) in fig. 3. The values which it is necessary to ascribe to x appear to be fairly reasonable, but, since the velocity is not highly sensitive to variations in x and the parameters occurring in (15) are not very accurately known, it would be unwise to regard the curve for x as having more than qualitative validity.

However, we may conclude from this analysis that the hypothesis of a non-uniform composition of helium above the λ-point is capable of accounting for the observed velocity curve, since the form of curve 3 (*c*) is very much what one would expect for a uniform liquid, such as " ideal He I " is assumed to be.

Finally we must see whether equation (16) predicts an attenuation of the right order of magnitude. Here the comparison between theory and experiment is even more uncertain than with the velocity, since α depends critically on the size of the inclusions, about which nothing is known. We shall therefore calculate the value of a which will lead to the

Fig. 4.

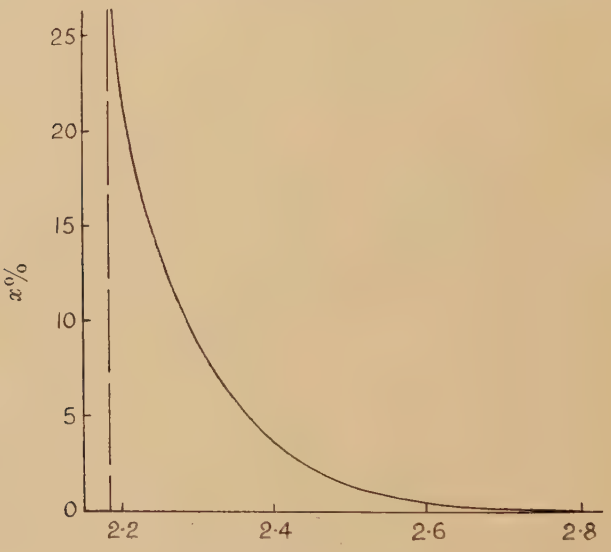

Temperature variation of concentration of inclusions.

right value of α at a given temperature, and see whether inclusions of this radius are likely, according to simple fluctuation theory, to be present at that temperature in the concentration, x, found above. It will be necessary to choose a value for C_2, and here again there is very little guidance from theory which will enable a wise choice to be made. According to the measurements of Keesom and Keesom (1935) the specific heat of He II in bulk rises, just below the λ-point, at least to 6 cals./gm. deg., but the rise is very rapid, and it is unlikely that the inclusions on the average take so high a value. We shall here assume C_2 to be 1·5 cals./gm. deg., or 0·22 cals./cm.^{3} deg. According to the recent data of Atkins and Chase the attenuation constant α, at 2·3° K. and a frequency of 14 Mc./s. is 0·27/cm., of which approximately 0·10/cm. is explicable in terms of viscous damping and thermal conduction in " ideal He I " (Pellam and Squire 1947). The difference, 0·17/cm. we

suppose to result from the presence of the inclusions. Putting $v_0 = 224{\cdot}3$ m./sec., $\Delta v = 4{\cdot}5$ m./sec. and $K = 4{\cdot}4 \times 10^{-5}$ cals./deg. cm. sec.* in equation (16), we find that the observed attenuation may be accounted for if the mean radius of the inclusions is about $2{\cdot}1 \times 10^{-7}$ cm., corresponding to a cluster of about 850 atoms.

In order to determine whether inclusions of radius $2{\cdot}1 \times 10^{-7}$ cm. might be present in such numbers as to occupy 9 per cent of the total volume, as required by our analysis of the velocity curve, we may carry out a simple calculation which, though based on quite inexact assumptions, should give a qualitatively correct answer. Suppose the liquid at 2·3° K. to be divided into regions whose volumes, V, are equal to the estimated volume of an inclusion, $3{\cdot}9 \times 10^{-20}$ cm^3. If these regions, having the properties of ideal He I, are regarded as weakly interacting with one another we may immediately calculate the proportion which through fluctuations have temperatures less than 2·18° K. This proportion, by standard fluctuation theory, is given by $\frac{1}{2}[1 - \mathrm{erf}\,(\Gamma.\delta T)]$ where $\delta T = 0{\cdot}12°$ K. and $\Gamma = \sqrt{(C_1 V/2kT^2)}$ deg.$^{-1}$, and substitution of numerical values leads to a value 11 per cent. The agreement with the desired value 9 per cent is probably better than the assumptions warrant, especially in view of the uncertainties in the values to be ascribed to various parameters occurring in the theory. We may, however, conclude that the suggested mechanism of the extra attenuation near the λ-point is capable in principle of explaining the magnitude of the effect.

As the λ-point is approached the attenuation rises very rapidly, and probably increases by a factor greater than 20. This cannot be explained on the assumption that the inclusions stay constant in volume, but, on the other hand, if they increase in size nearer the λ-point, as it is very plausible to assume, there is no difficulty in explaining the rapid rise, since α depends on a^2. Below the λ-point the attenuation drops again sharply, presumably as the liquid becomes more and more completely homogeneous, but we shall not attempt to calculate the attenuation when the liquid is mainly He II, with inclusions of He I, since in the absence of any adequate microscopic theory of He II the foundations of such a calculation would be even less firmly secure than those of the present work.

Acknowledgment.

I should like to express my thanks to Dr. K. R. Atkins and Mr. C. E. Chase for allowing me to make use of their results before publication.

References.

Atkins, K. R. and Chase, C. E., 1951 to be published in *Proc. Phys. Soc.*
Daunt, J. G., and Mendelssohn, K., 1946, *Proc. Roy. Soc.* A, **185,** 225.
Keesom, W. H., 1942 *Helium* (Elsevier).
Keesom, W. H., and Keesom, A. P., 1935, *Physica* **2,** 557.
Pellam, J. R. and Squire, C. F., 1947, *Phys. Rev.* **72,** 1245.

* I am indebted to Mr. C. Grenier for information concerning his as yet unpublished measurements of the thermal conductivity of He I.

CXXII. *The Synthesis of Elastic Dislocation Fields.*

By F. R. N. Nabarro,
Department of Metallurgy, The University of Birmingham†.

[Received June 13, 1951.]

Summary.

The static field of an infinitesimal loop of dislocation lying in its glide plane is calculated. The field of any plane loop lying in its glide plane may be obtained by integration of the result. The field produced by the sudden creation of an infinitesimal loop is calculated as a function of time. The field of an arbitrarily moving plane loop may be obtained by integration. The method is illustrated by simple examples.

§1. Introduction.

The process of plastic deformation in a crystal may be represented (*cf.* Cottrell 1949) by the following deformation of an isotropic elastic continuum. A cut is made over a finite area of a plane, the *glide plane*, and the opposite faces of the cut are moved relative to one another a distance **b** in a direction, the *glide direction*, which lies in the glide plane. The elastic deformation is thus a particular type of *dislocation*, as discussed by Volterra (1907). Burgers (1939) has shown that the static displacements produced by such a dislocation can be expressed by integrals along the line bounding the area which has slipped. We shall here express the same general result as a double integral over the area which has slipped, and extend the method to give the instantaneous displacements produced by a moving dislocation. In §2 we derive the static displacements produced by an infinitesimal loop of dislocation in an infinite body; §3 digresses to give the static displacements produced by such a loop at the centre of a finite sphere. In §4 the method of synthesis is illustrated by the screw dislocation, in which the cut surface is a half plane bounded by a line parallel to **b**, and the edge dislocation, in which the cut is made over a half plane bounded by a line perpendicular to **b**. The displacements produced if an infinitesimal loop of dislocation is suddenly created are calculated in §5, and, as an example of the method, the displacements produced by a rigid motion of a screw dislocation are calculated in §6.

§2. The Field of an Infinitesimal Loop of Dislocation Lying in its Glide Plane.

Consider an infinitesimal loop of dislocation with Burgers vector‡ $\mathbf{b}=(0, 0, -b)$ lying in the xz plane close to the origin. Let the area of

† Communicated by the Author.

‡ The vector **b** used in this paper is identical with the vector **f** of Burgers (1939). The current convention (*cf.* Frank 1951) is to take $\mathbf{b}=-\mathbf{f}$.

the loop be δA, while a typical element of its perimeter is $d\boldsymbol{\xi}$. The stress field of this dislocation in an infinite body may be found from the formula of Burgers (1939), which gives at the point $\mathbf{x}$ a displacement $\mathbf{u}$ of the form

$$\mathbf{u}=\mathbf{u}^*+\mathbf{u}^{**}+\text{grad}\,\psi, \quad \ldots\ldots\ldots \quad (1)$$

where

$$\mathbf{u}^*=\Omega\mathbf{b}/4\pi, \quad \ldots\ldots\ldots \quad (2)$$

$$\mathbf{u}^{**}=\frac{\mathbf{b}}{4\pi}\wedge\int\frac{d\boldsymbol{\xi}}{r} \quad \ldots\ldots\ldots \quad (3)$$

and

$$\psi=\frac{\lambda+\mu}{4\pi(\lambda+2\mu)}\int\mathbf{b}\wedge(\mathbf{x}-\boldsymbol{\xi})\,\frac{d\boldsymbol{\xi}}{r}. \quad \ldots\ldots \quad (4)$$

Here Ω is the solid angle subtended by the loop at the point $\mathbf{x}$, λ and μ are Lamé's elastic constants, and $r=|\mathbf{x}-\boldsymbol{\xi}|$.

In this case,

$$\left.\begin{aligned} 4\pi\mathbf{u}^*&=(0,\ 0,\ -b\delta Ay/r^3),\\ 4\pi\mathbf{u}^{**}&=(0,\ -b\delta Az/r^3,\ 0)\\ \text{and}\qquad 4\pi\psi&=(\lambda+\mu)b\delta Ayz/(\lambda+2\mu)r^3,\\ \text{leading to}\qquad B^{-1}u_x&=\frac{\lambda+\mu}{\lambda+2\mu}\,\frac{3xyz}{r^5},\\ B^{-1}u_y&=\frac{\lambda+\mu}{\lambda+2\mu}\left(\frac{3y^2z}{r^5}-\frac{z}{r^3}\right)+\frac{z}{r^3}\\ \text{and}\qquad B^{-1}u_z&=\frac{\lambda+\mu}{\lambda+2\mu}\left(\frac{3yz^2}{r^5}-\frac{y}{r^3}\right)+\frac{y}{r^3}, \end{aligned}\right\} \quad \ldots\ldots \quad (5)$$

where

$$B=-b\delta A/4\pi. \quad \ldots\ldots\ldots \quad (6)$$

This field may be derived from the " first type of simple solutions " of Boussinesq, given by Love (1927) at §§ 131, 132. In Love's notation it is

$$(u_x,\ u_y,\ u_z)=\tfrac{1}{2}\partial(u_2,\ v_2,\ w_2)/\partial z+\tfrac{1}{2}\partial(u_3,\ v_3,\ w_3)/\partial y. \quad \ldots \quad (7)$$

If u_{ij} is the component in the direction of x_j of the displacement at the point x_k produced by a force in the direction x_i at the origin, this displacement field is of the form

$$u_{kij}=\tfrac{1}{2}\left(\frac{\partial u_{ij}}{\partial x_k}+\frac{\partial u_{ik}}{\partial x_j}\right), \qquad i\neq k. \quad \ldots\ldots \quad (8)$$

The forces applied at the origin have zero resultant and zero moment. The corresponding diagonal terms with $i=k$ are " double forces without moment " (Love). The strength of an infinitesimal loop of dislocation is thus a tensor, in which one suffix represents the normal to the plane of the loop and one the Burgers vector. The non-diagonal terms represent elementary acts of slip, while the diagonal terms represent non-conservative motions (Nabarro 1951).

§ 3. A Loop at the Centre of a Sphere.

If the dislocation exists in a finite body with free surfaces, a complementary field must be added which neutralizes the traction across the boundary. For a sphere of radius R centred on the loop, such a field is given by

$$\left.\begin{aligned} \gamma B^{-1}u_x &= 48(\lambda+\mu)(2\lambda+7\mu)xyz, \\ \gamma B^{-1}u_y &= 48(\lambda+\mu)(2\lambda+7\mu)y^2z - 24(\lambda+\mu)(5\lambda+7\mu)r^2z \\ &\qquad + 5(27\lambda^2+56\lambda\mu+28\mu^2)R^2z \\ \text{and}\quad \gamma B^{-1}u_z &= 48(\lambda+\mu)(2\lambda+7\mu)yz^2 - 24(\lambda+\mu)(5\lambda+7\mu)r^2y \\ &\qquad + 5(27\lambda^2+56\lambda\mu+28\mu^2)R^2y, \end{aligned}\right\} \quad . \quad (9)$$

where

$$\gamma = 2(\lambda+2\mu)(19\lambda+14\mu)R^5. \quad . \quad . \quad . \quad . \quad . \quad . \quad (10)$$

These displacements may be derived by a superposition of two solutions of the types given by Love at § 172, taking $\omega_2 = yz$ and $\phi_2 = yz$.

On the surface $r = R$, the total displacement derived from (5) and (9) is given by

$$\left.\begin{aligned} \gamma B^{-1}u_x &= 210(\lambda+\mu)(\lambda+2\mu)xyz, \\ \gamma B^{-1}u_y &= 210(\lambda+\mu)(\lambda+2\mu)y^2z + 15\lambda(\lambda+2\mu)R^2z, \\ \text{and}\quad \gamma B^{-1}u_z &= 210(\lambda+\mu)(\lambda+2\mu)yz^2 + 15\lambda(\lambda+2\mu)R^2y. \end{aligned}\right\} \quad . \quad (11)$$

In spherical polar coordinates with Ox as axis, these become

$$\left.\begin{aligned} \gamma B^{-1}u_r &= 15(8\lambda+7\mu)(\lambda+2\mu)R^3 \sin^2\theta \sin 2\phi, \\ \gamma B^{-1}u_\theta &= 15\lambda(\lambda+2\mu)R^3 \sin\theta \cos\theta \sin 2\phi \\ \text{and}\quad \gamma B^{-1}u_\phi &= 15\lambda(\lambda+2\mu)R^3 \sin\theta \cos 2\phi. \end{aligned}\right\} \quad . \quad . \quad (12)$$

Suppose a homogeneous stress p_{ij} is exerted on the sphere before the dislocation is made. The work done by the displacements (12) against this stress is obtained by integrating $u_r p_{rr} + u_\theta p_{r\theta} + u_\varphi p_{r\varphi}$ over the surface of the sphere. The only components which do not vanish in the integration over ϕ are those arising from p_{yz} and p_{zy}, which are

$$\left.\begin{aligned} p_{rr} &= p_{yz} \sin^2\theta \sin 2\phi, \\ p_{r\theta} &= p_{yz} \sin\theta \cos\theta \sin 2\phi \\ \text{and}\quad p_{r\varphi} &= p_{yz} \sin\theta \cos 2\phi. \end{aligned}\right\} \quad . \quad . \quad . \quad . \quad . \quad . \quad (13)$$

The work done W is given by

$$\left.\begin{aligned} \gamma B^{-1}W &= 8(\lambda+2\mu)(19\lambda+14\mu)\pi R^5 p_{yz} \\ \text{or}\quad W &= -b\delta A p_{yz}. \end{aligned}\right\} \quad . \quad . \quad . \quad (14)$$

§ 4. Synthesis of the Edge and the Screw.

Returning now to the infinite body, we may take the loop to be rectangular, with $\delta A = \delta x\, \delta z$. By replacing z by $z-\zeta$ and integrating (5) over all ζ, we obtain the displacements produced by a pair of screw dislocations of opposite sign lying close to the z axis, and separated by δx. These are

$$u_x=0, \qquad u_y=0, \qquad u_z=-by\delta x/2\pi(x^2+y^2). \quad . \quad . \quad . \quad (15)$$

Replacing x by $x-\xi$ and integrating again from $\xi=-\infty$ to $\xi=0$, we obtain the displacements produced by a single screw dislocation along the z axis, which, apart from a constant, are

$$u_x=0, \qquad u_y=0, \qquad u_z=-(b/2\pi)\tan^{-1} y/x. \quad . \quad . \quad . \quad (16)$$

Alternatively, we may first integrate over all ξ to obtain a pair of edge dislocations close to the x axis, with displacements

$$\left.\begin{aligned} u_x &= 0, \\ u_y &= -\frac{b\delta z(\lambda+\mu)}{\pi(\lambda+2\mu)}\frac{y^2 z}{(y^2+z^2)^2} - \frac{b\delta z\mu}{2\pi(\lambda+2\mu)}\frac{z}{y^2+z^2}, \\ u_z &= -\frac{b\delta z(\lambda+\mu)}{\pi(\lambda+2\mu)}\frac{yz^2}{(y^2+z^2)^2} - \frac{b\delta z\mu}{2\pi(\lambda+2\mu)}\frac{y}{y^2+z^2}. \end{aligned}\right\} \quad . \quad . \quad (17)$$

To obtain an edge dislocation lying along the x axis, we integrate from $\zeta=-\infty$ to $\zeta=0$. The resulting displacements are, apart from a constant,

$$\left.\begin{aligned} u_x &= 0, \\ u_y &= -\frac{b(\lambda+\mu)}{2\pi(\lambda+2\mu)}\frac{y^2}{y^2+z^2} - \frac{b\mu}{4\pi(\lambda+2\mu)}\log(y^2+z^2), \\ u_z &= -\frac{b(\lambda+\mu)}{2\pi(\lambda+2\mu)}\frac{yz}{y^2+z^2} + \frac{b}{2\pi}\tan^{-1}\frac{y}{z}. \end{aligned}\right\} \quad . \quad . \quad (18)$$

§ 5. The Sudden Creation of an Infinitesimal Loop.

The movement of a dislocation in its glide plane may be regarded as the result of the continuous addition of infinitesimal loops to its boundary. If the displacement produced by the sudden creation of such a loop is known as a function of time, the field of a dislocation moving arbitrarily in its glide plane with subsonic speeds may be obtained by superposition. The known solutions for the field of a moving dislocation have each been obtained by some special artifice : the present method gives an explicit solution in the general case, although, as will be seen from § 6, its application in simple cases is rather laborious.

The displacement arising from the sudden creation of a loop of dislocation may be derived from that arising from the sudden application of a single force by the same process of differentiation and combination (7) as can be used to derive (5) from the known expressions for the static

displacements produced by a single force. Love (1904) has given the displacements arising from a single force suddenly applied and then continuously maintained. If the force is applied instantaneously, the results involve discontinuous functions, and the differentiation of these is not straightforward. It is more convenient to start from the formulæ of Stokes (1849) giving the displacement produced by a force which is an arbitrary function of the time, and to carry out the differentiations before passing to the special case of a force suddenly applied. A typical formula is given by Love (1927, § 212). The displacement produced at time t at the point x_k by a force in the x_i direction applied at the origin and proportional to $\chi(t)$ has a component u_{ij} in the direction of x_j given by

$$u_{ij}=\frac{\partial^2 r^{-1}}{\partial x_i \partial x_j}\int_{r/a}^{r/c} t'\chi(t-t')\,dt'+r^{-3}x_i x_j[a^{-2}\chi(t-r/a)-c^{-2}\chi(t-r/c)] \\ +\delta_{ij}r^{-1}c^{-2}\chi(t-r/c), \quad \ldots\ldots\ldots \quad (19)$$

where a and c are the speeds of dilatational waves and of shear waves. The displacements corresponding to the formation of a loop of dislocation in the orientation already considered are given, in analogy with (7), by

$$u_j=\partial u_{yj}/\partial z+\partial u_{zj}/\partial y. \quad \ldots\ldots\ldots \quad (20)$$

Substituting (19) in (20) leads to the expression

$$u_j=2\frac{\partial^3 r^{-1}}{\partial x_j \partial y \partial z}\int_{r/a}^{r/c} t'\chi(t-t')\,dt' \\ -\frac{x_j yz}{r^5}\left(12-2r\frac{d}{dr}\right)[a^{-2}\chi(t-r/a)-c^{-2}\chi(t-r/c)] \\ +\frac{1}{r^3}\frac{\partial(yz)}{\partial x_j}\left[2a^{-2}\chi(t-r/a)-3c^{-2}\chi(t-r/c)+r\frac{d}{dr}c^{-2}\chi(t-r/c)\right]. \quad \ldots \quad (21)$$

If the force is applied suddenly at time $t=0$ and then maintained, $\chi(t)=0$ for $t<0$, $\chi(t)=F$ for $t\geqslant 0$. The expression (21) then takes different forms in the three regions $t<r/a$, $r/a\leqslant t\leqslant r/c$, $t>r/c$. It may be written

$$t<r/a: F^{-1}u_j=0. \quad \ldots\ldots\ldots\ldots\ldots\ldots \quad (22)$$

$$r/a\leqslant t\leqslant r/c: F^{-1}u_j=\frac{x_j yz}{r^7}\left\{\frac{3r^2}{a^2}-15t^2-2r^3[a^{-3}\delta(t-r/a)-c^{-3}\delta(t-r/c)]\right\} \\ +\frac{1}{r^5}\frac{\partial(yz)}{\partial x_j}\left\{3t^2-\frac{r^2}{a^2}-r^3c^{-3}\delta(t-r/c)\right\} \quad \ldots\ldots \quad (23)$$

and

$$t>r/c: F^{-1}u_j=-\frac{3x_j yz}{r^5}\left(\frac{1}{c^2}-\frac{1}{a^2}\right)-\frac{1}{a^2 r^3}\frac{\partial(yz)}{\partial x_j}. \quad \ldots\ldots \quad (24)$$

In (23), terms have been omitted which occur only at the end points of the range, and are there finite, so that they contribute nothing to the integral over a distribution of loops. If the density of the medium is ρ_0, we have

$$a^2=(\lambda+2\mu)/\rho_0, \qquad c^2=\mu/\rho_0,$$

and (24) agrees with (5) if

$$F=-c^2B=bc^2\delta A/4\pi. \quad \ldots\ldots\ldots \quad (25)$$

§ 6. Rigid Motion of a Screw Dislocation in a Straight Line.

Consider a straight screw dislocation lying parallel to the z axis, and moving so that at time τ it intersects the plane $z=0$ at the point $(\xi(\tau), 0, 0)$, where $|\xi'(\tau)|<c$. The motion of the dislocation is equivalent to the creation of rows of infinitesimal loops of the type already discussed. The displacement corresponding to the creation of a single loop spreads out in a wave of finite thickness, bounded by the waves of dilatation and of shear. The displacement at $(x, y, 0, t)$ corresponding to the creation of a single loop at $(\xi, 0, \zeta, \tau)$ begins as soon as $t-\tau=r/a$, where

$$r^2=(x-\xi)^2+y^2+\zeta^2. \quad . \quad . \quad . \quad . \quad . \quad . \quad . \quad . \quad (26)$$

The component u_z arising from the point $\zeta=0$ does not vanish, and arrives when $t-\tau=\rho/a$, where

$$\rho^2=(x-\xi)^2+y^2. \quad . \quad . \quad . \quad . \quad . \quad . \quad . \quad . \quad . \quad (27)$$

According to (15), the resultant displacement obtained by integrating over all ζ is without dilatation in the final state. It does not follow from this alone that the disturbance spreads from the line of the dislocation with the speed c of a shear wave. For example, (Love 1927, § 213, (iv.)) the displacement around a centre of compression, which in the static case (*ibid.* § 132, (a')) is a pure shear, is propagated entirely with the velocity a of longitudinal waves. However, in the present case the resultant displacement is at all times parallel to the z direction, and independent of z. The dilatation always vanishes, and the disturbance spreads as a shear wave, being first observed when $t-\tau=\rho/c$. Disturbances from different parts of the dislocation line propagated with speeds lying between a and c arrive before this time, but continuously cancel one another.

In synthesizing the displacement, there are three situations to consider.

$t-\tau<\rho/a$: the longitudinal wave from the nearest element of the dislocation has not yet reached $(x, y, 0)$;

$\rho/a\leqslant t-\tau<\rho/c$: the longitudinal wave from the nearest element has arrived, but the shear wave has not ;

$t-\tau\geqslant\rho/c$: the displacement produced by the nearest element has reached its final value.

The displacements u_x and u_y are odd in ζ, and vanish on integration.

In the case $t-\tau<\rho/a$, the expression $t-\tau-r/a$ is negative for every element of the dislocation. It follows from (22) that u_z vanishes.

In the case $\rho/a\leqslant t-\tau<\rho/c$, the expression $t-\tau-r/a$ is negative when $\zeta^2>Z_a^2$ and zero or positive when $\zeta^2\leqslant Z_a^2$, where

$$\rho^2+Z_a^2=a^2(t-\tau)^2. \quad . \quad . \quad . \quad . \quad . \quad . \quad . \quad . \quad (28)$$

The expression $t-\tau-r/c$ is always negative. The contribution of elements with $\zeta^2>Z_a^2$ is zero, and the contribution of the remaining elements is given by (23) and (25) as

$$\frac{4\pi u_z}{bc^2y\delta\xi}=\int_{-Z_a}^{Z_a}\left\{\left(\frac{3}{r^5}-\frac{15\zeta^2}{r^7}\right)(t-\tau)^2+\frac{3\zeta^2}{a^2r^5}-\frac{1}{a^2r^3}\right.$$
$$\left.-2\zeta^2r^{-4}a^{-3}\delta(t-\tau-r/a)\right\}d\zeta, \quad . \quad . \quad (29)$$

where the integral is taken over the closed range. The terms in $\delta(t-\tau-r/c)$ have been omitted, since they vanish in this range. The terms not involving $\delta(t-\tau-r/a)$ are readily integrated, giving $4Z_a/a^5(t-\tau)^3$. The contribution of the δ function from the points $\zeta^2=Z_a^2$ exactly cancels this at all times in the range. There is thus no disturbance until the shear wave arrives.

In the case $t-\tau \geqslant \rho/c$, there is again no contribution from the points with $\zeta^2>Z_a^2$. When $Z_a^2 \geqslant \zeta^2 \geqslant Z_c^2$, the elements contribute according to (23), and when $\zeta^2<Z_c^2$ they contribute according to (24), where

$$\rho^2+Z_c^2=c^2(t-\tau)^2. \quad . \quad . \quad . \quad . \quad . \quad . \quad . \quad . \quad . \quad (30)$$

The contribution from the second region is given by

$$\frac{4\pi u_z}{bc^2y\delta\xi} = 2\int_{Z_c}^{Z_a}\left\{\left(\frac{3}{r^5}-\frac{15\zeta^2}{r^7}\right)[(t-\tau)^2-r^2/a^2]-\frac{12\zeta^2}{a^2r^5}+\frac{2}{a^2r^3}\right.$$
$$-2\zeta^2r^{-4}[a^{-3}\delta(t-\tau-r/a)-c^{-3}\delta(t-\tau-r/c)]$$
$$\left.-r^{-2}c^{-3}\delta(t-\tau-r/c)\right\}d\zeta, \quad . \quad (31)$$

taken over the closed range. The terms not involving δ functions yield

$$\frac{4Z_a}{a^5(t-\tau)^3}-\frac{4Z_c}{c^5(t-\tau)^3}+\frac{2Z_c}{c^3(t-\tau)^3}\left(\frac{1}{a^2}-\frac{1}{c^2}\right).$$

The δ functions yield

$$-\frac{4Z_a}{a^5(t-\tau)^3}+\frac{4Z_c}{c^5(t-\tau)^3}-\frac{2}{Z_cc^3(t-\tau)},$$

and the total contribution from this region is

$$\frac{4\pi u_z}{bc^2y\delta\xi}=\frac{2Z_c}{c^3(t-\tau)^3}\left(\frac{1}{a^2}-\frac{1}{c^2}\right)-\frac{2}{Z_cc^3(t-\tau)}. \quad . \quad . \quad . \quad . \quad (32)$$

The contribution from the region $\zeta^2<Z_c^2$ is given by

$$\frac{4\pi u_z}{bc^2y\delta\xi}=-\int_{-Z_c}^{Z_c}\left\{\frac{3\zeta^2}{r^5}\left(\frac{1}{c^2}-\frac{1}{a^2}\right)+\frac{1}{a^2r^3}\right\}d\zeta$$
$$=-\frac{2Z_c^3}{\rho^2c^5(t-\tau)^3}-\frac{2Z_c}{a^2c^3(t-\tau)^3}. \quad . \quad . \quad . \quad . \quad (33)$$

Adding (32) and (33) gives the total displacement in the region $t-\tau \geqslant \rho/c$ as

$$u_z=-\frac{by\delta\xi}{2\pi\rho^2}\cdot\frac{c(t-\tau)}{[c^2(t-\tau)^2-\rho^2]^{\frac{1}{2}}}. \quad . \quad . \quad . \quad . \quad . \quad (34)$$

As t increases, this tends to the static value given by (15).

In this particular problem the result could be obtained much more easily by noting that the displacement is ultimately equal to (15), and travels as a pure shear wave. This suggests a trial solution of the form

$$u_z=\frac{y}{\rho^2}f\left(\frac{\rho}{ct}\right). \quad . \quad . \quad . \quad . \quad . \quad . \quad . \quad . \quad . \quad (35)$$

The solution must obey the equation

$$\left(\frac{\partial^2}{\partial x^2}+\frac{\partial^2}{\partial y^2}-\frac{1}{c^2}\frac{\partial^2}{\partial t^2}\right)u_z=0, \quad \ldots\ldots \quad (36)$$

which is satisfied if

$$w(1-w^2)f''(w)=(2w^2+1)f'(w), \quad \ldots\ldots \quad (37)$$

where

$$w=\rho/ct. \quad \ldots\ldots \quad (38)$$

The solution of (37) subject to the boundary conditions at $w=0$ and $w=\infty$ leads at once to (34).

The total displacement is

$$u_z=-\frac{by}{2\pi}\int_{-\infty}^{\tau_0}\frac{\xi'(\tau)c(t-\tau)\,d\tau}{\rho^2[c^2(t-\tau)^2-\rho^2]^{\frac{1}{2}}}, \quad \ldots\ldots \quad (39)$$

where τ_0 is given by

$$[x-\xi(\tau_0)]^2+y^2=c^2(t-\tau_0)^2. \quad \ldots\ldots \quad (40)$$

For the particular case of steady motion, $\xi(\tau)=v\tau$, and (39) may be integrated by introducing the variable η, where

$$\cos\eta=\cos\psi/\cos\alpha,$$

$$\sin\psi=\rho/c(t-\tau)$$

and

$$\sin\alpha=vy/c[(x-vt)^2+y^2]^{\frac{1}{2}}.$$

This leads to the known result

$$u_z=-\frac{b}{2\pi}\tan^{-1}\frac{(1-v^2/c^2)^{\frac{1}{2}}y}{x-vt}. \quad \ldots\ldots \quad (41)$$

I am indebted to Dr. J. D. Eshelby for suggesting improvements in the presentation of this paper.

References.

Burgers, J. M., 1939, *Proc. K. Ned. Akad. Wet.*, **42**, 293.

Cottrell, A. H., 1949, *Progress in Metal Physics*, **1**, (London: Butterworth Scientific Publications), p. 77.

Frank, F. C., 1951, *Phil. Mag.*, **42**, 809.

Love, A. E. H., 1904, *Proc. London Math. Soc.* [2] **1**, 291; 1927, *The Mathematical Theory of Elasticity.*

Nabarro, F. R. N., 1951, *Phil. Mag.*, **42**, 213.

Stokes, G. G., 1849, *Trans. Camb. Phil. Soc.*, **9**, 1.

Volterra, V., 1907, *Ann. Ecole. Norm. Supér.* [3] **24**, 400.

CXXIII. *Observations on the Multiple Scattering of Ionizing Particles in Photographic Emulsions.*—Part V. *Scattering Measurements on Tracks of Slow Protons.*

By M. G. K. Menon and O. Rochat,
H. H. Wills Physical Laboratory, University of Bristol*.

[Received May 30, 1951.]

Summary.

The scattering constant has been determined by measurements of the multiple scattering along proton tracks ending in the emulsion. A value of $27{\cdot}8 \pm 0{\cdot}5$ has been obtained (for $\beta^2 \sim 0{\cdot}03$ and an average cell-size of $72\,\mu$).

A simple method involving the combined measurements of multiple scattering and residual range has been used to identify the particles. A parameter $P = 2{\cdot}37 \log \hat{\alpha}_{100\mu} + 1{\cdot}37 \log R$ was determined for each track (R being the range in microns and $\hat{\alpha}_{100\mu}$ the mean angle of multiple scattering—per $100\,\mu$—measured along the faster half of the trajectory); P is a linear function of the logarithm of the mass of the particle. A scale of values of P has been calibrated experimentally using tracks of protons from artificial sources and those of σ-mesons. Using this method tracks of 83 protons have been identified amongst a group of 136 particles of charge $|e|$ ejected from cosmic ray stars. The mean value of P for the 83 protons was found to be $4{\cdot}275 \pm 0{\cdot}013$. The resolution between π-mesons, protons, deuterons and tritons was found to be satisfactory. An appendix gives the coupling matrix calculated for the sagitta method, taking into account the loss of energy.

§ 1. Introduction.

The scattering constant as defined in a previous paper (Gottstein *et al.* 1951) can be determined by measuring the multiple scattering along tracks which end in the emulsion, and which are produced by particles of known mass.

The main advantage of this method is that the value of the initial energy of the particle can be determined reasonably well by measuring its residual range. The inaccuracy inherent in such a range measurement is of the order of 2 per cent—this being the probable error due to straggling (Rotblat 1950). The calculations are more complicated because, in contrast to the normal case in high energy tracks, the energy here can no longer be considered constant in that part of the track used for scattering measurements. The loss of energy along the track by ionization must be taken into account.

* Communicated by Professor C. F. Powell, F.R.S.

In a previous paper, Goldschmidt-Clermont *et al.* (1948) have used a statistical variable ϵ_i defined as the product of each angle α_i by the energy T_i corresponding to the centre of the cell. The mean $|\bar{\epsilon}|$ is a parameter which depends only on the mass of the particle and the scattering constant. In principle, this method enables one to carry on the measurements to the very end of the track—decreasing the cell size as the end is approached, and so increasing the statistical weight of the result. But such a procedure would make it difficult to determine the scattering constant, as energy is lost rapidly towards the end of the track and it is hard to eliminate effectively the Rutherford single scattering from the measurements.

However, if the scattering be measured in a part of the trajectory where the change of energy is not too large, then a constant cell length could be maintained for all the measurements, thereby introducing a simplification into the determination of the parameter ϵ.

In the present investigation, we have arbitrarily limited the scattering measurements to the faster half of the track. In our calculations, the average $\frac{1}{n}\Sigma_i|\alpha_i T_i|$ has been replaced by the statistically equivalent quantity $\left(\frac{1}{n}\Sigma_i|\alpha_i|\right) \times \left(\frac{1}{n}\Sigma_i T_i^{-2}\right)^{-1/2}$. The identical mathematical expectations and the slightly differing variances of these two parameters are indicated in the Appendix.

For the present investigation, we have employed 83 tracks of slow protons which ended in the emulsion. The experimental procedure adopted for identifying the particles producing these tracks is described below.

§ 2. Experimental Procedure.

1. *Selection of Tracks for Measurement.*

One hundred and fifty-four tracks ending in the emulsion, of length greater than 500 μ, originating from cosmic ray stars, have been systematically investigated. Tracks due to particles of charge greater than one (*i. e.* He, Li, Be, . . . nuclei) were identified by visual examination of the track for delta rays (Sorensen 1949, 1951) and by gap measurements (Hodgson 1950). Eighteen such tracks were found amongst the 154 tracks investigated. The remaining 136 tracks judged to be caused by particles of charge one, were used for the range and scattering measurements.

2. *Measurement of Range.*

The tracks were divided into segments of 48 μ and smaller. Horizontal and vertical projections were measured in each segment. In calculating the vertical projection in the unprocessed emulsion a shrinkage factor of 2·5 was adopted. From repeated measurements on the same track the total probable error in these determinations has been found to be less than 1 per cent. Tracks inclined at angles greater than 15° to the surface of the emulsion were not used.

3. *Measurement of Multiple Scattering.*

The first half of the range determined above was used to measure the multiple scattering. This distance was divided into "n" cells, each of size "s". "s" will be referred to as the "primary cell size". The tracks actually measured varied in length from 500μ to about 4000μ, so the numbers "n" and "s" have also varied. "s" was so chosen that "n" was at least equal to 30, the values of "s" being limited to sequence 8, 16, 24, . . . 48μ (8μ being the smallest unit on our eye-piece scale). In one eye-piece we used a scale of 48μ divided into segments of 8μ each, placed parallel to the displacement of the stage. The track was moved in steps of $s\mu$ along this scale. In the other eye-piece and perpendicular to this displacement, we used the scattering scale as described in previous papers. The position of the track was read on this scale at each step.

4. *Calculation of the Mean Angle* $\hat{\alpha}$.

Second differences were computed in cell-sizes which were integral multiples of the primary cell-size. This enabled us to choose the optimum cell length, defined as that for which the $\bar{d}$ has a value greater than four times the total noise in the cell. The noise of the microscope M4074 was determined for different cell sizes by use of a primary track 2 cm. in length, which had a finally determined mean angle of scattering of $0{\cdot}0007°/100\mu$ when measured in 4000μ cells. The results of these measurements have been described in a previous paper (Gottstein *et al.* 1951). Noise elimination as described in previous contributions (Menon *et al.* 1951) cannot be used in this case owing to the simplification we have introduced. A signal to noise ratio of at least four must be maintained to keep the influence of noise on the final result to within a few per cent. The absolute values of the second difference thus obtained were transformed into an angle $\hat{\alpha}$ expressed in degrees per 100μ.

§ 3. Identification of Mass.

Using this angle and the value of the range already measured, we have determined a parameter $P=1{\cdot}37\log R+2{\cdot}37\log\hat{\alpha}$ (R in μ and $\hat{\alpha}$ in degrees/100μ). This parameter is a linear function of the logarithm of the mass of the particle. It has been computed from the range energy relation expressed in the form of a power law $R=E^{1{\cdot}73}\times M$ and from the definition of $\hat{\alpha}$ (see Appendix).

Before P can be employed as a parameter to identify masses of the particles, a scale of values of P must be calibrated for particles of known mass. This calibration has been carried out in the following manner.

We chose twenty-four tracks of σ-mesons which ended in the emulsion and which were longer than 500μ. They have all been attributed to π^--mesons. The possibility that these σ-mesons are due to μ^--mesons is extremely small, for these reasons: the tracks were chosen from plates exposed in balloon flights at 65,000 ft. and 75 per cent of the σ-meson tracks

chosen had produced stars with more than two prongs. It is known that σ-stars produced by μ^--mesons are mostly 1-pronged (George and Evans 1951). The probability of their producing stars with two or more prongs is very small. It is therefore reasonable to assume that almost all the σ-meson tracks are in fact due to π-mesons.

By measuring the range and the scattering in the first half of the trajectory, one may compute a value of P for each of these tracks, and plot them in a histogram as in fig. 1 (A). These values are distributed

Fig. 1.

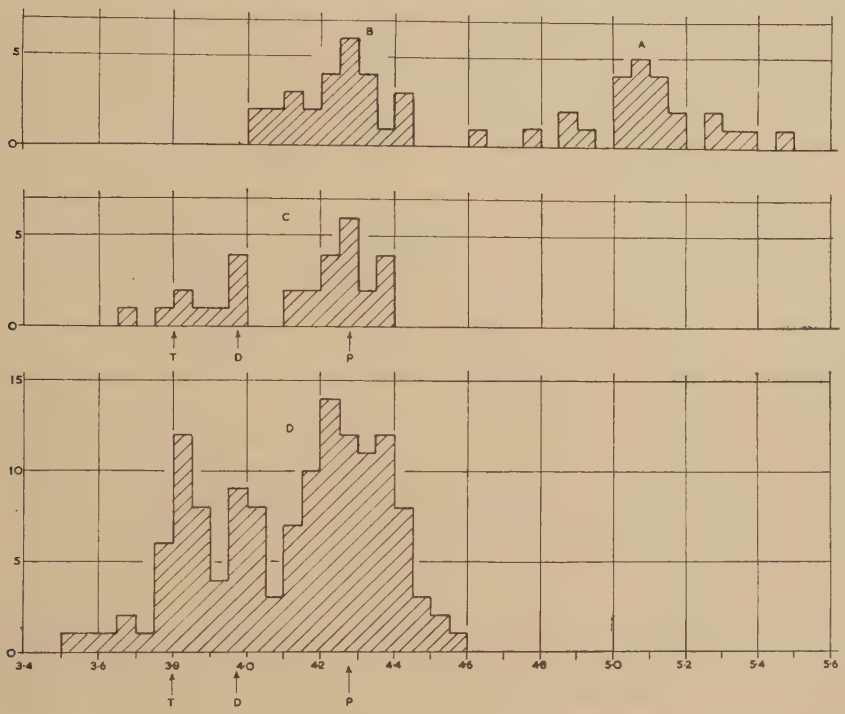

Histogram showing the values of the parameter $P=1{\cdot}37 \log_{10} R+2{\cdot}37 \log_{10} \hat{\alpha}$($\hat{\alpha}$ in °/100μ, R=total range in microns), for:

A—24 tracks of σ-mesons.

B—28 tracks of protons from the N^{14} (d, p) N^{15} reaction.

C—30 tracks identified previously by grain density versus multiple scattering.

D—136 tracks due to particles of charge 1 ejected from cosmic ray stars.

The ordinates give the number of tracks per interval of 0·05 of P.

The arrows, P, D, T, refer to the calculated values of the parameter P for protons, deuterons and tritons, assuming $P_\pi=5{\cdot}1$ and mass of proton/mass of π-meson=6·7.

with mean 5·1. Adopting P=5·1, for π-mesons, and a value 6·7 for the ratio of the mass of the proton to that of the π-meson, values of P for different particles may be calculated as: P(proton)=4.27, P(deuteron)=3·98, P(triton)=3·80.

The values of P(proton) were calibrated experimentally using tracks of protons ($1200\,\mu > \text{range} > 1000\,\mu$ which came to the end of their range in the emulsion) from the reaction $N^{14}(d, p)N^{15}$. The Q value of this reaction is 8·165 MeV. These were obtained in plates exposed to 8 MeV. deuterons in the Liverpool cyclotron. Fig. 1 (B) shows the P values for 28 of these tracks.

To study the overlap of the values P(proton), P(deuteron), P(triton), in a mixed group of particles, the calibration has been extended to include all particles of charge 1, using tracks ending in emulsion of length >3 mm. originating from cosmic ray stars. The particles producing these tracks had been identified in this laboratory, by measurements of the grain density and multiple scattering by Camerini, Fowler, Lock and Muirhead, who have very kindly given us their results. The P values obtained for this group of 30 tracks are shown as a histogram in fig. 1 (C).

We then determined the P values of 136 tracks (previously identified as being due to particles of charge 1). These were from cosmic ray stars in Ilford G5 plates, $400\,\mu$ thick, exposed in a high altitude balloon flight. The P values obtained have been plotted as a histogram in fig. 1 (D). The peak for P(protons) is in agreement with those obtained in fig. 1 (B) and (C). It is also consistent with the value of 4·27 obtained using $P\pi = 5{\cdot}1$ and $m_p/m_\pi = 6{\cdot}7$. Corson (1951) has made a plot of the parameter $p = \langle \alpha(x) \,.\, R^{0{\cdot}58}/\sqrt{x} \rangle_{av}$, where x and R (the cell-size and range respectively) are expressed in units of $100\,\mu$. He obtains a value of $\bar{p} \sim 5{\cdot}9$ for 76 proton tracks. Our results similarly plotted, give $p \sim 5{\cdot}6$. The agreement may in fact be even better than these figures show, since Corson remarks that since he uses a cell of $20\,\mu$ for a range of $500\,\mu$ his values are perhaps a little large, owing to noise introduced into the measurements.

To determine the scattering constant, we have taken the group lying between $4{\cdot}05 < P < 4{\cdot}60$ as protons. A certain number of protons which exhibit low multiple scattering would have been lost in the deuteron and triton peaks. On the other hand, the proton group will contain a certain number of deuterons and tritons as impurity. The magnitude of such contamination is less than 10 per cent, and its effect on the determination of the scattering constant will be very small.

§ 4. Determination of the Scattering Constant.

Using the identified group of slow protons, a plot has been made of $\log \hat{\alpha}$ against $\log R$. This is shown in fig. 2. The best line fitted to these points gives a slope of $-0{\cdot}554 \pm 0{\cdot}011$ (the error being the probable error). This value is in good agreement with that obtained (0·578) for the range-energy relation by more accurate methods. However, as the linearity of the regression line is not certain in the region considered, the scattering constant has been finally determined as shown in Table I.

The points on the $\log \hat{\alpha}$-$\log R$ plot (fig. 2) have been divided into groups using equal intervals of 0·1 along the $\log R$ axis. The coordinates of the

centres of gravity of these groups are given in columns 1 and 2 of Table I. Column 3 gives the effective range (=·72 R—see Appendix) and column 4 the corresponding energy as obtained from the range energy relation (Rotblat 1951, Catala and Gibson 1951, Bradner *et al.* 1950).

Fig. 2.

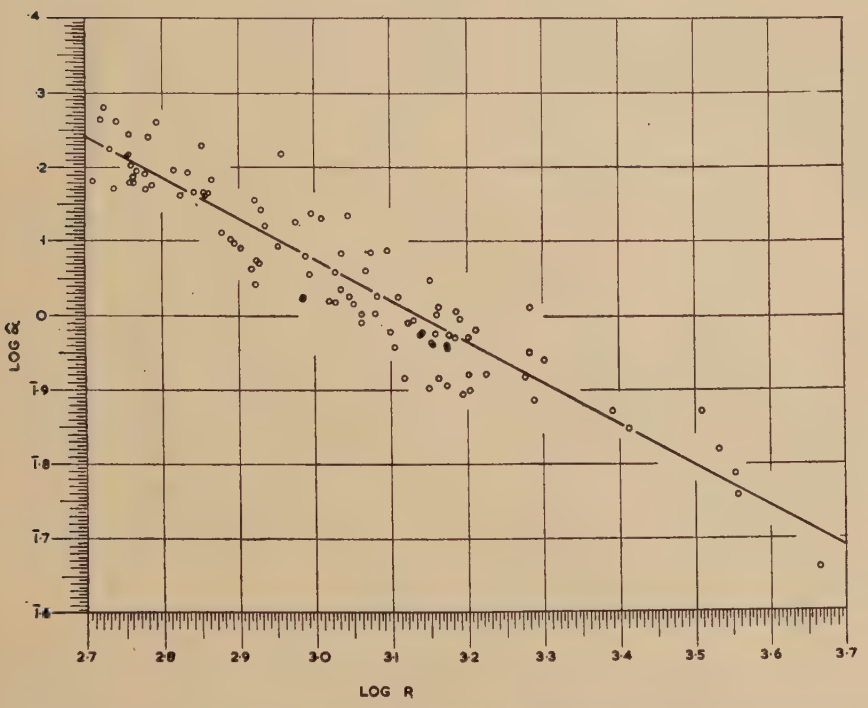

Plot of $\log_{10} \hat{\alpha}_{100\mu}$ versus $\log_{10} R$ for tracks having values of the parameter P in the interval $4{\cdot}05 < P < 4{\cdot}60$. The best line fitted to these points has a slope $-0{\cdot}554 \pm 0{\cdot}011$.

TABLE I.

log R	log $\hat{\alpha}$	$R_{eff} = 0{\cdot}72$ R	$T(R_{eff})$ in MeV.	$T(R_{eff}) \times \hat{\alpha}$
2·758	0·215	413	8·50	13·99
2·857	0·166	518	9·75	14·29
2·951	0·093	643	11·00	13·63
3·053	0·056	814	12·56	14·29
3·152	$\bar{1}$·965	1022	14·25	13·15
3·235	$\bar{1}$·944	1237	15·90	13·99
3·333	$\bar{1}$·902	1550	18·00	14·36
3·412	$\bar{1}$·845	1859	20·00	14·00
3·579	$\bar{1}$·765	2731	25·00	14·54
3·665	$\bar{1}$·658	3329	28·00	12·74

The product $\hat{\alpha}T(R_{eff})$ (which is equal to half the scattering constant in the units described previously) is given in column 5—the mean value of which is $13{\cdot}9 \pm 0{\cdot}25$. The final value of the scattering constant as thus obtained is $27{\cdot}8 \pm 0{\cdot}5$ (the errors given being the standard deviation).

Acknowledgments.

We are indebted to Professor C. F. Powell, F.R.S., for extending to us the hospitality and facilities of this laboratory. We would like to express our thanks to Miss R. Mitchell and Mrs. S. Rochat for their assistance with the scattering measurements. We are also thankful to Dr. W. M. Gibson for providing us with the proton tracks from plates exposed in the Liverpool cyclotron.

APPENDIX.

Approximation Involved in Calculating $|\hat{\alpha}|_{100\mu}$.

The n-dimensional distribution function of successive angles measured on the track between the points of residual ranges R_0 and R_n is characterized by a square matrix (A_{ik}). Its elements A_{ik} are equal to the quantities $\overline{\alpha_i \alpha_k}$—this being the expectation of the product of the ith angle by the kth.

These elements may be calculated using the range energy relation $T = K_a R^m$ in the case of the coordinate method, following Molière's theory (1951). Making the non-relativistic approximation $T\frac{2+\sigma}{1+\sigma} = 2T$, ($\sigma$ being the kinetic energy in terms of the rest mass) we obtain

(see equation, p. 1239).

In the present experimental investigation none of these terms exceeds 0·01. For the following argument they may be neglected.

The experimental procedure as described consists in calculating the arithmetic mean of " n " successive angles. This quantity being taken as proportional to the r.m.s. value, we may set

$$|\hat{\alpha}|_s = \frac{1}{n}\Sigma_i |\alpha|_i \sim \sqrt{\left(\frac{1}{n}\Sigma \alpha_i^2\right)}. \quad \ldots\ldots (2)$$

By definition, the expectation of the last term in (2) is given by

$$\sqrt{\left(\frac{1}{n}\Sigma_{ik} A_{ik}\delta_i^k\right)} = \frac{K_1}{2K_a}\sqrt{s}\sqrt{\left(\frac{\pi}{2}\right)}\sqrt{\left(\frac{1}{n}\Sigma_i R_i^{-2m} \ldots (1+\ldots)\right)}. \quad (3)$$

If we replace, in the square root, the Σ by the integral we get finally

$$|\hat{\alpha}|_s = \frac{K_1}{2K_a}\sqrt{s}\sqrt{\left(\int_{R_0}^{R_n} \frac{dR}{(R_0 - R_n)} . R^{-2m}\right)}. \quad \ldots\ldots (4)$$

Introducing

$$|\hat{\alpha}|_{100\mu} = \tfrac{1}{2}K_1/T_{(R_{eff})} = \frac{1}{2}\frac{K_1}{K_a} R_{eff}^{-2m}, \quad \ldots\ldots (5)$$

$$A_{ik}=s\left(\frac{K_1}{2K_a}\right)^2\cdot\frac{\pi}{2}\begin{bmatrix} R_1^{-2m}(1+\delta_1) & 0{\cdot}25\left(R_1-\frac{s}{2}\right)^{-2m}(1+\epsilon_1) & 0 & 0 \\ 0{\cdot}25\left(R_2+\frac{s}{2}\right)^{-2m}(1+\epsilon_2) & R_2^{-2m}(1+\delta_2) & 0{\cdot}25\left(R_2-\frac{s}{2}\right)(1+\epsilon_2) & 0 \\ 0 & (1+\epsilon_3).0{\cdot}25\left(R_3+\frac{s}{2}\right)^{-2m} & R_3^{-2m}(1+\delta_3) & (1+\epsilon_3)0{\cdot}25\left(R_3-\frac{s}{2}\right)^{-2m} \\ \cdots & \cdots & \cdots & \cdots \\ 0 & (1+\epsilon_i).0{\cdot}25\left(R_i+\frac{s}{2}\right)^{-2m} & R_i^{-2m}(1+\delta_i) & (1+\epsilon_i)0{\cdot}25\left(R_i-\frac{s}{2}\right)^{-2m} \end{bmatrix} \quad . \; . \; . \; (1)$$

R_i=residual range corresponding to the angle α_i, s=cell length.

K_1=scattering constant as defined in Gottstein *et al.* (1951); the change of the "logarithmic" term with range has been neglected here.

K_a=constant of the range energy relation.

The values of δ_i and ϵ_i are respectively $\delta_i=\frac{m(2m+1)}{10}\left(\frac{s}{R_i}\right)^2$ and $\epsilon_i=\frac{3m(2m+1)}{10}\left(\frac{s}{R_i}\right)^2+$ term in $\frac{s^3}{R^3}$.

we define an effective range

$$R_{eff}=\left[\frac{1}{R_0-R_n}\int_{R_n}^{R_0}\frac{dR}{R^{2m}}\right]^{1/-2m} \quad . \quad . \quad . \quad . \quad . \quad . \quad (6)$$

For

$$R_0=2R_n \quad \text{and} \quad m=0{\cdot}578, \quad R_{eff}=0{\cdot}72R_0.$$

The scattering constant will then be obtained from (5)

$$\frac{K_1}{2}=|\hat{\alpha}|_{100\mu}T_{(R_{eff})}. \quad . \quad . \quad . \quad . \quad . \quad . \quad . \quad (7\,a)$$

It is clear that $\frac{K_1}{2}$ is also the expectation of the quantity $\frac{1}{n}\Sigma_i|\alpha_i|T_{i(R_i)}$

$$\frac{K_1}{2}=\frac{1}{\sqrt{s}}\cdot\frac{1}{n}\Sigma|\alpha|_i T_{i(R_i)}. \quad . \quad . \quad . \quad . \quad . \quad . \quad (7\,b)$$

Thus this simplified method yields the same results as the more precise one in which each angle is multiplied by the corresponding energy.

The variance $\left(\frac{\delta K_1}{K_1}\right)$ for (7 *a*) is

$$\frac{\delta K_1}{K_1}=\sqrt{\left[\frac{\left(1+\frac{2}{16}\right)\int_{R_0}^{R_n}R^{-4m}\frac{dR}{R_n-R_0}}{2n\left(\int_{R_0}^{R_n}R^{-2m}\frac{dR}{R_n-R_0}\right)}\right]}=\frac{76{\cdot}5}{\sqrt{n}}\ \text{per cent}, \quad . \quad . \quad (8\,a)$$

whereas for the estimate given by (7 *b*) it is

$$\frac{\delta K_1}{K_1}=\sqrt{\left[\frac{\left(1+\frac{2}{16}\right)}{2n}\right]}=\frac{74}{\sqrt{n}}\,\text{per cent}. \quad . \quad . \quad . \quad (8\,b)$$

The variance given in (8 *a*) would be greatly increased in comparison with that in (8 *b*) if larger portions of the track were used.

References.

Bradner, Smith, Barkas and Bishop, 1950, *Phys. Rev.*, **77,** 462.

Catala and Gibson, 1951. *Nature, Lond.*, **167,** 553.

Corson, 1951 (private communication).

George and Evans, 1951, *Proc. Phys. Soc.* A, **64,** 193.

Goldschmidt-Clermont, King, Muirhead and Ritson, 1948, *Proc. Phys. Soc.*, **61,** 183.

Gottstein, Menon, Mulvey, O'Ceallaigh and Rochat, 1951, *Phil. Mag.*, **42,** 708.

Hodgson, 1950, *Phil. Mag.*, **41,** 725.

Menon, O'Ceallaigh, and Rochat, 1951, *Phil. Mag.*, **42,** 932.

Molière, 1951, *Z. Natur.* (in course of publication).

Rotblat, 1950, *Nature, Lond.*, **165,** 387 ; 1951, *Ibid.*, **167,** 550.

Sorensen, 1949, *Phil. Mag.*, **40,** 947 ; 1951, *Ibid.*, **42,** 188.

CXXIV. *Nuclear Transmutations Produced by Cosmic-Ray Particles of Great Energy.*—Part VI. *Experimental Results on Meson Production.*

By U. Camerini*, J. H. Davies, P. H. Fowler, C. Franzinetti†, H. Muirhead‡, W. O. Lock, D. H. Perkins and G. Yekutieli§,

H. H. Wills Physical Laboratory, University of Bristol||.

[Received July 30, 1951.]

[Plates XLII.–XLIV.]

Summary.

An analysis has been made of the secondary particles ejected from nuclear disintegrations observed in electron sensitive emulsions exposed to the cosmic radiation at 68,000 ft. Scattering and grain density measurements have been carried out on the tracks of 2000 particles associated with these stars. In addition, the grain density and angular distribution of 3070 shower particles and 1508 " grey " tracks have been measured.

For 200 stars, the energy of the primary particle which produced the disintegration was measured. A detailed analysis was made of such events. Single fast π-mesons of kinetic energy less than 1 BeV. are found to interact strongly with nuclear matter.

An estimate of the frequency of occurrence of neutral mesons was made from a consideration of the energy balance in stars of low multiplicity, n_s.

§1. Introduction.

In Parts I. to V. of the present series of papers a description has been given of the disintegrations produced in photographic emulsions by the high energy protons, neutrons and α-particles of the cosmic radiation. Parts I. and II. contained a phenomenological description of the principal features of the disintegrations observed at an altitude of 11,000 ft., and above 50,000 ft.; in Parts III. and IV. it was shown that a large proportion of the shower particles were π-mesons, which interact strongly with nuclei, and their distribution in energy was determined; and in Part V. evidence was given that neutral π-mesons are emitted, together with the charged π-particles, in the " showers ", that they have a lifetime less than 10^{-13} secs., and that their decay into two *quanta* gives rise to most of the soft component of the cosmic radiation.

In this and the final paper which follows, Part VII., an attempt has been made to elucidate the nature of the physical processes which occur within the nucleus under bombardment by energetic protons, processes which

* Now at the University of Rio de Janeiro, Brazil.
† Now at the University of Rome.
‡ Now at the University of Glasgow.
§ On leave from the Hebrew University, Jerusalem.
|| Communicated by Professor C. F. Powell, F.R.S.

result in the production of the " showers " of mesons, and nuclear fragments. This first paper contains a description of observations on 15,000 nuclear disintegrations recorded in plates " exposed " at 68,000 ft. In about 200 stars, the observed track of the primary particle which produced the disintegration was long enough to allow the energy to be determined. For such events a much more detailed analysis has been possible.

Part VII. contains an analysis of the new experimental material. In approaching the problem, it is assumed that the disintegrations can be described in terms of a succession of two-body interactions occurring in the nucleus (nucleon–nucleon and meson–nuclean) which can lead, if the interacting particles are sufficiently energetic, to the creation of π-particles. Recent observations, in this and other laboratories (O'Ceallaigh 1951, Fowler *et al.* 1951) strongly suggest that in the nuclear interaction of protons and neutrons of energy $\geqslant 10$ BeV. the production of more massive mesons may become important. But at the rather lower energies, <10 BeV., with which we have been mainly concerned, any such process, and those involving the creation of pairs of nucleons, if they occur, can hardly play an important role.

§ 2. Nomenclature.

In describing the observations, it will be convenient to adopt the nomenclatures given in Part I. A closer analysis has been found desirable, however, in the case of the more heavily ionizing particles. The tracks produced by the particles emerging from nuclear disintegrations are therefore divided into three classes :—

(i.) *Tracks of " shower " particles.* These are tracks in which the grain-density, g, is less than 16 grains per 50μ ; in the conditions of the experiment, this value corresponds to a particle with the electronic charge and a specific ionization less than 1·4 times the minimum value, i min. The great majority of such tracks are produced either by π-mesons of energy greater than 80 MeV., or by protons of energy greater than 500 MeV. The total number of such tracks associated with a given " star " is denoted by n_s.

(ii.) " *Grey* " *tracks.* These are tracks with a grain density in the interval from 16 to 80 grains per 50 μ, and their number for any star is represented by N_g. They can be produced by protons with energy in the interval from 25 to 500 MeV. Only a very small proportion of the protons emitted during the " evaporation " of highly excited nuclei have energies as great as 25 MeV. Most of the " grey " tracks are therefore due to protons, recoiling from fast nucleons and produced at an early stage of the disintegration. Some, however, are due to deuterons and tritons, and about 18 per cent to π-mesons of energy less than 80 MeV.

(iii.) " *Black* " *tracks.* These tracks have a grain density greater than 80 grains per 50 μ, and their number is denoted by N_b. They are due to protons of energy less than 25 MeV. : to deuterons and tritons of energy

less than 50 MeV. and 75 MeV., respectively ; and to α-particles less than 800 MeV.

The sum N_g+N_b is represented by N_h. A " star " is characterized in terms of N_h+n_s together with a suffix to denote the nature of the particle producing the disintegration ; viz., n, p, π, α—for neuton, proton. π-meson or α-particle respectively. Stars with $n_s \geqslant 2$ are referred to as " showers ".

§ 3. Scope of the Observations.

In an examination of 87 c.c. of emulsion, 15,300 nuclear disintegrations or " stars " were observed. Measurements of scattering and grain density were made on 2000 of the tracks associated with these stars, the only criterion for selection being that the track, in the emulsion, was longer than 3 mm.

Measurements of grain density and of the angular distribution of the ejected particles were also made on the tracks of 3070 shower particles, and 1508 grey tracks including those which were shorter than 3 mm. In addition, all stars in which the track of the primary particle was long enough to allow the energy to be determined, were analysed in detail.

§ 4. Composition of Stars.

The distribution of the 15,300 nuclear disintegrations according to the number of shower particles, n_s, and the number of heavily ionizing particles, N_h, is shown in Table I. The results given are those recorded by the observers ; but a more detailed study of individual stars, selected at random, indicated that the errors in the observations of both N_h and n_s were small.

It will be convenient to describe first the distributions in the values of the energy, mass and angular distribution of the different types of secondary particles; and where possible, the variation of these quantities with the star parameters N_h and n_s.

4.1. " *Shower Particles* ".

Of the 2000 tracks for which the scattering parameter $\bar{\alpha}$ was determined, 470 were shower particles. These were sub-divided into three groups—according to whether they could be identified as mesons, or protons ; or whether their nature was uncertain. We denote particles of the three types by the symbols π_s, p_s and π, p, respectively.

π_s. Mesons with kinetic energy in the interval from 80 to 1100 MeV. The particles in this group constitute about 60 per cent of the total number of shower particles.

p_s. Protons of energy between 500 and 800 MeV. (20 per cent of the total).

π, p. Particles with a mean angle of scattering, $\bar{\alpha}$, less than 0·0226 degrees per 100 μ. For such particles, the grain density in the tracks, both of mesons and protons, is equal to the minimum value, and the two types of particle cannot be distinguished in the conditions of the experiment. (20 per cent of the total.)

The distribution in energy of the π_s particles for stars of different types indicates that there is no significant dependence on either N_h or n_s. In other words, the energy distribution of the mesons is nearly the same for disintegrations in which a heavy nucleus of silver and bromine is completely

TABLE I.

ANALYSIS OF 15,300 STARS OBSERVED IN PLATES FLOWN AT 68,000 FT. N_h = NUMBER OF HEAVILY IONIZING PARTICLES ($g > 1.5 g_{min}$); n_s = NUMBER OF SHOWER PARTICLES ($g < 1.5 g_{min}$).

N_h / n_s	3	4	5	6	7	8	9	10	11	12	13	14	15	16	17	18	19	20	21	22	23	24	25	26	27	28	29	>30	Totals.
0 n	2499	2132	1499	938	576	367	238	169	124	100	89	67	47	37	29	14	18	11	7	3	4	1	1	3	2	1		1	8977
p	225	310	356	305	204	137	116	92	75	45	49	53	32	32	22	12	10	11	9	8	3	2	4	1	1	1	1		2117
1 n	133	194	195	199	128	97	88	63	51	53	28	34	23	13	25	15	18	3	8	1	2	1	1	2	1	1		1	1378
p	91	146	151	135	96	79	52	50	44	36	28	25	24	15	15	5	11	6	10	5	1	8	6	3	2	3		3	1063
2 n	33	36	44	51	37	26	26	23	20	17	16	27	17	15	15	9	3	4	2	7		1	2	1		2		3	437
p	24	42	28	49	32	24	29	29	22	20	20	23	20	10	13	7	7	7	3	8	1	2	3	2	1	1		2	424
3 n	9	5	8	7	6	10	5	4	4	5	2	5	2	2		1	2		1		2				2			1	83
p	13	15	25	17	14	14	12	12	18	10	11	16	12	7	1	7	4	5	2	1	1	6	2	1	1				229
4 n	3	6	7	6	7	2	6	2	2	2	1	4		2		3	1		2	1	1	1		1	1	1		1	61
p	3	11	15	11	11	9	9	10	5	4	6	2	5	6	8	1	4	5	4	2	5	4	2	3	3		1		148
5 n	3	2	1	4	3	1	1	5	1	4	2		1			4	1	1	1		1			2					37
p	8	5	8	9	7	5	6	6	5	5	2	4	4	4	3	2	1	2	2	1	1	3	1	1	1	1			97
6 n		2		3	4	1	3	1	1		5	1	2	1		1		1	1	2		2		1					28
p	5	5	3	7	5	2	5	2	2	5	2	6	2	1	3	4	1	1	3	3	1	1		1					68
7 n												1	1		2													6
p	1	2	1	2	2	1	3	4		5		2	6		1	1	1		1	2				2		1	2		39
8 n				1		2											1												4
p			2	1	4		1	3	3	3		1	1	2	1	2	1		1	2	3	2			1				34
9 n		1		1		1								1														6
p	1	1	1	2		1	1			1				2				1						3	1		1		14
10n														1			1												4
p		2	1		2		1				1	1		1		1			1	1	2		1						13
11n										1																			0
p					1			3					1			1													6
12n																													0
p					1								1							1									3
13n																													0
p				1		1	1					2		1		1				1		1							9
14n										1																			1
p																													0
>15n																1	1	2	2	1	1	1							3
p			1	1		1								2		1	1	1	1	1	1	1							11

Grand Total :- 15,300

disrupted [as for those in which only a few heavily ionizing particles emerge, many of which are due to the disruption of light elements such as carbon or oxygen ; and it is the same for " showers " in which many mesons are created as for those in which there are only a few. This feature

is displayed in Table II., which shows values of the average kinetic energy of the particles for stars with different values of N_h and n_s. It may be emphasized that although we are delaing here with the low-energy end of the energy spectrum of the ejected mesons, it contains more than 60 per cent of all these particles produced in the disintegratons.

TABLE II.

Average kinetic energy of the π-mesons of energy E, where 1100 MeV $>$ E $>$ 80 MeV for stars of different types.

n_s	1	2–4	5–∞
E	385$\pm$40	340$\pm$35	395$\pm$40
N_h	3–8	9–14	15–∞
E	385$\pm$45	360$\pm$40	360$\pm$30

A similar analysis of the distributions in energy of the protons, p_s, and unidentified particles, (π, p), is subject to large statistical errors, but the results are given in Tables III. *a* and III. *b*. These show the proportions of protons and unidentified particles, (π, p), among the shower particles of all types, for different kinds of stars. The most important fact established by the results is that the proportion of these energetic particles (π, p) is greater for large than for small showers. If we consider all the stars in which a given number of shower particles, n_s, is produced the proportion of fast shower particles (π, p) is greater for the small than for large values of N_h.

TABLE III. *a*.

Number of π-p particles per shower particle.

		N_h 3–8	N_h 9–∞	N_h 3–∞
n_s	1	0·15$\pm$0·04	0·09$\pm$0·05	0·13$\pm$0·03
n_s	2–4	0·22$\pm$0·05	0·22$\pm$0·05	0·22$\pm$0·03
n_s	5–∞	0·41$\pm$0·09	0·14$\pm$0·04	0·23$\pm$0·04
n_s	1–∞	0·23$\pm$0·03	0·16$\pm$0·02	0·20$\pm$0·02

TABLE III. *b*.

Number of proton shower particles per shower particle.

		N_h 3–8	N_h 9–∞	N_h 3–∞
n_s	1	0·21$\pm$0·04	0·18$\pm$0·06	0·20$\pm$0·04
n_s	2–4	0·16$\pm$0·04	0·13$\pm$0·04	0·14$\pm$0·04
n_s	5–∞	0·05$\pm$0·03	0·12$\pm$0·03	0·10$\pm$0·03
n_s	1–∞	0·16$\pm$0·03	0·13$\pm$0·02	0·14$\pm$0·02

We shall see later that the first of these facts is a simple consequence of the greater average energy of the primary particles of stars with greater multiplicity ; and that the second is due to secondary interactions and loss of energy of the shower particles in escaping from the nucleus in which they are produced.

In order to calculate the average energy required to produce the π, p particles, it is necessary to make assumptions about the proportions of π-mesons and protons among them. This has been done in the following way : the energy spectrum of the μ-mesons in the cosmic radiation, most of which are produced by the decay in flight of π-particles, has been determined by Sands (1950). From this spectrum, the energy distribution of the parent π-particles can be computed ; and thence, from the low energy distribution of π-mesons observed in the present experiments, the total number to be expected among the (π, p) particles can be calculated. The result is about two-thirds of all the (π, p) particles, and the rest are therefore attributed to protons. Assuming that this proportion is constant for stars of all types, the average energy of a (π, p) particle is found to be 1930 MeV.

Using this value, and taking into account the rest-energy of the π-particles, the average energy of the shower particles can be found for stars of different types. The results are shown in Table IV. : they reflect the different proportions of fast shower particles (π, p) in different kinds of stars.

TABLE IV.

Average total energy of shower particles ($\pi_s+p_s+\pi$, p) as a function of N_h and n_s.

n_s	1	2–4	5–∞
E	750$\pm$40 MeV	850$\pm$40 MeV	910$\pm$45 MeV
N_h	3–8	9–14	15–∞
E	855$\pm$40 MeV	775$\pm$55 MeV	730$\pm$45 MeV

4.2. *Angular Distributions.*

The angular distribution of the shower particles with respect to the line of motion of the charged primary particles has been determined by observations on more than 1000 " stars ". The results have been separated into a number of classes according to the characteristics of the stars and are shown in figs. 1 and 2. Most of the shower particles are emitted in directions making angles, θ, less than 40° with that of the primary particle, but some are ejected backwards, $\theta > 90°$. The angular distribution of the backward-moving particles is nearly isotropic.

Fig. 1 shows that the " width " at half-maximum of the angular distributions decreases—but only very slowly—as n_s, the number of shower particles in a star increases ; fig. 3 shows the variation with multiplicity, n_s, of the median angle of the distribution, η, for stars of a given type. The observations can be easily interpreted in terms of the increase of the average energy of the primary particles required to produce stars of increasing multiplicity. This involves an increase in the velocity of the C-system of the interacting nucleons, and therefore an increasing tendency for the mesons to be thrown forward, in the L-system, in directions near that of the primary particle.

The "half-widths" of the angular distributions increase with the value of N_h (fig. 3), an effect which can be interpreted in terms of interactions of the shower particles with the parent nucleus. Such interactions will contribute, first, to excitation energy of the nucleus, and thus to the

Fig. 1.

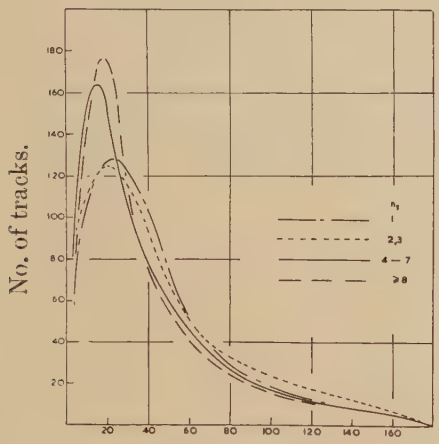

The angular distributions of shower particles in the laboratory system for different ranges of multiplicity. The ordinate gives the number of tracks per angular interval.

Fig. 2.

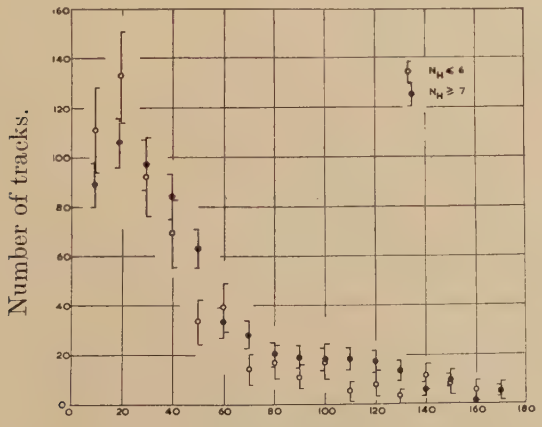

The angular distribution of shower particles for stars of $N_h \leqslant 6$ and $N_h \geqslant 7$.

completeness of the disintegration of the nucleus, *i. e.* to an increase in N_h, and, secondly, to a scattering of the emerging mesons, and so to the breadth of the angular distributions.

The fraction of the shower particles projected at angles greater than 90° to the direction of the primary, is denoted by B. Observations on

this quantity also have an important bearing on the question of secondary interactions of the shower particles in escaping from the parent nucleus, and it will be convenient to refer to it as the " backward fraction ". As shown in fig. 4, it decreases only slowly with increase in the value of n_s, the multiplicity of the star. There is, however, a strong dependence on N_h. Thus, taking all stars with shower particles, $n_s \geqslant 1$, the value of B is equal to $0{\cdot}113 \pm 0{\cdot}016$ for $N_h \leqslant 7$; and to $0{\cdot}171 \pm 0{\cdot}012$ for $N_h > 7$. Almost all stars for which $N_h > 7$ must be due to the disintegration of the heavy elements in the emulsion, silver and bromine ; and also some, at least, of those for which $N_h \leqslant 7$. It follows that the ratio of the backward fraction due to the disintegration of the heavier elements, B_H, to that for the lighter elements, B_L, must be greater than $17{\cdot}1/11{\cdot}3$, *i. e.* $B_H/B_L > 1{\cdot}5 \pm 0{\cdot}24$.

Fig. 3.

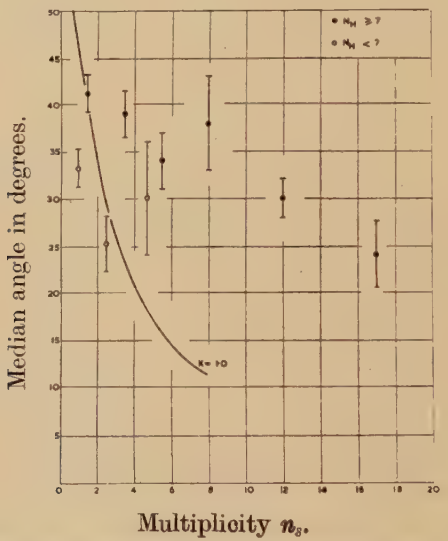

The variation of the median angle of the showers with the multiplicity, for stars of $N_h \geqslant 7$ and $N_h < 7$. The curve shows the variation expected on the assumption of multiple production in a single nucleon–nucleon collision ($K = 1{\cdot}0$).

4.3. " *Grey* " *Tracks.*

The grey tracks are due almost entirely to protons, deuterons and tritons, and the results of a study of the distribution in energy and the relative proportions of the different types of particles have been given in Part IV. These quantities appear to be constant for stars of different types, with the exception of type O_n, and fig. 5 shows their average number per star for different values of n_s.

From a knowledge of the number and the average kinetic energy of the particles producing the " grey " tracks the average energy required to produce the heavily ionizing particles which appear as " grey " and

" black " tracks has been calculated. Following the procedure described in Part I. (Brown *et al.* 1949) the total energy E_{N_h} of these particles, including neutrons of the same speeds, may be calculated. The results may be expressed by the realtion :—

$$E_{N_h}=f(N_h)=155\ N_h-100\ \text{MeV}.\ (N_h>1).$$

This formula applies for stars of all types with the important exception of type $O_{\prime\prime}$. The formula given in Part I., viz : $E_{N_h}=37N_h+4N_h^2$, was obtained using a selection of stars which were predominantly type $O_{\prime\prime}$ for low values of N_h.

Fig. 4.

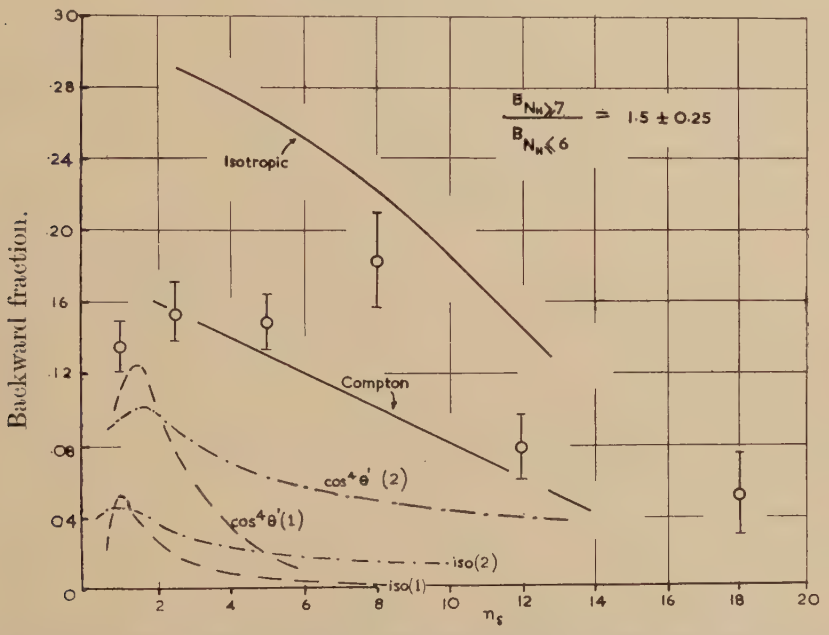

The variation of backward fraction with multiplicity. Experimental points ⊼. Curves marked "iso" calculated variation on the assumption of pure multiple production with isotropic angular distribution of the mesons in the C-system of the colliding nucleons for (1) and (2) generations. " $\cos^4\theta'$ " variation calculated on the assumption of an angular distribution in the C-system of form $\cos^4\theta'\sin\theta' d\theta'$. The full line curves indicate the fraction projected backward on the assumption that each meson is elastically scattered by a nucleon in its exit through the nucleus, either by Compton-type scattering, or by scattering isotropic in the C-system of meson and nucleon, with cross-section independent of energy.

The angular distributions of the particles which produce the grey tracks, divided into three groups according to the energies of the particles, are shown in fig. 6. The observed tendency for the fast protons to be emitted at only small angles to the direction of motion of the primary particle is in accord with the results of Crussard (1950), Harding (1951) and Osborne (1951).

4.4. " *Black* " *Tracks.*

The " black " tracks are emitted almost isotropically, and their observed energy " spectrum " is consistent with the view that they arise as a result of the evaporation of the nucleons from a highly excited nucleus (Harding, Lattimore and Perkins 1949).

§5. Stars Produced by Primary Particles of Known Energy.

In analysing the experimental material, a track has been identified as due to a singly-charged primary particle producing a star if it satisfies the following conditions :—

(1) Its grain-density must be less than 16 grains per 50 μ.

(2) The track must be in the upper hemisphere.

Fig. 5.

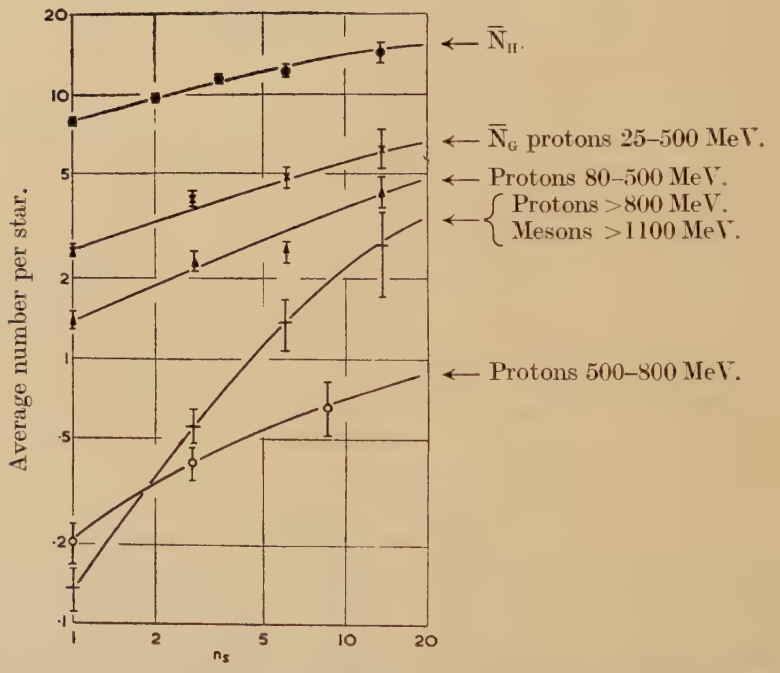

Variation with multiplicity of the number of protons and mesons of different energies and of the number of heavily ionizing particles N_h.

(3) For stars of higher multiplicity, $n_s > 2$, the track of the particle assumed to be the primary must be not widely inclined to the average direction of the secondary shower particles.

(4) The energy of the assumed primary particle, if measurable by the scattering method, must be sufficiently great to have produced the star and the shower particles.

Of 2000 tracks on which scattering measurements and grain counts have been made, 200 satisfied these conditions.

It is well known that mesons produced in nuclear interactions may be emitted backwards, the direction of motion being nearly opposite to that of the parent particle. It is therefore possible to make errors of identification and to attribute a track to a primary particle when it was, in fact, due to an ejected meson—the true primary particle being a neutron. Such errors are most serious in the case of stars of low multiplicity. A star produced by a fast neutron in which a single fast meson is ejected vertically upwards, type 1_n, may be wrongly classed as of type 0_p. The proportion of such errors can be estimated in the following ways :—

Fig. 6.

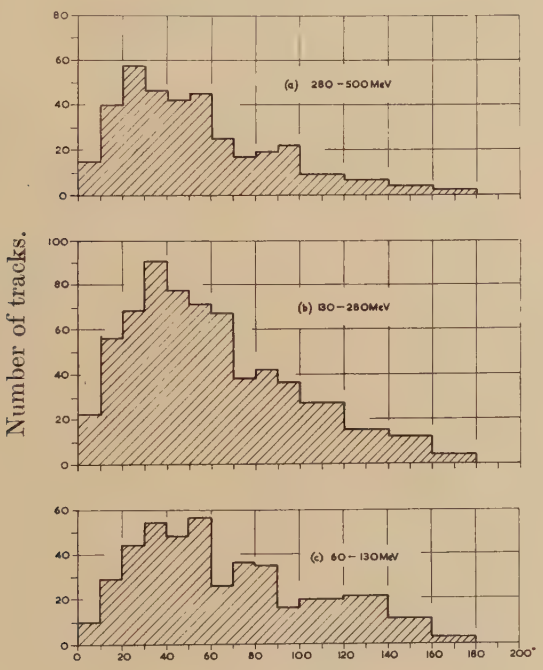

The angular distribution of the " grey " protons as a function of energy.

The fraction of secondary shower particles from stars of type 1_p which have directions of motion in the upper hemisphere, is found to be 0·15. If it is assumed that the angular distribution of the secondary fast particles produced in stars of type 1_n is similar to that in type 1_p, then it follows that only 10 per cent of the " primary " particles of stars of type 0_p are, in fact, secondary particles. The probability of wrongly identifying a charged primary particle in events from which several shower particles are emitted is small, because the average energy of " backward " moving shower particles is low so that the scattering measurements prove them to be insufficiently energetic to have produced the star.

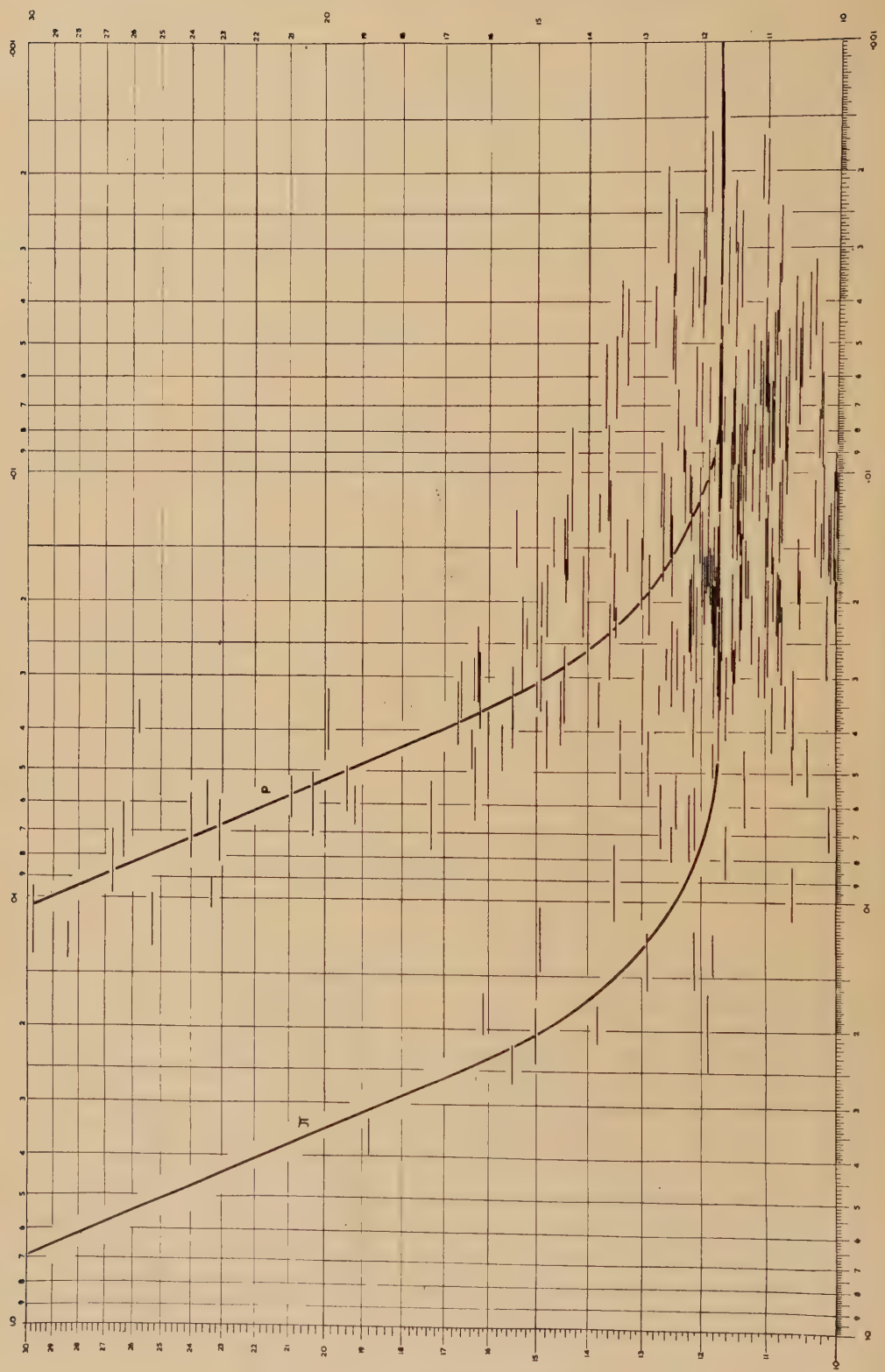
Grain density—grains per 50 microns.
Mean deviation $\bar{a}$ in degrees per 100 microns.
p
π

Fig. 7.

A plot of the values of g and $\bar{\alpha}$ for all the track of " primary " particles identified by these criteria is shown in fig. 7. The distribution in energy of the particles—deduced from the results shown in fig. 7, after correction for geometrical factors and with the assumption that all the fastest particles (π, p) are protons, is represented in fig. 8.

It is possible to determine directly the distribution in energy of the π-mesons among the primary particles in the interval $<10^3$ MeV. Extrapolating the results to greater energies, it was found that only about 15 per cent of the fast primaries (π, p ; E $<1{\cdot}2$ BeV.) are due to π-mesons. A second estimate of this ratio was obtained by the following method :—

The energy spectrum of the secondary (π, p) particles is known, and the cross-section for their interaction with nuclei is close to the geometrical value. It is therefore possible to estimate how many of the high energy

Fig. 8.

Integral spectrum of " primary " protons and π-particles.

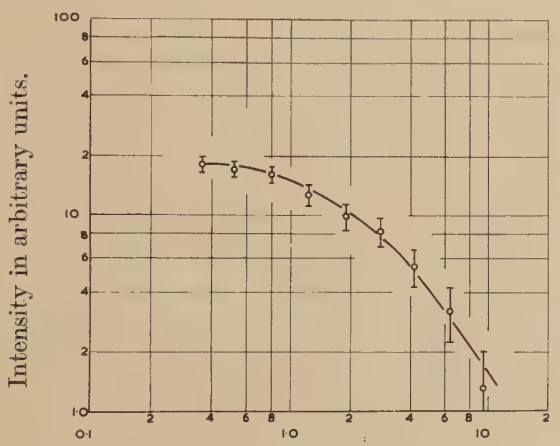

Energy in BeV.

The integral distribution of the " primary " protons and π, p particles.

(π, p) particles, produced in nuclear disintegrations in the plate assembly, will interact with another nucleus in the local matter. Such calculations show that only about 10 per cent of the fast primaries (π, p) have been generated in the plate assembly and, because of the short life-time of the π-mesons and the very weak interaction of μ-mesons, most of the others must be protons. Further, some of the fast (π, p) primaries locally generated are protons, thus only about 6 per cent of the fast primary particles of energy $>10^3$ MeV. can be attributed to π-mesons.

Similar calculations allow estimates to be made of the proportion of primary particles of lower energy which it should be possible to identify as π-mesons. The expected number thus obtained, for the particular conditions of the experiment, is 40, a number in good agreement with that observed, viz., 43.

5.1. *Variations of $\overline{n}_s$, $\overline{N}_g$ and $\overline{N}_h$ with the Energy of the Primary Particle.*

The energy of sufficient primary particles has been measured to allow the characteristics of the stars to be studied as a function of the primary energy, and fig. 9 shows the variation of $\overline{n}_s$, $\overline{N}_g$ and $\overline{N}_h$ with E_p.

Fig. 9.

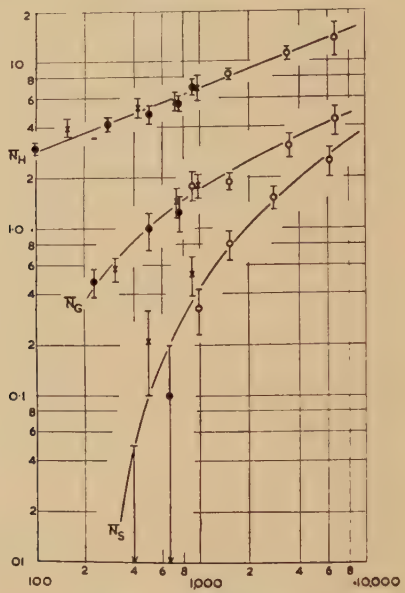

Variation of $\overline{N}_h$, $\overline{N}_g$, and $\overline{n}_s$ with the kinetic energy of the primary particle ; $\times$-stars produced by π-mesons ; ● proton initiated stars ; ○ stars initiated by " π, p " particles.

Fig. 10.

$\overline{E}_{grey}$ versus primary energy.

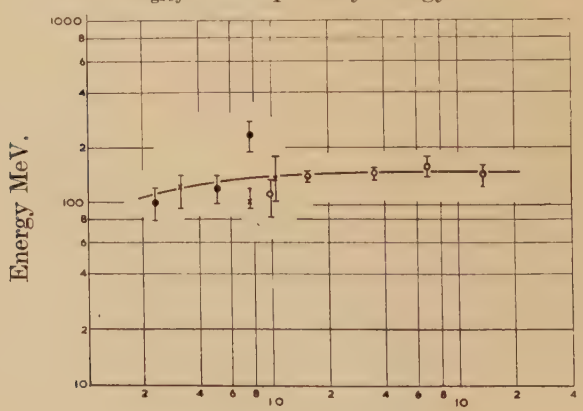

The average energy of a " grey " proton as a function of primary energy for stars initiated by mesons ($\times$), by protons (●), and by " π, p " particles (○).

Fig. 9 also includes the results of observations on showers produced by α-particles of great energy. For these events the mean multiplicity per nucleon has been plotted against the mean energy per nucleon. The results are in good accord with those for primary protons, with which they have been incorporated. Fig. 10 shows the variation with primary energy, E_p, of the average energy of the particles producing the grey tracks.

The distributions of the individual values of n_s, for a number of intervals in the value of E_p, are shown in fig. 11. There is a wide spread in the values of n_s for a given value of E_p, so that the multiplicity of a shower gives only a rough indication of the energy of the primary particle which produced it. We have been unable, except rarely, in very favourable cases, to measure the energy of primary particles above 20 BeV., and very few above 10 BeV. In analysing showers of high multiplicity we have, therefore, sometimes taken the observed value of n_s as an indication of E_p, but the results are then subject to large errors.

5.2. *Secondary Particles from Stars with Primaries of Known Energy.*

Whenever possible, detailed measurements have been made on the scattering, grain-density and range of the secondary particles arising in the disintegrations produced by primary particles of known energy. It will be convenient to consider separately the results for different classes of primary particles ; for protons, π-mesons and π, p particles :—

(a) *Primary protons with energy from* 0·2 *to* 0·9 *BeV.*

Among thirty-four stars produced by protons in this range of energy, only one secondary meson was identified. Allowing for geometrical factors, the estimated frequency of occurrence of the charged secondary mesons was found to be $0{\cdot}07 \pm 0{\cdot}07$ per star.

(b) *Primary π-mesons with energy between* 0·2 *and* 1·1 *BeV.*

In contrast with the above result for primary protons, seven secondary mesons have been identified in a study of thirty-seven stars produced by π-mesons, a result which, allowing for geometrical factors, corresponds to $0{\cdot}46 \pm 0{\cdot}23$ secondary mesons per disintegration. Details of the observations on the seven secondary particles and the associated disintegrations are given in Table V. It will be seen that the mesons commonly emerge from these nuclear encounters with small kinetic energy. A similar observation has been made for 90 MeV. mesons by Bernardini, Booth, Lederman and Tinlot (1950, 1951).

Pl. XLIII. shows an event which is remarkable in that two secondary mesons are generated by the incident meson.

(c) *Fast primary particles : ratio of the cross-sections for elastic and inelastic scattering.*

When a fast particle interacts with a nucleus, some of its energy may or may not be expended in the production of mesons. Following Heisenberg (1949), we may refer to the two types of collisions as "inelastic" and "elastic" respectively. By determining the average multiplicity $\bar{n}_s$ for different values of $\bar{E}_p$, and by making allowance both

Fig. 11.

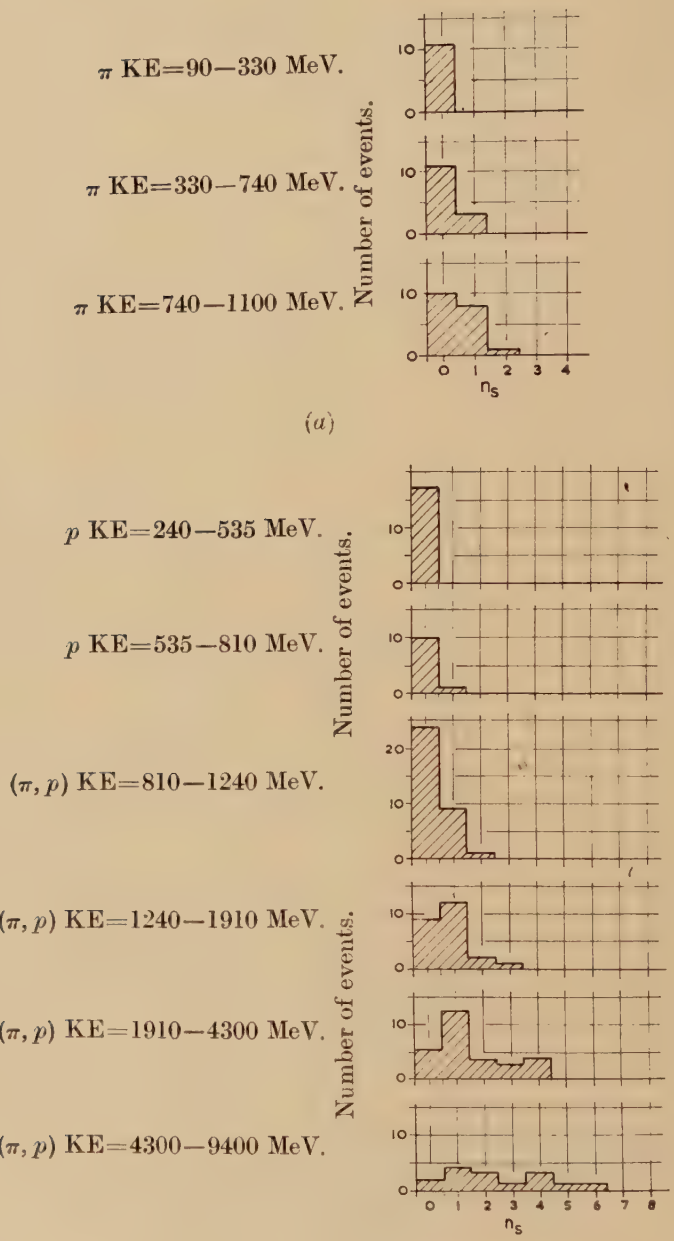

Distribution of multiplicity, n_s, in stars produced by (*a*) π-mesons, (*b*) protons and "π, p" particles, as a function of energy.

for the shower particles which are protons and for the neutral mesons which are not recorded, we can estimate the proportion of elastic and

inelastic collisions made by primary particles of different energy. In making the analysis, it has been assumed that the mesons have a probability of 2/3 of being charged (Carlson *et al.* 1950).

TABLE V.

Star Type	Kinetic energy of incident meson (MeV.)	Kinetic energy of emergent meson (MeV.)	% energy loss
$2+0_\pi$	79 ± 8	67 ± 13	15
$7+1_\pi$	640 ± 100	40 ± 8	94
$6+1_\pi$	755 ± 150	450 ± 90	43
$5+0_\pi$	825 ± 180	17 ± 3	98
$6+0_\pi$	900 ± 190	29 ± 6	97
$3+1_\pi$	1040 ± 210	120 ± 20	88
$3+2_\pi$	1050 ± 200	$\begin{cases}375\pm70\\365\pm70\end{cases}$	70

Fig. 12.

Proportion F of 0_p stars versus primary energy.

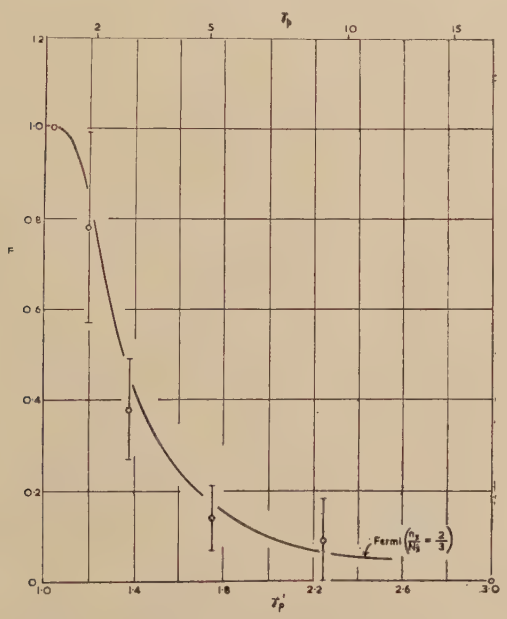

Proportion of " 0_p stars " plotted as a function of γ_p, the total energy of the primary proton in terms of its rest energy. The curve represents the values predicted by Fermi's theory. (See text.)

Fig. 12 shows the proportion of primary particles which do *not* produce shower particles, for different values of the primary energy E_p. For $E_p=1{\cdot}6$ BeV. (total energy $\gamma_p=2{\cdot}7$), half the primary particles do not produce shower particles, and the curve shows the rapid fall of the cross-section for " elastic " scattering as the energy of the primary particle

increases. The theoretical minimum value of E_p for the production of a π-meson of energy 80 MeV., is 360 MeV. The results shown in fig. 12 indicate that for values of $E_p < 1600$ MeV. most of the collisions are not completely inelastic.

The full curve in fig. 12 represents the values deduced from Fermi's theory (Fermi 1950, 1951) (see also Part VII.). These predicted values take into account production of mesons of all energies, including those of less than 80 MeV. which are too slow to appear among the " shower particles ". Such particles are few, however, so that their inclusion does not seriously invalidate a comparison between the theoretical curve and the experimental results. The agreement between them is seen to be satisfactory.

5.3. *The Production of Neutral Mesons; Missing Energy.*

It is now established that neutral as well as charged π-mesons are produced in energetic nuclear encounters. An estimate of their frequency of occurrence has been made by comparing the total energy represented by the secondary particles emitted from stars of a given class with the mean energy of the primary particles producing them. It has thus been shown that there is some missing energy which it is reasonable to attribute to the creation of neutral mesons.

The analysis was restricted to stars, with $n_s \leqslant 4$, produced by primary particles of velocity βc, where $\beta > 0{\cdot}7$. The upper limit to n_s was applied in order to avoid the inclusion of large numbers of primary particles of energy greater than 10 BeV. If such particles were included, large errors would have been introduced in this analysis. The limit to the value of β was introduced because primary particles of lower velocity cannot be identified with certainty. The results obtained are summarized in Tabel VI.

Column (1) shows the observed frequency of the different kinds of tracks. Values of the average kinetic energies of the particles in group (*a*) have been taken from the results of Harding *et al.* (1949); the other values in column (2) have been determined from the present observations. For the groups P, D, T, the energies quoted in columns (2), (3), (4), (5), are for each proton, whether ejected individually or as part of a deuterium or tritium nucleus. It has then been assumed that the total number of neutrons of energy greater than 25 MeV. is equal to 1·25 times the number of these protons. Column (6) gives the total number of nucleons, or nesons, associated with one ejected charged patticle (*i. e.* one track) of the type under consideration.

The results show that the mean energy represented by the secondary nucleons, $\bar{E}_n$, is 1458 ± 60 MeV.; and by the ejected mesons, $\bar{E}_\pi$, $\chi(630 \pm 40)$ MeV., where χ is the ratio of the sum of neutral and charged mesons to the charged mesons alone. The total energy associated with the " average " star is then $\bar{E}_p = \bar{E}_n + \chi \bar{E}_\pi$. The average energy of the primary particles of this group, directly observed, was found to be

$\overline{E}_p = 2700 \pm 150$ MeV. It follows that $\chi = E_p - E_{nucleon}/E_\pi = 2{\cdot}0 \pm 0{\cdot}3$, a value which corresponds to a ratio of neutral to charged mesons of $1{\cdot}0 \pm 0{\cdot}3$. This result does not depend significantly on the assumed proportions of mesons and protons among the (π, p) particles, but only on the correction factor for the " grey " and " shower " particles.

Carlson, Hooper and King (1950) have estimated the ratio of neutral to charged mesons produced in nuclear disintegrations, by observing the materialization of the γ-rays into which the neutral mesons decay. They restricted their observations to showers with $n_s \geqslant 3$, average value 4·5, and found a value $N_{\pi^0}/N_{\pi\pm} = 0{\cdot}45 \pm 0{\cdot}10$. Gregory and Tinlot (1951), using a cloud chamber, obtained a value of $\sim 0{\cdot}3$.

Table VI.

Type of track		No. per star	Kinetic energy per track	Binding energy per track	Total energy per track	Energy per star (uncorrected)	Correction factor for neutral particles	Total energy per star
Black	P, D, T,	3·6	10	8	18	65	2·75	179
	α	1·8	10	3	13	23	1	23
Grey	P, D, T,	2·48	131	8	139	344	2·25	775
	π	0·22	47	140	187	41	χ	41χ
Shower,	P	0·18	625	8	633	114	2·25	256
	π	0·60	395	140	535	321	χ	321χ
π–p	P	0·063	1582	8	1590	100	2·25	225
	π	0·127	1960	140	2100	266	χ	266χ

All energies in MeV.

The discrepancy between the present result for stars with $\bar{n}_s = 1{\cdot}1$ and that obtained for showers with $\bar{n}_s = 4{\cdot}5$, may be attributed, at least in part, to the fact that by selecting small values of n_s, we also favour the selection of showers in which the ratio of neutral to charged mesons is large, and *vice versa*. In nuclear encounters which lead to the production of a given number of mesons, it may be assumed that the division between charged and neutral particles in any individual case will be subject to statistical fluctuations. If we therefore impose a restriction $n_s > 4$, we shall include in the sample stars with four charged and no neutral mesons, four charged and one neutral, etc. Because of the rapid fall in the number of stars as n_s increases, such observations will tend to give a lower value of the ratio N_{π^0}/N_π.

Acknowledgments.

We have pleasure in thanking Professor C. F. Powell, F.R.S., for his constant interest and encouragement ; Miss M. Stott, Miss M. Merritt, Mrs. M. L. Andrews, Mrs. M. J. Harris and Mr. M. J. Harris for assistance with the measurements ; Miss J. Burnell and Dr. H. K. Heitler for the diagrams ; Miss P. Dyer and Mr. A. R. Gattiker for the photographs ; and the team of microscope observers of this laboratory for their careful scanning of the plates.

This work has been carried out as part of a programme of research supported by the Department of Scientific and Industrial Research, and two of us (J. H. D. and W. O. L.) are indebted to this body for maintenance grants.

References.

Bernadini, G., Booth, E. T., Lederman, L., and Tinlot, J. H., 1950, *Bombay Conference on Fundamental Particles*, 1951. *Phys. Rev.* **82,** 105.

Brown, R. H., Camerini, U., Fowler, P. H., Heitler, H., King, D. T., and Powell, C. F., 1949, *Phil. Mag.*, **40,** 862, (I).

Camerini, U., Coor, T., Davies, J. H., Fowler, P. H., Lock, W. O., Muirhead, H., Tobin, N., 1949, *Phil. Mag.*, **40,** 1073 (II).

Camerini, U., Fowler, P. H., Lock, W. O., and Muirhead, H., 1950, *Phil. Mag.*, **41,** 413 (IV).

Carlson, A. G., Hooper, J. E., and King, D. T., 1950, *Phil. Mag.*, **41,** 701 (V).

Crussard, 1950, *Bombay Conference on Fundamental Particles.*

Fermi, E., 1950, *Prog. Theor. Phys.*, **5,** 570 ; 1951, *Phys. Rev.*, **81,** 863.

Fowler, P. H., 1950, *Phil. Mag.*, **41,** 169. (III).

Fowler, P. H., Menon, M. E. K., Powell, C. F., and Rochat. O., 1951, in course of publication.

Gregory, B. P., and Tinlot, J. H., 1951, *Phys. Rev.*, **81,** 675.

Harding, J. B., 1951, *Phil. Mag.*, **42,** 63.

Harding, J. B., Lattimore, S., and Perkins, D. H., 1949, *Proc. Roy. Soc.* A, **196,** 325.

Heisenberg, W., 1949, *Z. Phys.*, **126,** 569.

O'Ceallaigh, C., 1951, in course of publication.

Osborne, L. S., 1951, *Phys., Rev.*, **81,** 239.

Sands, M., 1950, *Phys. Rev.*, **77,** 180.

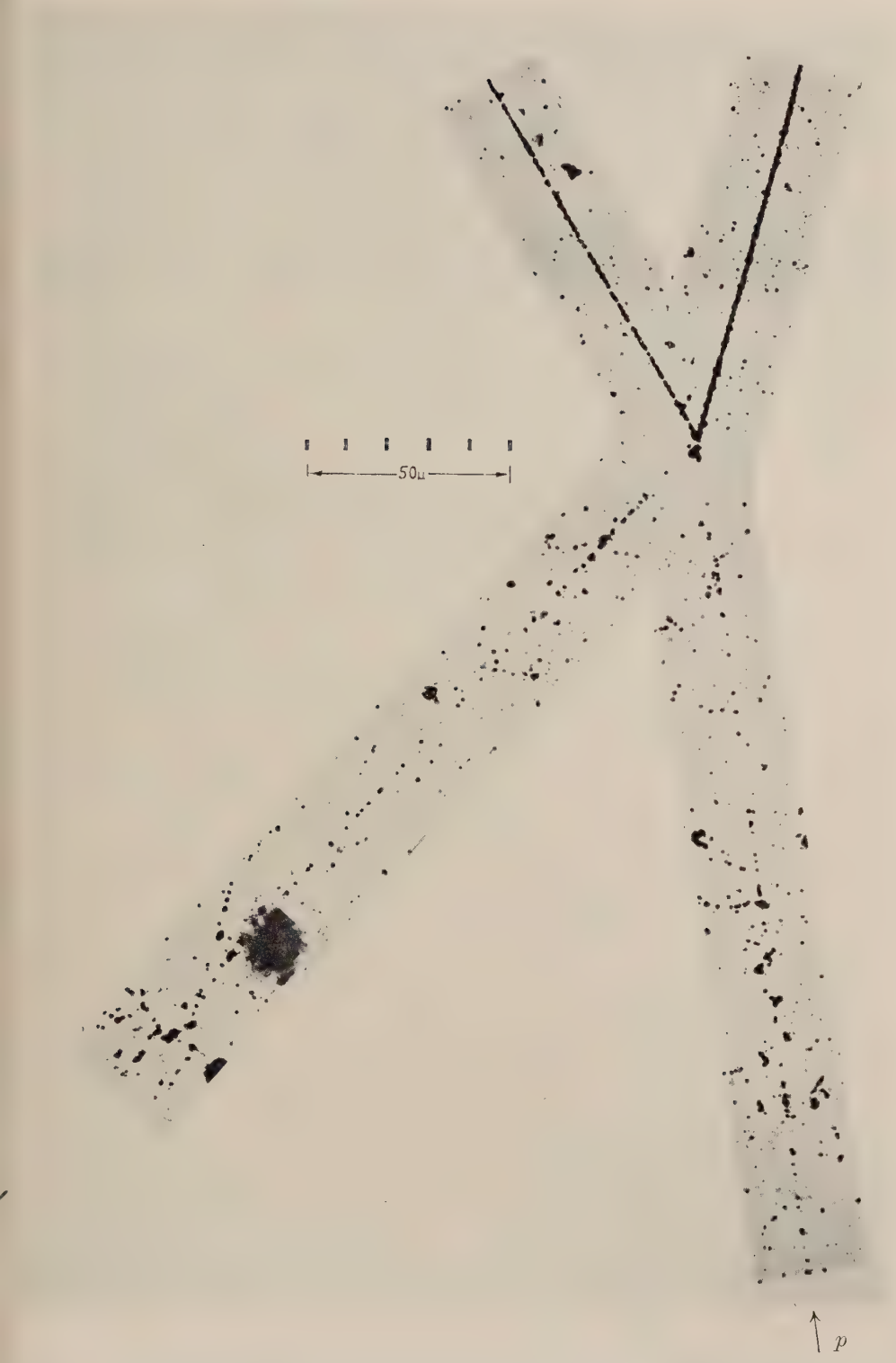

A star of type $2+1p$ in which a meson of 120 MeV. kinetic energy is produced, the primary proton having an energy of 600 MeV.

To face page 1260

Disintegration initiated by a π-meson of kinetic energy 1085 MeV. in which two π-mesons of energy 365 and 375 MeV. are produced, together with a proton of 270 MeV.

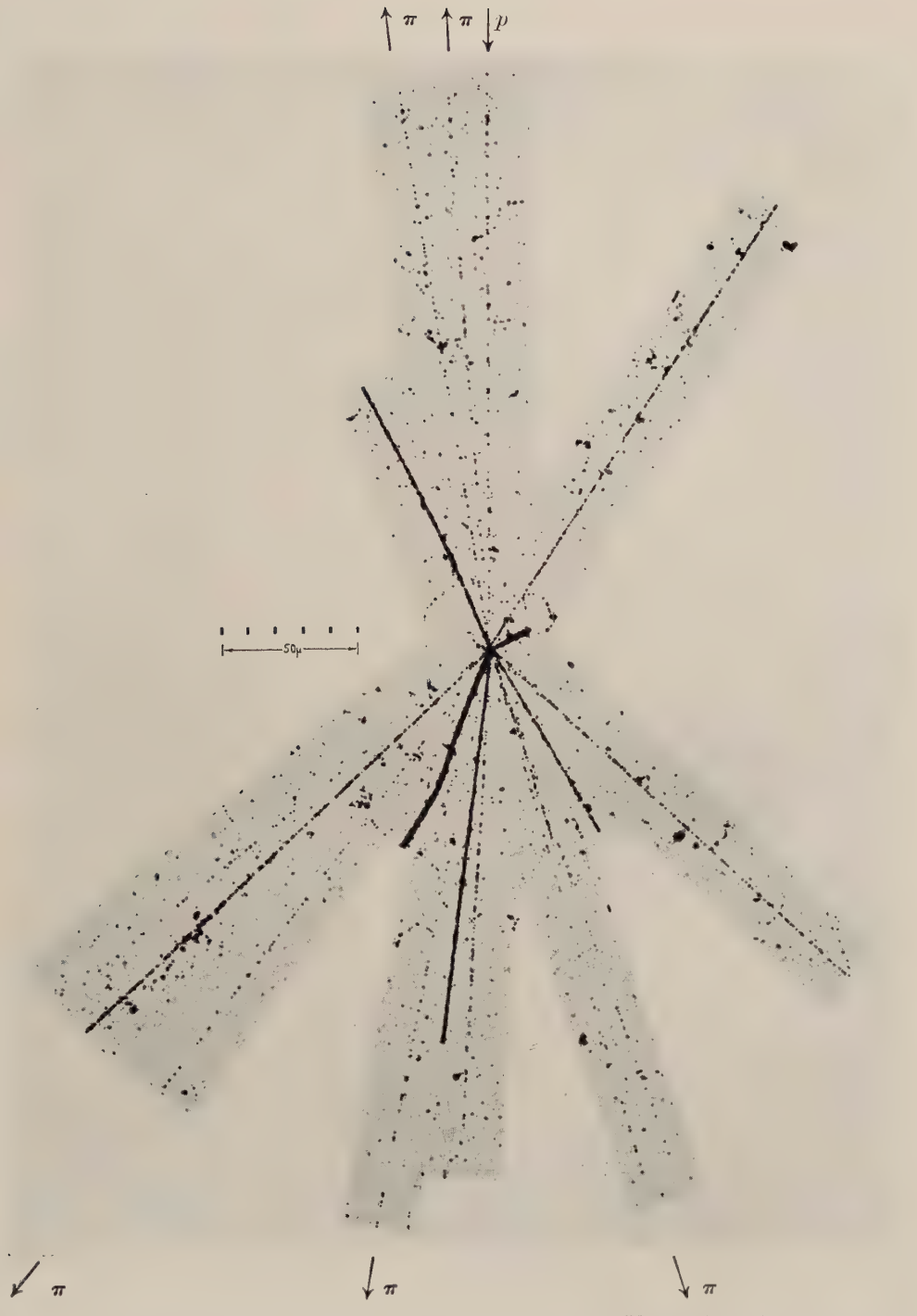

A star of type $11+8p$ in which two mesons of energy ~80 MeV. are ejected backwards in the laboratory system. Three of the forward shower particles have been identified as π-mesons.

CXXV. *Nuclear Transmutations Produced by Cosmic Ray Particles of Great Energy.*—Part VII. *Interpretation of the Experimental Results.*

By U. Camerini, J. H. Davies, C. Franzinetti, W. O. Lock, D. H. Perkins and G. Yekutieli.
H. H. Wills Physical Laboratory, University of Bristol *.

[Received July 30, 1951.]

Summary.

The observations presented in the preceding paper are analysed and compared with the current theories of meson production. In making the analyses, account is taken of the interaction with the parent nucleus both of the recoil nucleons and the created mesons.

It is found that the observations do not provide decisive evidence in favour of either plural or multiple meson production. The experimental results can be explained in terms of either the multiple theory with secondary generation of mesons, or the plural theory assuming many-body collisions.

Some other conclusions arising from the work are given at the end of this paper.

§ 1. Introduction to the Analysis.

The simplest conditions for studying the generation of mesons in nucleon–nucleon collisions would be provided by experiments in which fast nucleons collided with protons in a hydrogen target, but such observations have hitherto been impracticable. Although such collisions must occur in a photographic emulsion, they are rare, and we are therefore forced to attempt to infer the nature of the complex physical processes which take place in the nucleus from the results of the collisions of the nucleons with the mixture of nuclei found in the emulsion. In addition to hydrogen, which is the most common element, this mixture contains a variety of nuclei which can conveniently be divided into two groups; the heavier, mostly silver and bromine; and the lighter, carbon, nitrogen and oxygen.

In approaching this problem, the basic assumption is made that the disintegrations can be described in terms of encounters between individual pairs of nucleons. Unfortunately, the experimental data available do not permit a definite proof of the correctness of this assumption. If the physical processes taking place cannot be described in terms of such collisions, the interpretation of the experimental results becomes very difficult, for no theoretical guidance, regarding many-body problems is yet available.

* Communicated by Professor C. F. Powell, F.R.S.

If, however, the disintegrations can always be described in terms of a number of elementary collisions, nucleon–nucleon and meson–nucleon, the problem is reduced to an enquiry into their characteristics, and we have to determine the following quantities :

(i.) The cross-sections for radiative and elastic scattering, and their variation with the energy of the incident particle.

(ii.) The probability of radiating as mesons a fraction, K, of the energy of the two colliding particles which is available in the C-system, and the dependence of K on the primary energy.

(iii.) The distributions in energy, and in angle of emission, of all the secondary particles involved ; for radiative collisions, the number of mesons created ; and the dependence of all these distributions on K, and on the primary energy.

The analysis proceeds as follows :

The experimental results are first compared with predictions based on the pure plural theory of meson production (Heitler–Janossy 1949, 1950) in which it is assumed that the mesons are produced individually in interactions between pairs of nucleons. Secondly, a similar comparison is made for the pure multiple theories (Heisenberg 1949, Fermi 1950, 1951) in which it is assumed that many mesons may be produced in a single collision. An attempt is then made to reduce the observed discrepancies by considering both for the plural and the multiple theories the secondary generation of mesons by recoiling nucleons and, for the multiple theory only, the effect of meson–nucleon interactions.

§ 2. Pure Plural Theory.

The plural theory, as originally stated by Heitler and Janossy (1949) was based upon the following assumptions : (*a*) in each nucleon–nucleon collision only one meson is produced ; (*b*) the mean free path for collision of a nucleon in the nucleus is of the order of the inter-nucleon distance ; (*c*) the nucelus is completely transparent to the created mesons.

(a) *Comparison of observations with the Heitler–Janossy Theory.*

In the pure plural theory, the total number of mesons, charged and neutral is given by the number of encounters, N_s, made by the primary particle in traversing the nucleus, for it is assumed that one meson is created at each collision ; it follows that

$$N_s = \frac{\log(\gamma_p - 1) - \log(\gamma_c - 1)}{-\log(1-\sigma)} + 1. \quad . \quad . \quad . \quad . \quad (1)$$

In this formula γ_p is the total energy of the primary particle in terms of its rest-mass energy and γ_c is the " cut-off " energy in the same units, below which the primary cannot generate mesons. σ, assumed to be a constant, is the fraction of the kinetic energy lost by a primary particle

in each collision ; Heitler takes $\sigma=0{\cdot}25$. The recoiling nucleon takes a fraction α of the primary energy, the meson $(\sigma-\alpha)$. If we consider only those mesons for which $\gamma_s \geqslant 1{\cdot}7$ (shower particles), then the cut-off is given by

$$(\sigma-\alpha)\mathrm{R}(\gamma_c-1)=1{\cdot}7\ ;\ \mathrm{R}=\frac{\mathrm{M}_p}{\mathrm{M}\pi}=6{\cdot}7.$$

The variation of n_s with E_p, taking $n_s=\frac{2}{3}\mathrm{N}_s$ is then determined by σ and α only. Heitler assumes further that $\alpha=\sigma-\alpha=\frac{1}{8}$ and γ_c then equals 3·1. The value of N_s given by relation (1), multiplied by a factor $\frac{2}{3}$ is plotted in fig. 1, and shows good agreement with the experimental results for values of $n_s \leqslant 6$.

Fig. 1.

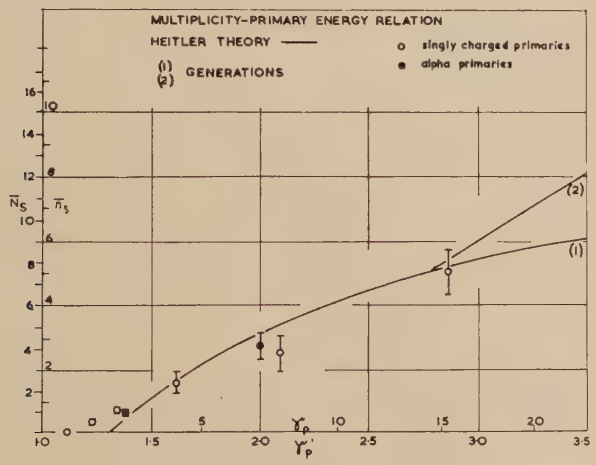

Variation of average multiplicity with primary energy ; comparison of the experimental results with the predictions of the plural theory. γ_p=total energy of the primary proton, in terms of its rest energy. For the α-particles the multiplicity per nucleon is plotted against energy per nucleon.

Messel (1951) suggests a value of $(\sigma-\alpha) \sim 1/3$, and that the remaining energy is divided symmetrically between the two nucleons. The multiplicity using these parameters is somewhat higher than the values shown in fig. 1.

Heitler and Janossy suggest that at high primary energy the recoil nucleons can themselves produce mesons, thus accounting for showers of very high multiplicity. The contribution of the recoils is shown in curve (2), fig. 1.

According to the above picture of plural production, the ratio of mesons to recoil nucleons, *generated in meson producing collisions* will be less than or equal to unity. We cannot of course measure directly the number $\mathrm{S}_{\mathrm{rad}}$ of recoil nucleons originating exclusively from meson-producing collisions. However, if we consider all nucleons emerging with energies

above 80 MeV. we shall certainly obtain an upper limit for S_{rad}. In Table I. and fig. 2 we have displayed as a function of n_s the ratio of charged plus neutral mesons {$=3/2\times$(no. of identified mesons$+0{\cdot}66\times$ no. of (π, p) particles)}, to the number of nucleons above 80 MeV. energy {$=2\times$(no. of protons between 80 and 800 MeV.$+0{\cdot}33\times$no. of (π, p) particles)}. The data are taken from fig. 5 of Part VI.

TABLE I.

n_s	No. of mesons including neutrals	No. of nucleons >80 MeV.	Ratio $\left(\frac{\text{nucleons}}{\text{mesons}}\right)$
1	1·65	3·30	0·50
2	2·4	4·60	0·52
5	6·2	7·60	0·81
10	13·0	10·6	1·23
20	26·8	14·2	1·9

Fig. 2.

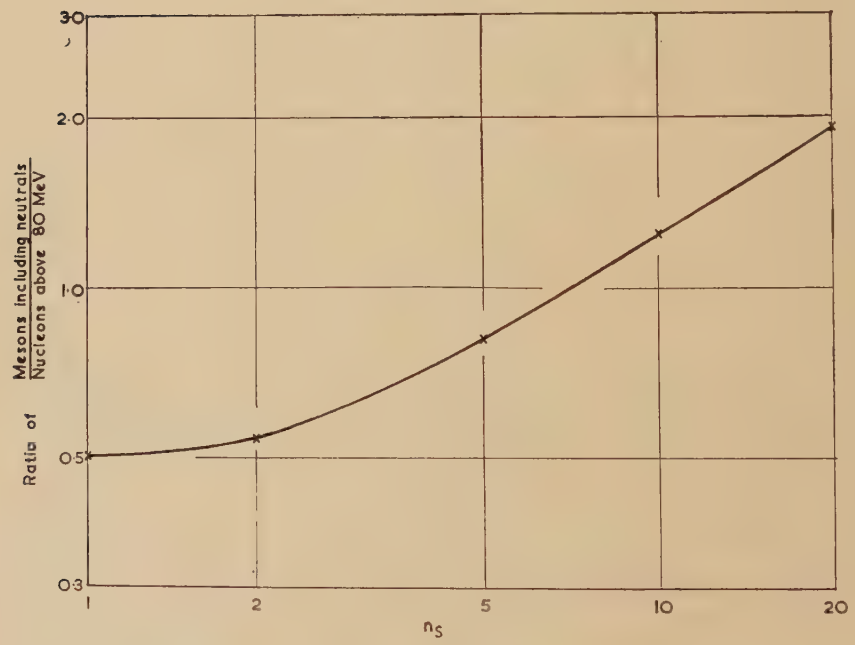

Thus at high multiplicity ($n_s>10$), the ratio exceeds unity, and thus there appears to be more than one meson produced per radiative collision. This conclusion would not be affected by choosing a somewhat lower limit (*i. e.* <80 MeV.) for the energy of nucleons recoiling from radiative collisions. The results in Table I. depends also on the proportions of mesons and protons in the (π, p) particles (see Part VI.). However, any variation in these proportions cannot affect the ratio of mesons to nucleons by more than 30 per cent.

(b) *Modifications of the Plural Theory.*

In an attempt to meet these difficulties, Heitler and Janossy (1950) and Heitler and Therreaux (Heitler 1950, 1951), have modified the plural theory in the following manner. The primary nucleons and the successive recoil nucleons are assumed to be confined within a very narrow cone. It is then visualized that at a certain stage in the disintegration, n moving nucleons may all be interacting with the same nucleon " at rest " giving n further mesons, but only one more recoil nucleon. After m stages of this process, there will be $m(m+1)/2$ mesons, with only $(m+1)$ recoil nucleons. With this assumption Therreaux finds that the percentage of recoil protons amongst the shower particles decreases with increasing n_s, and that the number of " grey " recoil protons is almost constant for $3<n_s<20$.

The degradation of energy as such a cascade develops will, however, lead to an increased angular spread of the emitted particles. If so, the true picture lies between the two extremes ; that in which the ratio of mesons to recoil nucleons is equal to $m/2$, and that of the original theory, where there are equal numbers of mesons and recoil nucleons.

A ratio of mesons to recoil nucleons lying somewhere between these extreme values is certainly compatible with our observations. On the assumption of a contribution from such many-body collisions therefore, the predictions of the plural theory are in accord with the experimental data.

§ 3. Pure Multiple Theory.

The multiple theory of meson production, in its simplest form, assumes : (*a*) that the mesons are created in a single nucleon–nucleon collision; and (*b*) that the nucleus is transparent to both the recoiling nucleons and the mesons. Heisenberg (1950) has calculated the variation of $\overline{N}_s$ with γ_p. He assumes that the mesons are produced with an energy distribution in the C-system of the colliding nucleons which is independent of γ_p, except that it extends up to a maximum value which varies with the total available energy in the system. This assumed spectrum is of the form $f(\gamma_s')d\gamma_s'=d\gamma_s'/\gamma_s'^2$, where γ_s' is the total energy of a meson in the C-system in terms of its rest-mass. If the theory gives an adequate picture of meson production, the form of the spectrum can be determined from the present experimental observations, provided certain conditions are satisfied. The method is as follows :

In the case of 23 showers, it was possible to determine the energy both of the primary particle and of one or more secondary shower particles by observations on the scattering parameter $\bar{\alpha}$. Assuming that all the primary particles are protons and that all the shower particles of a particular event are mesons produced in a single nucleon–nucleon collision, a Lorentz transformation enables the energy and direction of motion of the mesons in the C-system to be determined. It is also assumed, tentatively, that any loss of energy and change of direction of a meson in its escape from the nucleus can be neglected.

In making the transformation, it is convenient to measure energy in terms of the rest energy of the particle, and velocity as a ratio to that of light.

Let γ_p=total energy of primary particle in the L-system ;

γ'_p=total energy of primary particle in the C-system.

It follows that :

$\gamma'_p=\sqrt{[(\gamma_p+1)/2]}$.

The total kinetic energy of the two nucleons in the C-system in terms of the meson rest-mass is, before collision,

$$2R(\gamma'_p-1)$$

and the amount radiated as mesons is

$$\epsilon=2R(\gamma'_p-1)K,$$

where K=degree of inelasticity, and R, the ratio of the masses of the proton and meson, equals 6·7.

The maximum energy which a single meson can take is either

$$\epsilon'=\epsilon, \text{ or } \epsilon'=\frac{R(\gamma'^2_p-1)}{\gamma'_p} \quad . \quad . \quad . \quad . \quad . \quad . \quad . \quad (2)$$

whichever is the smaller.

Now γ'_s and θ', the energy of the meson, and its angle of emission with respect to the line of motion of the primary, in the C-system, are related to the corresponding quantities γ_s and θ in the L-system by the transformations :—

$$\gamma'_s=\gamma_s\gamma'_p-\sqrt{(\gamma_s^2-1)}\,.\,\sqrt{(\gamma'^2_p-1)}\,.\cos\theta, \quad . \quad . \quad . \quad . \quad (3)$$

$$\tan\theta'=\frac{\sin\theta}{\gamma'_p(\cos\theta-\beta_{p'}/\beta_s)}, \quad . \quad . \quad . \quad . \quad . \quad . \quad . \quad . \quad . \quad (4)$$

$$\tan\theta=\frac{\sin\theta'}{\gamma'_p(\cos\theta'+\beta_{p'}/\beta_{s'})}. \quad . \quad . \quad . \quad . \quad . \quad . \quad . \quad . \quad (5)$$

Each secondary is given a geometrical weighting factor $g(\theta)$, which is introduced to take account of the relative probability of observing long tracks for different values of θ. The analysis is confined to those stars of which the energy of the primary particle has been determined, and this can only be done for long tracks nearly parallel to the surface of the emulsion. Shower particles ejected at angles near $\theta=0°$ and $\theta=180°$ with respect to the line of motion of the primary particle will therefore have a much greater chance of remaining in the emulsion than those with $\theta=90°$. The observations therefore lead to a series of weighted values of θ' and γ_s', the angle of emission and the energy, respectively, of the meson in the C-system.

The angular distribution of all such mesons is given in Table II.

TABLE II.

θ' (in degrees)	0—30	30—60	60—90
Number Observed	34±23	70±30	99±35
Isotropic distribution	27	74	102

Within the large statistical errors, it is consistent with an isotropic distribution. The ratio of backward to forward-moving mesons is 0·95±0·44, a result consistent with the value expected from symmetry considerations.

Fig. 3.

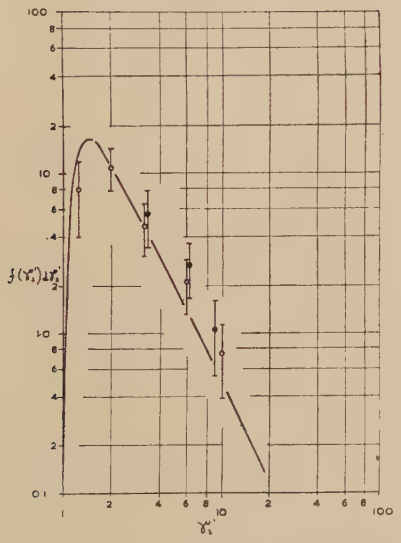

The energy spectrum of the mesons in the C-system derived on the assumption of a single nucleon–nucleon collision. γ_s' is the total energy of the meson in terms of the rest energy.

● K=0·5 ; ○ K=1.0. The curve represents the spectrum p^2dp/γ^4.

Collecting together all values of γ_s', we obtain a distribution in energy $f(\gamma_s')d\gamma_s'$. This however cannot be compared directly with Heisenberg's spectrum which corresponds to infinite available energy in the C-system of the interacting nucleons. To make the necessary corrections to the observations, we divide by the factor $p(\gamma_s')$ representing the observed fraction of showers having primaries such that γ_p' is greater than the value given either by $\gamma_s'=2\mathrm{RK}(\gamma_p'-1)$

or by $\mathrm{R}(\gamma_p'^2-1)/\gamma_p'$

whichever is smaller.

The corrected distribution $f(\gamma_s')\,d\gamma_s'$ is shown in fig. 3, for K=1 and for K=0·5. The peak at $\gamma_s'\sim 2$ is presumably a consequence of the

conservation of momentum in the C-system. The distribution can be represented analytically by the equation

$$p^2dp/\gamma_s'^4,$$

where $p=\sqrt{(\gamma_s'^2-1)}$, which falls off at high energies as $1/\gamma_s'^2$. This is in satisfactory agreement with the spectrum chosen by Heisenberg.

It may be mentioned that, even if the pure multiple theory is inadequate, valuable information may be obtained by making such transformations in favourable cases.

3.1. *Yield Curve on Pure Multiple Theory.*

The average number of mesons produced in the collision is

$$\overline{N}_s'=\frac{\epsilon}{(\gamma_s')_{av}},$$

where

$$(\gamma_s')_{av}=\int_1^{\epsilon'}\gamma_s' f(\gamma_s')\,d\gamma_s' \Big/ \int_1^{\epsilon'} f(\gamma_s')d\gamma_s'. \quad . \quad . \quad . \quad . \quad . \quad (6)$$

The number of mesons classed as shower particles (energy in L-system $\gamma_s>1{\cdot}7$) is

$$\overline{N}_s=\chi\overline{N}_s',$$

where the factor χ is nearly unity, and is easily calculated. In reaching this result, an isotropic angular distribution of the mesons in the C-system has been assumed. If one-third of all the mesons produced are neutral, the average number of mesons which appear as shower-particles is $\overline{n}_s=(2/3)\overline{N}_s$; and n_s is therefore determined as a function of $\epsilon=2RK(\gamma_p'-1)$. The results for three values of K, 1·0, 0·7 and 0·3—are shown in fig. 4. It will be seen that with low values of γ_p, the results indicate a small mean value of K, contrary to the Heisenberg assumption, K=1. For such values of γ_p, some of the collisions will be completely elastic—see fig. 12, Part VI.—and the remainder correspond to a finite value of K, which must, as shown by energy considerations, be near unity. If only a single meson-producing collision occurs in the nucleus, a mean value of K, near to unity, must be assumed to obtain agreement with the experimental results for large values of γ_p.

The yield curve according to Fermi's theory is included in fig. 4. At high energies, the predicted average multiplicity appears to be too small, though presumably the agreement could be improved by a suitable choice of his fundamental parameter Ω.

Fluctuation of n_s in stars produced by protons of given energy.

The results represented in fig. 11 of Part VI. which show the large fluctuations in the values of n_s for stars produced by primary protons of a given energy may be due to :—

(*a*) variations in the kinetic energy of individual mesons in the C-system ;

(*b*) variations in the degree of inelasticity, K, of the collisions ; and

(*c*) statistical fluctuations in the ratio of charged to neutral mesons.

Assuming on the average, that 2/3 of the mesons are charged, the effect of (*c*) is readily calculated. The spread then predicted in Fermi's theory is found to be in good agreement with experiment.

The effect of (*a*) was computed numerically on the Heisenberg theory, for different values of K. Assuming a spread in K, and *mean* values of K as deduced from the yield curve (fig. 4), there is again found to be satisfactory agreement with the observations.

Fig. 4.

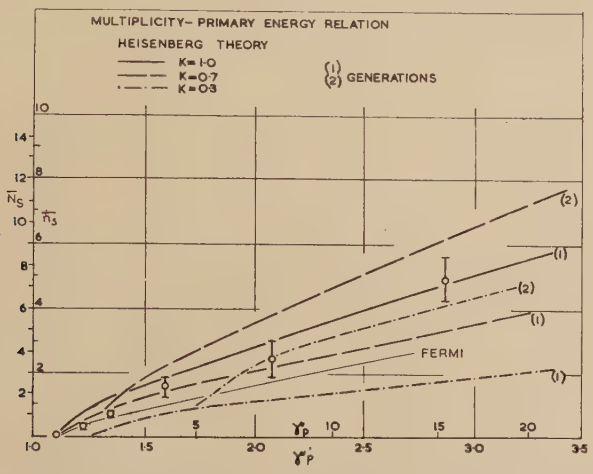

Variation of average multiplicity with primary energy ; comparison of the experimental results with the predictions of the multiple theory. $\gamma'_p = \sqrt{[(\gamma_p+1)/2]}$ = energy of nucleon in C-system.

3.2. *Angular Distribution of mesons in the Laboratory System.*

The question may now be asked " How far does the assumption of a single meson-producing collision, without secondary interactions of the mesons in their escape from the nucleus, explain the observed angular distribution ? ". It has been found by calculation that the form of the observed angular distribution of the mesons in the L-system cannot be uniquely explained in terms of simple assumptions regarding their energy and angular distribution in the C-system. On the other hand, the median angle η, and the backward fraction of the emitted mesons B, as observed in the L-system, do not depend so critically on the assumed features of the distributions in the C-system. Thus assuming only that equal numbers of mesons are projected backwards and forwards in the C-system, the medain angle is given by equation (5)

$$\tan \eta = 1/\gamma'_p(\beta_{p'}/\beta_{s'}) \quad . \quad . \quad . \quad . \quad . \quad . \quad . \quad . \quad (7)$$

or since $\beta'_p/\beta'_s \sim 1$, $\tan \eta = 1/\gamma_{p'}$. The value of $\tan \eta$ given by this equation is an upper limit because a small proportion of mesons, emitted backwards

with low velocity in the C-system, will appear in directions $\theta<\eta$ in the L-system.

The variation of η with n_s, as calculated from equations (6) and (7), is shown in fig. 3 of Part VI. The observed median angle decreases much more slowly with increasing n_s than the simple theory predicts, and this is evidence against a pure multiple process. The difference in the observed value of B for $N_h \leqslant 7$ and $N_h > 7$ also indicates that secondary interactions play a role.

If the angular distribution of mesons in the C-system is of the form $F(\theta')d\theta' = \cos^n\theta' d\theta'$, the fraction of mesons with velocity β'_s which travel backwards in the L-system is given by the equation

$$B = \frac{1}{2}\left[1 - \left(\frac{\beta_{p'}}{\beta_{s'}}\right)^{n+1}\right]; \quad \beta_{s'} > \beta_{p'}. \qquad . \quad . \quad . \quad . \quad . \quad (8)$$

If shower particles only are considered ($\gamma_s > 1{\cdot}7$), the above formula is slightly modified.

Using the spectrum $f(\gamma'_s)d\gamma'_s$ we can therefore find the value of B as a function of γ'_p or γ_p by numerical integration. Again using the γ'_p versus $\bar{n}_s$ relation, we get a curve relating B with average multiplicity $\bar{n}_s$.

It is found that the actual slope and peak of the curve does not depend very strongly on the value of n ; the absolute magnitude however, varies almost linearly with $(n+1)$ as can be seen by binomial expansion of (8). The curves (fig. 4, Part VI.), were calculated for $K=1$ and $n=0$ and $n=4$ respectively. The slope of these curves is quite different from the experimental B versus n_s relation. The correct slope can be secured by assuming secondary nucleon–nucleon collisions (see 4.1) and in order to account for the absolute magnitude of B we have to postulate an anisotropic component in the C-system angular distribution. Alternatively, it may be assumed that elastic scattering of the mesons by nucleons can occur, a possibility which is considered in more detail in § 5.

§ 4. Multiple Theory with Secondary Processes.

4.1. *Secondary nucleon–nucleon collisions.*

The agreement between the experimental observations and the predictions of the pure multiple theory may be considerably improved by assuming that a second generation of mesons is created. Such mesons may be produced in collisions involving nucleons recoiling from the primary particle. In considering such effects, we first neglect any secondary interactions of the mesons in escaping from the nucleus.

If such secondary generation occurs, a simple Lorentz transformation is no longer valid, for the mesons are created in several collisions involving nucleons of different energy. If, however, we make a statistical study of a large number of showers, produced by primary particles of similar energy, it is sufficient to assume an effective value of γ'_p, γ'^*_p. γ'^*_p is a mean value of γ'_{p1} and γ'_{p2}, the values of γ'_p for the first and second

generation, suitably weighted according to the number of mesons arising in each. If it is assumed that the nucleus is so large that all meson-producing collisions which are energetically possible actually occur, then it may be shown that $\gamma_p'^*/\gamma_p'$ is nearly independent of the value of K; and that it lies within the limits 0·8 and 1.

The above considerations indicate that the average values for γ_s' for the secondary particles $(\gamma_s')_{av}$, as deduced from the spectrum of § 3 in which it is assumed that they are produced in a single collision, are at most, 10 per cent too large. The errors are thus not greater than those due to the poor statistical weight of the observations at present available. It is therefore reasonable to estimate the proportion of mesons due to secondary generation, using the value of $(\gamma_s')_{av}$ and the results are included in fig. 4. The calculations have been made for three values of K=0·3, 0·7 and 1·0.

4.2. *Angular distributions including effects due to secondary generation.*

As previously mentioned, the assumption both of secondary generation, and of anisotropy in the angular distribution of the mesons in the C-system, is needed to explain the observations on the backward fraction, B. The calculations have been made assuming K=1, and neglecting the spread in multiplicity n_s for a given primary energy γ_p. It is reasonable to suppose however, that these simplifications will not seriously affect the general trend of the theoretical curves. For a given value of γ_p, the average meson energy in the C-system will be greater than $(\gamma_s')_{av}$ if $n_s<\bar{n}_s$; see equation (6). The backward fraction will therefore also be greater. The reverse is true if $n_s>\bar{n}_s$. Thus the general slope of the theoretical curve should remain almost unaffected.

When K<1, calculation of the backward fraction is very complicated, for the nucleons from the first collision recoil at an angle to the direction of motion of the primary particle. This must lead to a broadening of the angular distribution of which it is difficult to estimate the magnitude.

4.3 *Variation of Multiplicity n_s, with star size N_h.*

If the secondary generation of mesons plays an important role at high primary energies, it will be more likely to occur in heavy than in light nuclei. Stars with $N_h>8$ must almost always be due to the disintegration of silver or bromine nuclei, whilst stars of smaller N_h may be due either to the disintegration of nuclei of the light elements carbon, nitrogen or oxygen, or to those of silver and bromine. If therefore we consider stars produced by primary particles of the same energy, secondary generation, more likely in heavy nuclei, would contribute to making the average multiplicity of stars with $N_h>8$ greater than those with $N_h<8$. On the other hand, any reabsorption of mesons in the parent nucleus will tend to reduce the number of mesons and increase the number of recoiling nucleons.

In view of these considerations, we have plotted the average multiplicity n_s, as a function of primary energy, Ep, for the two classes of stars ; see fig. 5. Included in the figure are the results of Salant *et al.* (1950) for primary particles of energy between 1 and 8 BeV., and for those of energy greater than 8 BeV. (average energy 14 BeV.). At high energies, there is a significant difference between the average multiplicities of the two types of stars. It is reasonable to infer that secondary processes frequently take place in heavy nuclei bombarded by protons of great energy, and that re-absorption of the mesons is relatively unimportant.

Fig. 5.

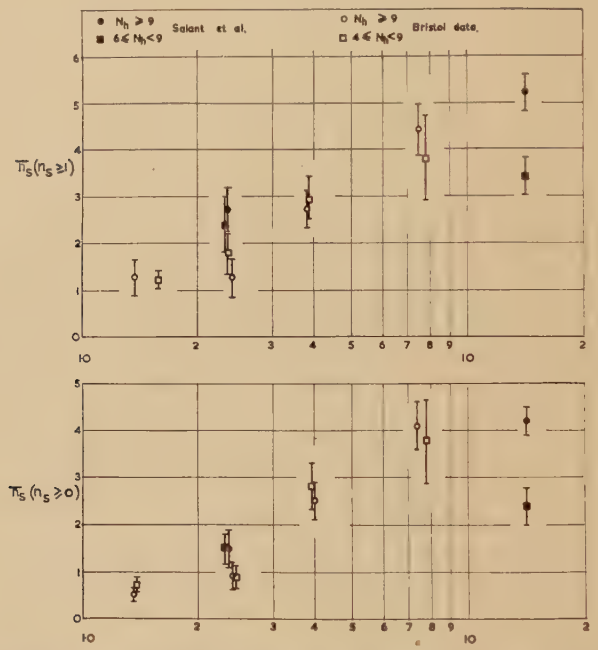

Observed variation of average multiplicity with kinetic energy of the primary particle in BeV, for stars of different prong number N_h.

It may be remarked that the results of Salant *et al.* relate to stars of $N_h = 2-8$ and $N_h \geqslant 9$, while our figures are for stars of $N_h = 4-8$, and $N_h \geqslant 9$. This may explain the difference between the two sets of observations at 2·4 BeV.

§ 5. Meson–Nucleon Interactions.

Hitherto any interaction of the mesons with the parent nucleus has been neglected, and an attempt has been made to explain the experimental results in terms of nucleon–nucleon collisions alone. The results given in 5·2 (*b*) of Part VI., show, however, that meson have a strong interaction with nucleons, and we now consider the effects of such interactions.

5.1 *Elastic Scattering of Mesons.*

In order to estimate the effect of the elastic scattering of mesons during their escape from the parent nucleus, we have considered two possibilities. In the first, the scattering process is regarded as analogous to the Compton effect, the relative probability of different angles of scattering being similar to that in electro-magnetic case. On being scattered, a meson may then be deflected through a large angle and may lose a large fraction of it energy. On the second assumption, the scattering is regarded as " isotropic " ; the cross-section for the interaction is assumed to be constant irrespective of the energy of the meson, and after the encounter, all directions of motion of the meson, in the C-system of the interacting particles, are equally probable.

In calculating the effect of such scattering, we have made the simplifying assumption, that the original angular distribution of the mesons can be represented by a δ-function ; *i.e.* all mesons are initially projected in the line of motion of the primary nucleon. Assuming each meson to be once scattered in escaping from the nucleus, the fraction B′ of the mesons which emerge in the backward hemisphere can be calculated for a given value of the primary energy γ_p. The calculation depends upon the known distribution in the values of γ_s, and the energy " spectrum " $f(\gamma_s')\,d\gamma_s'$. These quantities and the relation between $\bar{n}_s$ and γ_p allow the two curves in fig. 4 of Part VI. to be computed. The actual magnitude of B′ will be greater than that calculated since the initial angular distribution of the mesons is certainly quite broad. A slight error is introduced when the curves are taken as plots of B′ against n_s, instead of $\bar{n}_s(\gamma_p)$, because of the spread of n_s for a given primary energy. This effect has already been considered in 4.2.

It is reasonable to suppose that any backward fraction unaccounted for by the Lorentz transformation is due to large-angle scattering, and this view is supported by the fact that the angular distribution of the mesons in the backward hemisphere is nearly isotropic.

The backward fraction due to single scattering calculated by the above method is certainly an underestimate. Comparison of the observed and calculated values of B therefore allows us to obtain an upper limit (for $n=1$, equation (8)) for the probability of large-angle scattering, and the value thus obtained is 0·3. For the nuclei considered, this value indicates that the cross-section for the scattering process is of the order of 1/10 the geometrical cross-section per nucleon.

In the scattering process, the meson projects a nucleon, and this particle, if a proton, produces a " grey " track. The above value of the cross-section is consistent with the observed slow increase of $\overline{N}_g$ with n_s. The ratio $Q=B(N_h>8)/B(N_h\leqslant 8)=1{\cdot}5\pm 0{\cdot}25$. If Q′ represents the ratio (B heavy nuclei)/(B light nuclei), then from the effect arising purely from the Lorentz transformation, one expects $Q'\sim 1{\cdot}0$; from scattering alone a value of $Q'=1{\cdot}8$. Since the observed value does not represent complete separation of light and heavy nuclei, the observed value of Q′, 1·5, is in reasonable agreement with that predicted from scattering alone.

5.2 *Reabsorption of Mesons in the Nucleus.*

The evidence presented in section 4.3 of Part VI. precludes the possibility that any substantial fraction of fast mesons created in the primary act, or acts, can be re-absorbed and annihilated by nucleons, in the parent nucleus. The average total energy of such a meson is ~860 MeV., and the disappearance of this energy would result in a considerable increase in N_h. Thus if strong absorption takes place N_h should increase rapidly with increasing n_s, which is contrary to the observations.

5.3. *Generation of Mesons in Meson–Nucleon Collisions.*

In traversing nuclear matter, a very energetic meson may produce further mesons in two ways : (i.) First, it may be elastically scattered by a nucleon ; and this nucleon may recoil with sufficient energy to produce one or more mesons in collision with another nucleon. (ii.) Secondly, in the scattering process, the meson may generate further mesons directly.

A meson primary originates, of course, as a shower particle and, to be identified, it must have an energy less than 1100 MeV. Such a particle can have only a small probability of producing further mesons by process (i.) since it cannot transfer more than 880 MeV. in collision with a nucleon, and the average value is only ~ 500 MeV. We should therefore expect to observe only the elastic scattering of such particles, and the result of their collision with a nucleus should commonly be a " star " without shower particles.

As described in Part VI. (see Table V. and Pl. XXXVI.) one star has been observed in which an incident meson of 1050 ± 200 MeV. energy produces two mesons of energy 375 ± 70 MeV. and 365 ± 70 MeV. and a recoil proton of 270 ± 50 MeV. On process (i.) it follows from the conservation laws that one of the mesons should be ejected backwards, which is contrary to observation. Thus the event can only be explained in terms of process (ii.).

By analogy with the nucleon–nucleon collisions which result in the creation of mesons, we may refer to the reproductive process (ii.) as " inelastic scattering ". Heitler estimates that for mesons in the range of energy under consideration, the ratio of inelastic to elastic scattering is ~10 per cent. This value suggests that among the 37 examples of stars produced by π-mesons which we have observed, there should be one in which the primary particle leads to the emission of two identifiable mesons ; and we have seen that one such event has been found.

Although meson production occurs rarely in the nuclear interactions of π-mesons of energy less than 1 BeV., it is reasonable to suppose that it becomes important at higher energies. This view is supported by the experiments of Rosser and Swift (1951) who have exposed photographic emulsions, at an altitude of 2860 m., above and below 30 cm. of lead. They found that the ratio of charged primaries to neutral primaries for disintegrations with $n_s \geqslant 2$ was $0{\cdot}86 \pm 0{\cdot}21$ above the lead, and $1{\cdot}76 \pm 0{\cdot}48$

below it. For the following reasons they suggest that the difference is due to mesons created in the lead :—

The average energy of a primary nucleon which produces a penetrating shower of $n_s \geqslant 2$ is of the order of 4 BeV. If the observed showers are attributed to fast nucleons recoiling from the π-mesons, then the incident π-mesons must have an energy greater than this value, *i. e.* >4 BeV. The number of π-mesons of such great energy is not sufficient, from this point of view, to account for the magnitude of the effect observed. On the other hand, the results are readily explained if it is assumed that π-mesons of energy greater than 1 BeV. can produce showers of π-mesons directly, the cross-section for the process being approximately equal to the geometrical value.

§ 6. Production of Mesons by Energetic α-Particles.

It is reasonable to suppose that, in producing mesons by collisions with a nucleus, a relativistic α-particle will act as a beam of four nucleons. Included in fig. 1 are the results obtained in studying showers produced by α-particles of known energy. For such showers, the multiplicity per nucleon has been plotted against the energy per nucleon, and the agreement between these results and those for proton primaries gives support for the above view.

§ 7. Conclusions.

The conclusions which follow from the present experiments may be briefly summarized as follows :—

(i.) At low energies (<1 BeV.) most of the nucleon–nucleon collisions are completely elastic. The " inelastic " scattering cross-section does not become comparable with that for " elastic " scattering until an energy of about 2 BeV. is reached.

(ii.) For a given value of the primary energy, a wide range in the number of charged mesons emitted is observed in different disintegrations. The multiplicity, n_s, therefore gives an unreliable indication of the primary energy.

(iii.) Assuming pure " multiple " production, the energy and angular distributions of mesons in the C-system of the two colliding nucleons can be calculated. The angular distribution thus found is approximately isotropic ; the energy spectrum can be represented by p^2dp/γ^4 (p=momentum, γ=energy).

(iv.) The simple theory is of multiple production, with no secondary radiative collisions, is inadequate. To obtain agreement with experiment, it must be assumed that mesons are also produced in secondary nucleon–nucleon and meson–nucleon colilisions.

(v.) The modified plural theory, which considers meson production in many-body collisions by both the primary nucleon and the recoil nucleons, also gives satisfactory agreement with the experimental data.

(vi.) The observations therefore do not provide a decisive test between the two theories, and there appears to be nothing to choose between them regarding economy of hypothesis. The multiple picture introduces a strong-coupling theory, whereas on the plural picture it seems necessary to postulate many-body collisions.

(vii.) The number of neutral mesons ejected from stars of multiplicity between 0 and 4 is found to be $1{\cdot}0 \pm 0{\cdot}3$ times the number of charged mesons.

(viii.) Re-absorption of fast mesons by the parent nucleus in which they are created is very improbable, although such a process may explain the very large stars (N_h) of small multiplicity, n_s.

The cross-section for elastic scattering of these mesons by the nucleons (Compton-type scattering) is $\sim$10 per cent of the geometrical value.

(ix.) On the contrary, single fast π-mesons of energy less than 1 BeV. interact strongly with nuclear matter ; in $\sim$50 per cent of the cases they emerge from an encounter with a nucleus having lost a large fraction of their energy. It is not possible, from the present observations, to decide whether in the remaining cases, the mesons are absorbed, or whether they suffer charge exchange, so that the outgoing meson is undetected.

Acknowledgments.

We have pleasure in thanking Professor C. F. Powell, F.R.S., for his interest and encouragement during the analysis, and Professor W. Heitler for several informative discussions and permission to quote the unpublished calculations of M. Therreaux. We wish especially to express our thanks to Dr. H. Messel, for his very thorough and painstaking rading of a preliminary draft of this work, and for many useful suggestions and criticisms.

This work has been carried out as part of a programme of research supported by the Department of Scientific and Industrial Research, and one of us (W. O. L.) is indebted to this body for a maintenance grant.

References.

Fermi, E., 1950, *Prog. Theor. Phys.*, **5**, 570 ; 1951, *Phys. Rev.* **81**, 863.

Heisenberg, W., 1949, *Z. Phys*,. **126**, 569.

Heitler, W., and Janossy, L., 1949, *Proc. Phys. Soc.*, A **62**, 364, 669 ; 1950, *Helv., Phys., Acta.*, **23**, 417.

Heitler, W., 1950., *Bombay Conference on Fundamental Particles* ; 1951, Private Communication.

Lewis, H. W., Oppenheimer, J. R., and Wouthuysen, S. A., 1948, *Phys. Rev.*, **73**, 127.

Messel, H., 1951, *Proc. Phys. Soc.* A, **64**, 726.

Rosser, W. E. V., and Swift, M. W., 1951, Private Communication.

Salant, E. O., Hornbostel, J., Fisk, C. B., and Smith, J. E., 1950, *Phys. Rev.* **79**, 184.

CXXVI. *Associated Penetrating Particles of Cosmic Rays Underground.*

By H. J. J. Braddick, W. F. Nash and A. W. Wolfendale,
The Physical Laboratories, University of Manchester*.

[Received July 19, 1951.]

Abstract.

Two cloud chambers have been used at a depth underground equivalent to 26 m. of water in a study of the penetrating cosmic ray particles. Pairs of associated penetrating particles have been observed originating in lead plates in the chamber and also entering it from above. It is considered that the process is one in which a μ-meson produces a penetrating secondary of mean energy $\sim 10^9$ eV., the penetrating secondary being either a μ-meson or a π-meson. The cross-section for the process is estimated to be about 5×10^{-29} cm.^{2} per nucleon for lead and of the same order of magnitude for sandstone.

§ 1. Introduction.

The discovery of associated pairs of penetrating particles underground was first reported by Braddick and Hensby (1939) as a result of cloud chamber experiments at a depth of 60 metres water equivalent. It is probable that these events are not identical with penetrating showers as observed at sea level, for it is known that the primaries responsible for penetrating showers are so attenuated as to be negligible at this depth.

Pairs of penetrating particles have also been observed under thick absorbers at sea level by Shutt (1946) who interpreted them as pairs of μ-mesons.

The present work was undertaken to verify and elucidate these results. Cloud chambers have been operated in a cave at 26 m.w.e. depth, using simple counter control and a number of events involving associated penetrating particles (A.P.P.) were photographed stereoscopically. While the work was in progress underground phenomena involving A.P.P. have been reported by George and Evans (1950), using photographic emulsions, and by Greisen *et al.* (1951), using counter arrangements. The relation of these results to ours will be discussed.

It seems likely that the events described are secondary to μ-mesons and that the interaction of μ-mesons with matter is greater than was thought.

* Communicated by Professor P. M. S. Blackett, F.R.S.

§ 2. Experimental Arrangement.

The apparatus was installed in a cave at Stockport under 2600 gm./cm.^{2} of rock, which was mainly red sandstone of mean density 2 gm./c.c. The vertical cosmic-ray intensity was about $\frac{1}{4}$ of that at sea level. Two cloud chambers were used at different times, they were installed in the same position with their centres 170 cm. below the roof. The whole cave was maintained at a temperature of 18° C.

In the first series of experiments the apparatus consisted of a cloud chamber of normal design 30 cm. in diameter and 13 cm. deep, with a lead plate 2 cm. thick placed across the centre. This plate was used to distinguish between electrons and penetrating particles, electrons usually being recognized by the production of electron showers on passing through the plate.

In order to investigate further the properties of A.P.P. a multiple plate chamber was constructed. The chamber was 40 cm. $\times$ 39·5 cm. $\times$ 36 cm. in size and could contain up to thirteen 1 cm. lead plates. The chamber was illuminated through the back and the expansion was produced by the symmetrical lateral movement of two rubber diaphragms on opposite sides of the chamber.

The selection system usually consisted of a simple 3-fold counter telescope. Only one penetrating particle passing through the central part of the chamber was therefore required to cause an expansion.

§ 3. Experimental Results.

3.1. *Cylindrical cloud chamber. Series I.*

Two thousand two hundred photographs were taken with the arrangement shown in fig. 1 *a*. The counting rate of the 3-fold counter system was 81 ± 2 per hour, being $\frac{1}{4}$ of that at sea level. The total time during which the chamber was available to record incoming particles (sensitive time) was 27·5 hours.

Thirteen photographs of this series each showed two penetrating particles which were considered associated (the criteria for acceptance as associated will be stated later).

3.2. *Cylindrical cloud chamber with 3 cm. lead above. Series II.*

The second series of photographs was taken with the arrangement shown in fig. 1 *b*. The 3 cm. lead absorber above the chamber was used to increase the probability of degrading any electronic component. The position of the counters was not exactly the same as before and the triple coincidence rate was 50 ± 2 per hour.

Two thousand six hundred photographs were taken, the total sensitive time being 52 hours. Twelve apparent A.P.P. were observed, four of which had originated in the lead absorber above the chamber.

3.3. *Cylindrical cloud chamber with 3 cm. lead above and a split counter tray below. Series III.*

To increase the efficiency of detecting A.P.P. relative to random associations of particles, a split counter tray was placed below the chamber as shown in fig. 1 *c*. This arrangement was sensitive to electron

Fig. 1.

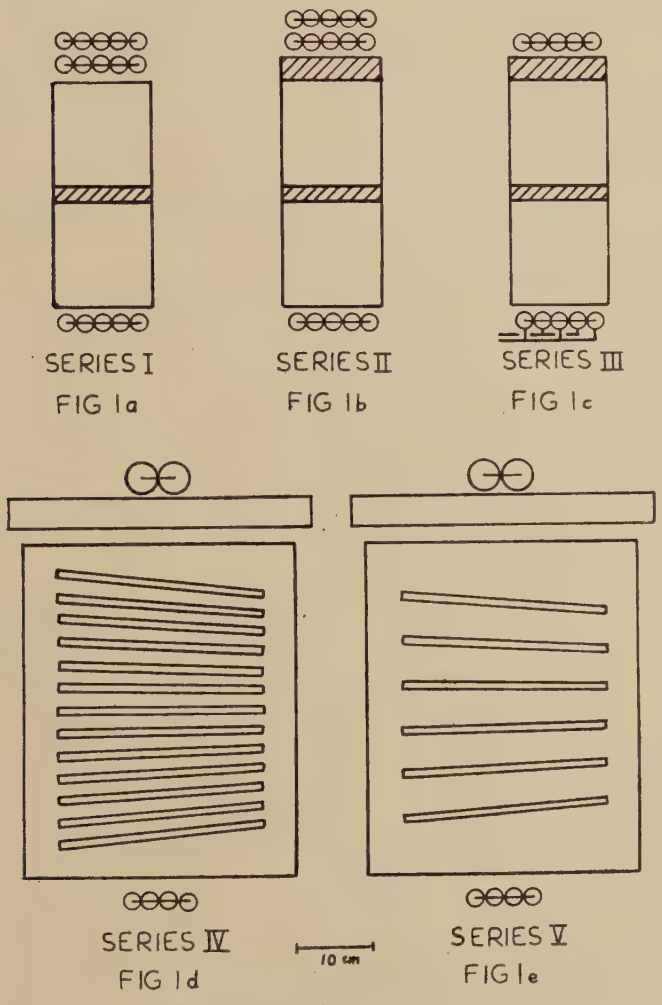

Experimental arrangements.

showers in addition to A.P.P. The counting rate was $8 \pm 0{\cdot}9$ per hour at sea level and $5 \pm 0{\cdot}4$ per hour underground. The total number of photographs taken was 2400 and the total sensitive time was 480 hours. Thirty photographs showed apparent A.P.P., of which twelve originated in the 3 cm. lead absorber above the chamber.

3.4. *Multiple plate cloud chamber containing thirteen* 1 *cm. lead plates. Series IV.*

For all the observations with the multiple plate chamber a simple threefold counter telescope was used. The arrangement is as shown in fig. 1 *d* and the counting rate was 12·5 per hour. In a sensitive time of eighteen hours, 215 photographs were taken, each showing at least one particle penetrating all the plates.

One pair of apparent A.P.P. was observed to originate in one of the lead plates. One small penetrating shower was observed and one pair of A.P.P. originating in the sandstone above the chamber was found.

3.5. *Multiple-plate cloud chamber containing six* 1 *cm. lead plates. Series V.*

In order to increase the visibility of the tracks and to make it possible to distinguish possible "heavy" tracks from contamination α-particles, alternate plates were removed.

One thousand two hundred and seventy-six photographs, showing at least one particle penetrating all the plates, were taken with this arrangement. Seven examples of pairs of A.P.P. originating above the chamber and traversing the lead plates were observed. Two cases of pairs of A.P.P. originating in the lead plates in the chamber and one penetrating shower produced in a lead plate in the chamber were found. Two photographs showed three penetrating particles entering and traversing the chamber. For ease of comparison an analysis of all the penetrating events observed is given in the table below.

Table I.

Series	Total sensitive time in hrs.	No. of apparent pairs produced		No. of penetrating showers produced	
		In lead	Externally	In lead	Externally
I.	27·5	—	13	—	0
II.	52	4	8	0	0
III.	480	12	18	0	0
IV.	18	1	1	1	0
V.	142	2	8	2	2

§ 4. Discussion of Results on Pairs of Associated Penetrating Particles.

4.1. *Random associations.*

It is necessary to consider the possibility that these pairs of A.P.P. are due to random associations. When the pairs are produced in the lead inside the chamber the probability of random association is negligible. When the pairs are produced above the chamber we impose the following criteria :—

(*a*) The pairs must be visually contemporary in the chamber and parallel or diverging downwards.

(*b*) On reprojection the pairs must appear coplanar to within about 2°.

The number of random associations expected on criterion (*a*) is approximately 1 in 1000 for the cylindrical chamber and approximately 20 in 1000 for the multiple plate chamber. Criterion (*b*) reduces these figures by a factor of about 20. Many of the pairs rejected due to criterion (*b*) are probably genuine pairs of associated penetrating particles, for which the lack of coplanarity is due to the effect of scattering in the lead or sandstone.

4.2. *Knock-on electrons.*

Mesons traversing matter are known to give energy to electrons by collision (knock-on process), and it is necessary to consider whether any of the events appearing as cases of pair production are really events of this type. In the arrangements IV. and V., where the particles are observed to penetrate several plates without the production of electron showers, the probability of their being electrons is negligible.

In the arrangements I., II. and III. the particles are observed penetrating only one plate in the chamber and the probability of their being electrons must be calculated.

Consider the arrangement used in series II. and III. A meson accompanied by a knock-on electron produced in the 3 cm. lead above the chamber where both particles penetrate the 2 cm. lead plate inside the chamber, would probably satisfy the criteria for acceptance as a pair. The theoretical energy distribution of electrons knocked-on by the meson spectrum was obtained, and for each energy the probability of the electron emerging from the upper plate and passing without multiplication through the lower plate was calculated. For the final electron distribution, the scattering distribution of fig. 2 was calculated and compared with the observed scattering.

It is seen that very few of the pair particles which show small deflections are likely to be knock-on electrons, although the few particles which are scattered through large angles could be explained in this way.

A further indication that the pair events in general are not knock-on electrons is given by the fact that there is no correlation between the angle between the particles of a pair and the angle of scattering of the more scattered particle. In a knock-on process, a small pair angle would be correlated with high electron energy and small scattering angle. We may conclude that most of the pairs of associated penetrating particles, observed in series II. and III. and originating in the lead above the chamber, are genuine.

In series I. the same argument may be applied to pairs which originate in the sandstone roof, and we conclude that the pairs are genuine.

In series II. and III. any electrons which originate in the roof would have to pass through two lead plates to qualify as components of pairs, and we consider that all the pairs enumerated are genuine. The possibility that electrons secondary to meson bremsstrahlung might simulate A.P.P. has been considered and found to be negligible.

From the above considerations, it is clear that associated penetrating particles do exist. It is now necessary to consider whether the production of these A.P.P. can be explained by known processes.

4.3. *Nature of primaries.*

The nucleon component which is mainly responsible for the production of penetrating showers at sea level is highly absorbed with an absorption length $\sim$100 gm./cm.^{2}. Thus the probability that a nucleon arrives at the underground station is $\sim e^{-26}$. This is far too small to account for the observed number of pairs.

The possibility that these events are π-meson induced is excluded if it is assumed that the absorption length for π-mesons is the same as that for nucleons. However, the behaviour of high energy π-mesons (energy $\sim 10^9$ eV.) is not at all clear. It is possible to eliminate π-mesons from sea level as the primaries responsible for pairs observed

Fig. 2.

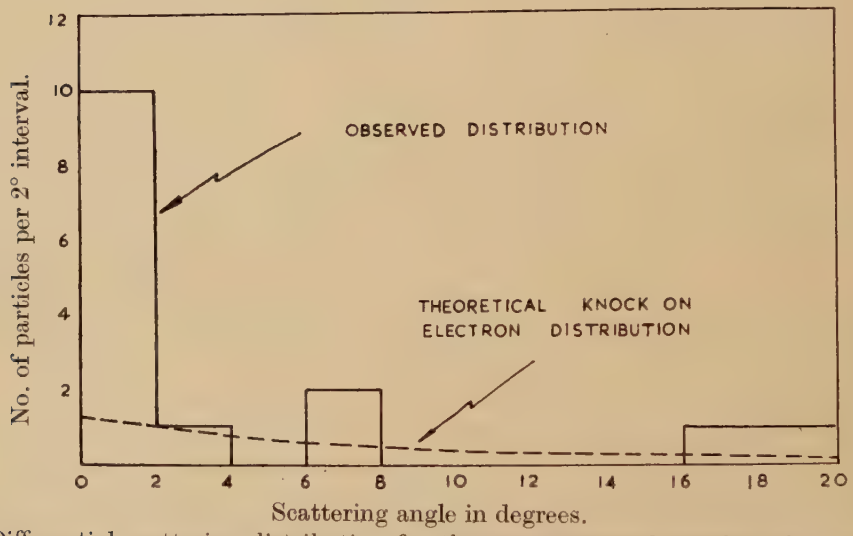

Differential scattering distribution for the more scattered member of a pair, originating in the lead absorber above the chamber, in Series II. and III.

underground on the following considerations. Let us assume as the most unfavourable case that all mesons with $E > 10^{11}$ eV. at sea level are π-mesons since π-mesons of this energy produced near the top of the atmosphere will not have had time to decay before they reach sea level. Such π-mesons would be 1/4000 of the total cosmic ray flux at sea level. In addition there are at sea level a small number of π-mesons produced locally; these have however limited range and decay to form μ-mesons. In order to account for the observed rate of production of pairs of A.P.P. in terms of production by π-mesons, all the high energy π-mesons must reach the underground station and then must all interact in 3 cm. Pb. This is obviously impossible.

The above considerations eliminate nucleons and π-mesons as the source of pairs. Unless we assume that these events are induced by unknown particles the only particles which remain in sufficient numbers are μ-mesons.

4.4. *Nature of the pair particles.*

In these experiments the main indication of the nature of the pair particles is given by their scattering on traversing the lead plates in the cloud chambers.

Fig. 3.

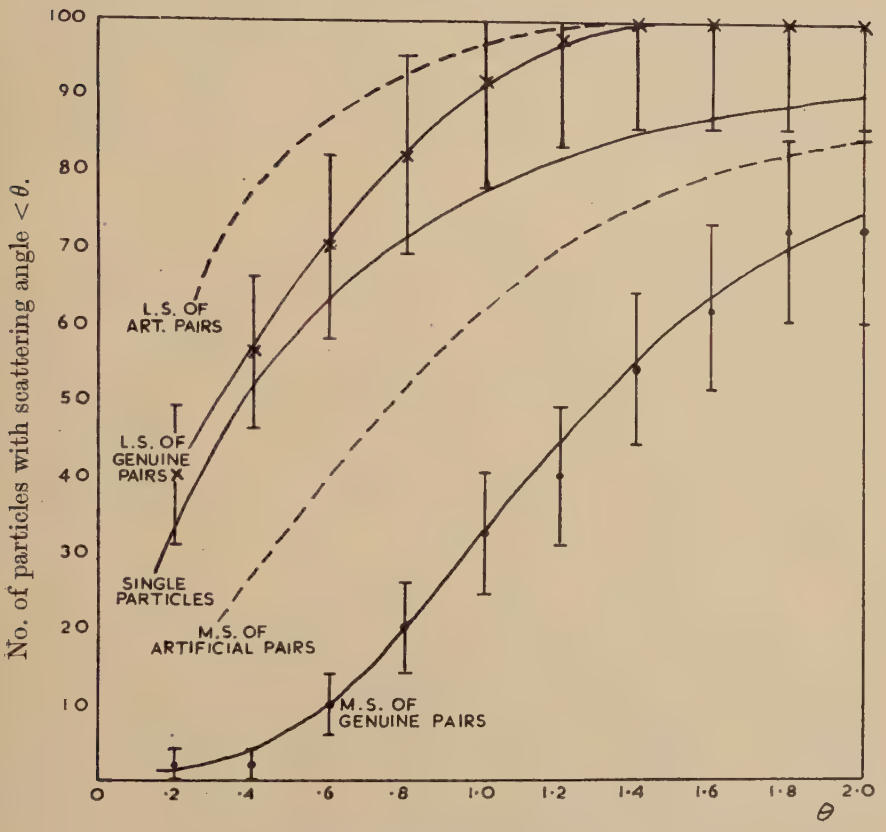

Scattering angle in degrees.

Comparison of the integral scattering distributions.

In series I., II. and III. accurate scattering measurements were possible to within 0·1° and the scattering of each member of the pair in the 2 cm. lead block was measured using a low power microscope fitted with a goniometer eyepiece. The pair particles were divided into two groups, containing respectively the less and more scattered members (L.S. and M.S.) of each pair. The integral scattering distributions, together with that for single particles, are shown in fig. 3. It is

seen that the less scattered members can be correlated with the single particles, *i. e.* the normal μ-mesons beam present at the station. On the other hand, the more scattered members are obviously not the normal μ-mesons. In order to determine whether the difference in the distributions is due to the method of analysis the scattering angles for single penetrating particles were measured, these were taken in pairs and the distributions for the more and less scattered members of these artificial pairs plotted. It can be seen that the difference in the distributions for the genuine pairs cannot be explained in this way. It is concluded that the more scattered member or penetrating secondary, as we will call it, is probably a μ-meson of mean energy $\sim 10^9$ eV., although the possibility of its being a π-meson cannot be ruled out.

Observations in series IV. and V. show that as a rule the penetrating secondary has energy greater than 10^9 eV., only one case being observed where it has energy less than this. This result is not consistent with that just given.

TABLE II.

Cross-section for production of pairs of A.P.P. in lead.

Series	Metres of Pb. traversed by s	Observed No. of pairs accepted	Corrected No. of pairs produced	Interaction length in metres of Pb.	Cross-section in cm.^{2}/nucleon
II.	78	3	3	26	$5{\cdot}7\times10^{-29}$
III.	1150	9	30	38	$4{\cdot}0\times10^{-29}$
IV. } V. }	89	3	3	30	$5{\cdot}0\times10^{-29}$

4·5. *Cross-section for the production of pairs in lead.*

Assuming that the primary responsible for the production of a pair is a μ-meson, and that the interaction is between the μ-meson and a nucleon, it is possible to calculate a cross-section for the process.

In the results of series III. corrections have been applied for loss of efficiency due to (*a*) the split tray arrangement, and (*b*) the narrow angle pairs lost due to the finite size of the counters.

Angular distribution of pair particles.

A histogram of the angular distribution of pair particles originating in the lead absorber in series II. and III. is shown in fig. 4. A correction has been applied for narrow angle pairs lost in the split tray experiments as mentioned previously.

4.6. *Pairs entering from outside the chamber.*

Quantitative results for these events are difficult to evaluate owing to the effects of scattering in the sandstone. A pair of A.P.P. originating

in the sandstone and being scattered through an appreciable angle before entering the cloud chamber will be rejected under the criteria for selection mentioned in § 4.1.

The angular distribution is very similar to that for pairs originating in the lead, indicating that the events are of a similar nature.

Cross-section for production of pairs of A.P.P. in sandstone.

This determination demands a knowledge of the angular distribution and energy of the pair particles since these quantities determine how thick a layer of sandstone is effective. From what has been said previously concerning the nature of the pair particles it seems probable that the penetrating secondary is a meson (μ or π) of mean energy $\sim 10^9$ eV.

Fig. 4.

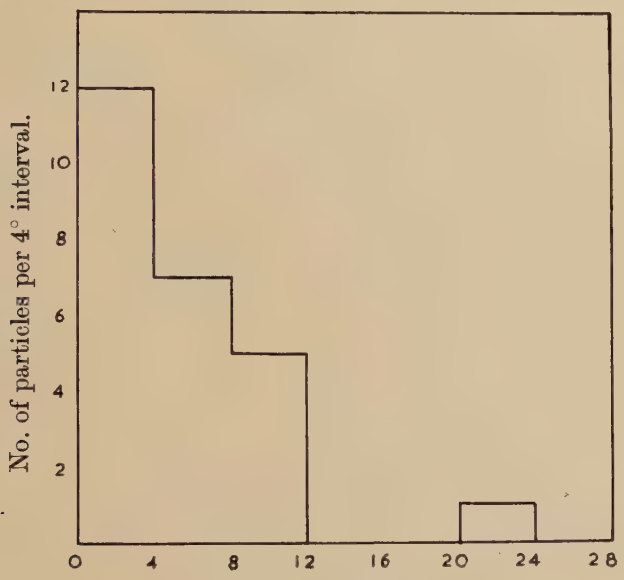

Pair angle in degrees.

Corrected angular distribution of pair particles, originating in the lead absorber above the chamber, in Series II. and III.

Assuming a unique energy of formation of 10^9 eV. for the penetrating secondary an estimate of the cross-section for sandstone can be made; this neglects the effects of scattering previously mentioned and so the value obtained for the cross-section is a lower limit.

An estimate of the absolute lower limit to the value of the cross-section for sandstone production can be made by assuming that the penetrating secondary has infinite energy (instead of 10^9 eV.), in this case the whole thickness of sandstone above the equipment contributes to the flux of pairs crossing the cloud chambers. This calculation has been made assuming the Gaussian distribution of pair angles approximating to the histogram in fig. 4.

The cross-sections calculated are 1/3 of those given in Table II. Thus the cross-section for sandstone production of pairs is in any case greater than 5×10^{-30} cm.^{2} per nucleon.

Apparent pairs produced in air.

Three cases in each of series I. and V. have been found in which pairs of A.P.P. appear to have originated in the air above the cloud chambers. The pair angles and probable angles of scattering in the lead plates inside the cloud chambers are such that the cases cannot be explained in terms of scattering in the roofs of the chambers. The probability that these cases are examples of the random association of two particles is low, but this possibility cannot be entirely ruled out. Further investigations must be carried out before this phenomenon can be established.

Table III.

Cross-section for production of pairs of A.P.P.'s in sandstone assuming a unique energy of formation of 10^9 eV.

Series	No. of single mesons traversing chamber	No. of pairs observed	Cross-section in cm.^{2}/nucleon
I.	2200	9	5×10^{-29}
II.	2600	8	$3{\cdot}5\times10^{-29}$
III.	24000	18	$1{\cdot}5\times10^{-29}$
IV. V.	1500	5	3×10^{-29}

§5. Penetrating Showers.

In series IV. and V. two cases have been observed of penetrating showers of low multiplicity produced in the chamber. These showers differ from those observed at sea level in that the penetrating particles are emitted at large angles to the direction of the incident particle.

Two cases have been found where three A.P.P. enter the cloud chamber, and in each case one of the penetrating particles suffers two large angle deflections in the lead plate. It is probable that these deflected particles are π-mesons from a penetrating shower produced in the sandstone. Several cases of three or more parallel A.P.P. incident obliquely in the cloud chamber and penetrating a few lead plates have been observed, these are probably remnants of the penetrating particles present in extensive air showers.

§6. Comparison with other Observations.

Braddick and Hensby (1939) using an arrangement similar to that for series I.–III. at 60 mwe. found five cases of pairs of A.P.P. out of 2000 photographs taken with a counter selection system requiring one penetrating particle. This rate is similar to that found in this

investigation. George and Trent (1951), using a cloud chamber containing two 3 cm. lead plates, have found two cases of pairs of A.P.P., out of 1500 photographs, originating in the upper lead plate and traversing the lower one without deflection. Both these experiments were carried out at a depth of 60 mwe. These experiments show about the same cross-section as ours, and this result is in provisional agreement with the hypothesis that the pairs are produced by μ-mesons. However, the statistical weight of these experiments is as yet very low. Experiments by Shutt (1946) at sea level using a cloud chamber under 88 cm. lead showed the existence of pairs of A.P.P. The cross-section calculated from Shutt's results is $\sim 10^{-29}$ cm.^{2}/nucleon for pair production in lead and agrees with that found in the present investigations within the statistical errors involved. George and Jason (1947), using a penetrating shower counter set requiring at least three A.P.P. at a depth of 60 mwe., found no coincidences in 45 days continuous recording. George and Trent (1949), however, using a counter set of lower selectivity, found events which could be explained in terms of the production of penetrating groups of mesons of low multiplicity, by mesons. A cross-section of 5×10^{-29} cm.^{2}/nucleon has been calculated for the production of these showers in lead, this value compares well with that found in this investigation for the production of pairs. George and Evans (1950) have found stars and penetrating showers produced by μ-mesons in photographic emulsions exposed underground. The cross-sections found for these events are $\sim 10^{-29}$ cm.^{2}/nucleon for stars and $\sim 4 \cdot 10^{-30}$ cm.^{2}/nucleon for penetrating showers. The shower particles observed by George and Evans are π-mesons and the most probable multiplicity is about three : a multiplicity of shower particles as high as eight has been observed. The two cases in the present investigation in which three penetrating particles are observed are probably events of this type. The majority of the pairs of A.P.P. observed in our experiments cannot be explained in terms of penetrating showers containing two penetrating particles, since the total cross-section for shower production calculated by George and Evans is only $4 \cdot 10^{-30}$ cm.^{2} per nucleon and showers containing only two particles form a small proportion of the showers observed. It is likely that the production of a pair of A.P.P. is an event of a more elementary type than the production of a penetrating shower. If heavy particles are associated with these events it seems certain that they would have been observed in photographic plate experiments, and we are led to infer that the interaction observed is one in which a μ-meson produces only a single penetrating secondary.

Conclusions.

(1) μ-mesons produce penetrating secondaries on passing through matter, one penetrating secondary being produced in each event.

(2) The cross-section for this process is $\sim 5 \times 10^{-29}$ cm.^{2}/nucleon for lead and of the same order of magnitude (certainly greater than 5×10^{-30} cm.^{2}/nucleon) for sandstone.

(3) The penetrating secondary is probably a μ-meson of mean energy $\sim 10^9$ eV., but there is a possibility that it is a π-meson.

Acknowledgments.

We are glad to record our indebtedness to Professor P. M. S. Blackett for his interest in these experiments, to Dr. J. G. Wilson, Dr. E. P. George and Dr. P. T. Trent for discussion. We thank also Stockport Corporation for permission to work in the cave, and its officers for help in examining the caves and determining their position. W. F. Nash and A. W. Wolfendale are indebted to the D.S.I.R. for maintenance grants.

References.

Braddick, H. J. J., and Hensby, G. S., 1939, *Nature*, **14,** 1012.
George, E. P., and Evans, J., 1950, *Proc. Phys. Soc.*, **63,** 1248.
George, E. P., and Jason, A. C., 1949, *Nature*, **160,** 327.
George, E. P., and Trent, P. T., 1949, *Nature*, **164,** 838.
George, E. P., and Trent, P. T., 1951, Private communication.
Greisen, K., Cocconi, G., and Bollinger, L. M., 1951, *Phys. Rev.*, **82,** 294.
Shutt, R. P., 1946, *Phys. Rev.*, **69,** 261.

CXXVII. *On Field Theories with Non-localized Interaction.*

By Jerzy Rayski,
Nicolas Copernicus University, Torun, Poland*.

[Received June 13, 1951.]

Summary.

It is shown that a method of direct quantization of field equations (completely avoiding the canonical formalism) is applicable to a wide class of fields with a non-local interaction. In §1 the extended source theory of Peierls and McManus is quantized and discussed. The S-matrix is computed by the method of C. N. Yang. A general rule for an immediate transcription of the traditional S-matrix elements into the new form is given. In §2 another type of a non-local interaction is discussed and it is shown that all the usual covergence difficulties may be easily avoided if we give up the strict localizability of charge, energy, etc., and if we abandon the postulate of gauge invariance of the second kind. This is acceptable since it is possible to guarantee the integral conservation laws without the continuity equations and to secure a vanishing photon rest mass by other devices, not necessarily by the formal gauge invariance. In the limit $\lambda \to 0$ where λ is a fundamental length, the discussed field theory goes over into the traditional quantum electrodynamics.

§1. Quantization of the Peierls and McManus Field.

Let us discuss first the field described by Peierls and McManus (1948) with the following Lagrangian

$$L = L^{(0)} + L', \quad . \quad . \quad . \quad . \quad . \quad . \quad . \quad . \quad (1)$$

where $L^{(0)}$ is the usual Lagrangian for the electromagnetic and spinor fields without interaction while the interaction part L' is

$$L' = \tfrac{1}{2} \int d^4x \{ j_\mu(x), A_\mu^R(x) \}, \quad . \quad . \quad . \quad . \quad . \quad . \quad . \quad (2)$$

where

$$\{a, b\} = ab + ba, \quad . \quad . \quad . \quad . \quad . \quad . \quad . \quad . \quad . \quad (3)$$

while

$$a^R(x) = \int d^4x' F(x - x') a(x'), \quad . \quad . \quad . \quad . \quad . \quad . \quad . \quad (4)$$

where $F(x)$ is a function of the argument $x_\mu x_\mu$. In order to get a correspondence with the tranditional theory $F(x)$ should be a delta-like function

$$F(x) = \frac{1}{(2\pi)^4} \int d^4k \exp(ik_\mu x_\mu) f(k_\mu^2, \lambda), \quad . \quad . \quad . \quad . \quad . \quad (5)$$

* Communicated by Professor R. E. Peierls, F.R.S.

where the Fourier transform $f(k_\mu^2, \lambda)$ is a function of $k_\mu k_\mu$ and of a parameter λ with the dimension of length. We may assume, *e. g.*

$$f(k_\mu^2, \lambda)=1/1+(\lambda^2 k_\mu^2)^2 \quad \text{or} \quad f(k_\mu^2, \lambda^2)=\exp\{-(\lambda^2 k_\mu^2)^2\}, \quad . \quad . \quad (6)$$

which become unity in the limit $\lambda \to 0$. We notice the following properties :

$$\int d^4x \mathrm{F}(x)=1, \quad f(0, \lambda)=1 \quad . \quad . \quad . \quad . \quad . \quad . \quad . \quad (7)$$

whence we get the identity

$$\mathrm{A}_\mu^{(0)\mathrm{R}} \equiv \mathrm{A}_\mu^{(0)}, \quad . \quad . \quad . \quad . \quad . \quad . \quad . \quad . \quad (8)$$

where the index zero means an unperturbed field obeying the Laplace equation

$$\Box \mathrm{A}_\mu^{(0)}=0. \quad . \quad . \quad . \quad . \quad . \quad . \quad . \quad . \quad (9)$$

The interaction part of the Lagrangian may also be written as

$$\mathrm{L}'=\tfrac{1}{2}\int d^4x\{j_\mu^{\mathrm{R}}(x), \mathrm{A}_\mu(x)\}. \quad . \quad . \quad . \quad . \quad . \quad . \quad . \quad (10)$$

The Lagrange equations are

$$\Box \mathrm{A}_\mu=-j_\mu^{\mathrm{R}}, \quad . \quad . \quad . \quad . \quad . \quad . \quad . \quad . \quad (11')$$

$$\gamma^\mu \frac{\partial \psi}{\partial x_\mu}+m\psi=(ie/2)\{\gamma^\mu \psi, \mathrm{A}_\mu^{\mathrm{R}}\}, \quad . \quad . \quad . \quad . \quad (11'')$$

$$\frac{\partial \bar{\psi}}{\partial x_\mu}\gamma^\mu - m\bar{\psi}=-(ie/2)\{A_\mu^{\mathrm{R}}, \bar{\psi}\gamma^\mu\}. \quad . \quad . \quad . \quad . \quad (11''')$$

The above equations are invariant under the usual gauge transformation

$$\mathrm{A}_\mu \to \mathrm{A}_\mu - \frac{\partial \Lambda}{\partial x_\mu}, \quad \psi \to \psi \exp(-ie\Lambda), \quad . \quad . \quad . \quad . \quad (12)$$

where

$$\Box \Lambda=0. \quad . \quad . \quad . \quad . \quad . \quad . \quad . \quad . \quad (12')$$

To prove the invariance we use the fact that Λ^{R} is identical with Λ. Equations (11) may be replaced by the equivalent integral equations expressed by means of retarded and advanced potentials (compare C. N. Yang (1950) and G. Källén (1950).

$$\mathrm{A}_\mu(x)=\mathrm{A}_\mu^{\mathrm{in}}(x)+\int d^4x' \mathrm{D}^{\mathrm{ret}}(x-x') j_\mu^{\mathrm{R}}(x'), \quad . \quad . \quad . \quad . \quad (13')$$

$$\psi(x)=\psi^{\mathrm{in}}(x)+(e/2i)\int d^4x' \mathrm{S}^{\mathrm{ret}}(x-x')\{\gamma^\mu \psi(x'), \mathrm{A}_\mu^{\mathrm{R}}(x')\}, \quad . \quad (13'')$$

$$\bar{\psi}(x)=\bar{\psi}^{\mathrm{out}}(x)+(e/2i)\int d^4x' \{\mathrm{A}_\mu^{\mathrm{R}}(x'), \bar{\psi}(x')\gamma^\mu\}\mathrm{S}^{\mathrm{ret}}(x'-x), \quad . \quad (13''')$$

where $$\mathrm{D}^{\mathrm{ret}}=\overline{\mathrm{D}}-\tfrac{1}{2}\mathrm{D}, \quad \mathrm{S}^{\mathrm{ret}}=\overline{\mathrm{S}}-\tfrac{1}{2}\mathrm{S}, \quad . \quad . \quad . \quad . \quad . \quad . \quad (14)$$

$$\mathrm{A}_\mu(x)=\mathrm{A}_\mu^{\mathrm{out}}(x)+\int d^4x' \mathrm{D}^{\mathrm{adv}}(x-x') j_\mu^{\mathrm{R}}(x'), \quad . \quad . \quad . \quad . \quad (15')$$

$$\psi(x)=\psi^{\mathrm{out}}(x)+(e/2i)\int d^4x' \mathrm{S}^{\mathrm{adv}}(x-x')\{\gamma^\mu \psi(x'), \mathrm{A}_\mu^{\mathrm{R}}(x')\}, \quad (15'')$$

$$\bar{\psi}(x)=\bar{\psi}^{\mathrm{in}}(x)+(e/2i)\int d^4x' \{\mathrm{A}_\mu^{\mathrm{R}}(x'), \bar{\psi}(x')\gamma^\mu\}\mathrm{S}^{\mathrm{adv}}(x'-x), \quad . \quad (15''')$$

where $$\mathrm{D}^{\mathrm{adv}}=\overline{\mathrm{D}}+\tfrac{1}{2}\mathrm{D}, \quad \mathrm{S}^{\mathrm{adv}}=\overline{\mathrm{S}}+\tfrac{1}{2}\mathrm{S}. \quad . \quad . \quad . \quad . \quad . \quad (16)$$

We may write equations (13′) and (15′) also in the form

$$\mathrm{A}_\mu^{\mathrm{R}}(x)=\mathrm{A}_\mu^{\mathrm{R\ in\ (out)}}(x)+\int d^4x' \mathrm{D}^{\mathrm{R\,R\ ret\ (adv)}}(x-x') j_\mu(x').$$

By adding together the equations (13) and (15) we get

$$A_\mu^R(x)=A_\mu^{(0)R}(x)+\int d^4x' \bar{D}^{RR}(x-x')j_\mu(x'), \quad . \quad . \quad . \quad . \quad . \quad . \quad (17')$$

$$\psi(x)=\psi^{(0)}(x)+(e/2i)\int d^4x' \bar{S}(x-x')\{\gamma^\mu\psi(x'), \quad A_\mu^R(x')\}, \quad . \quad (17'')$$

$$\bar{\psi}(x)=\bar{\psi}^{(0)}(x)+(e/2i)\int d^4x' \{A_\mu^R(x'), \quad \bar{\psi}(x')\gamma^\mu\}\bar{S}(x'-x), \quad . \quad (17''')$$

where $A_\mu^{(0)}$, $\psi^{(0)}$, $\bar{\psi}^{(0)}$ mean half the sum of the ingoing and outgoing waves, *e. g.*

$$A_\mu^{(0)}=\tfrac{1}{2}(A_\mu^{in}+A_\mu^{out}). \quad . \quad . \quad . \quad . \quad . \quad . \quad . \quad (18)$$

By subtracting the equations (13) and (15) we get

$$A_\mu^{R\,in}(x)-A_\mu^{R\,out}=\int d^4x' D^{RR}(x-x')j_\mu(x'), \quad . \quad . \quad . \quad . \quad . \quad . \quad (19')$$

$$\psi^{in}(x)-\psi^{out}(x)=(e/2i)\int d^4x' S(x-x')\{\gamma^\mu\psi(x'), \quad A_\mu(x')\}, \quad . \quad . \quad (19'')$$

$$\bar{\psi}^{in}(x)-\bar{\psi}^{out}(x)=-(e/2i)\int d^4x' \{A_\mu(x'), \quad \bar{\psi}(x')\gamma^\mu\}S(x'-x).$$

$$. \quad . \quad . \quad (19''')$$

The traditional Hamiltonian formalism is not adequate for the quantization of fields with a non-local interaction. On the other hand it is possible to quantize directly the fundamental integral equations (13) and (15) or the equivalent (17) and (19) by assuming the usual (interaction-free) commutation relations for the ingoing and outgoing waves. The same relations hold for $A_\mu^{(0)}$, $\psi^{(0)}$ and $\bar{\psi}^{(0)}$:

$$[A_\mu^{(0)}(x), \quad A_\nu^{(0)}(x')]=i\delta_{\mu\nu}D(x-x'), \quad . \quad . \quad . \quad . \quad . \quad . \quad . \quad . \quad . \quad (20')$$

$$\{\psi^{(0)}(x), \quad \bar{\psi}^{(0)}(x')\}=-iS(x-x'), \quad . \quad . \quad . \quad . \quad . \quad . \quad . \quad . \quad . \quad (20'')$$

$$\{\psi^{(0)}(x), \quad \psi^{(0)}(x')\}=\{\bar{\psi}^{(0)}(x), \quad \bar{\psi}^{(0)}(x')\}$$

$$=[A_\mu^{(0)}(x), \quad \psi^{(0)}(x')]=[A_\mu^{(0)}(x), \quad \bar{\psi}^{(0)}(x')]=0. \quad (20''')$$

The commutation relations between the perturbed waves follow automatically from the field equations (13) or (15) or (17) which may be solved successively in a power expansion of the coupling parameter e. For the quantization of the field equations it is essential to symmetrize the expression for the product of ψ and A_μ^R since these quantities do not commute with each other in case of a non-local interaction. We should also use the symmetrized current

$$j_\mu=(ie/2)[\bar{\psi}, \quad \gamma^\mu\psi]. \quad . \quad . \quad . \quad . \quad . \quad . \quad . \quad . \quad (21)$$

Although we do not know the exact form of the commutation relations between the perturbed wave functions (as the exact solution of the field equations is not known), we may surely find some general properties of the commutators or anticommutators, *e. g.*, the anticommutator between two perturbed spinor functions must be a covariant function of the argument $x_\mu-x'_\mu$:

$$\{\psi_\alpha(x), \bar{\psi}_\beta(x')\}=-iU_{\alpha\beta}(x-x'). \quad . \quad . \quad . \quad . \quad . \quad (22)$$

which follows from the invariance of the formalism under space and time translations. Hence, for the perturbed wave functions taken at the same space-time point x_μ we have the same commutations relations as for the unperturbed ones

$$U_{\alpha\beta}(0)=S_{\alpha\beta}(0), \quad . \quad . \quad . \quad . \quad . \quad . \quad . \quad . \quad (23)$$

since we may translate the common point x_μ to the infinite past (or future) where we have to do with the ingoing (or outgoing) waves only.

This last property enables the proof of the validity of the continuity equation for the perturbed current j_μ. By multiplying (11'') and (11''') to the right or left by $\bar{\psi}$ and ψ we get

$$\frac{\partial}{\partial x_\mu} j_\mu=(1/4)\gamma^\mu_{\alpha\beta}[\{\psi_\alpha(x), \bar{\psi}_\beta(x)\}, A^R_\mu(x)]=0, \quad . \quad . \quad . \quad (24)$$

since the anticommutator between two field functions taken at the same point is (from (23)) a number and, thus, commutes with everything. Also the averaged current obeys the continuity equation

$$\frac{\partial}{\partial x_\mu} j^R_\mu=0. \quad . \quad . \quad . \quad . \quad . \quad . \quad . \quad . \quad (24')$$

Due to (24) the problem of auxiliary condition is the same as in the usual quantum electrodynamics

$$\frac{\partial}{\partial x_\mu} A_\mu |\rangle=0. \quad . \quad . \quad . \quad . \quad . \quad . \quad . \quad . \quad (25)$$

We may develop the Lorentz condition in a Taylor series and show, as usual, that all terms of the expansion vanish (due to (11') and (24')) if two initial conditions

$$\frac{\partial}{\partial x_\mu} A_\mu(\vec{r}, t)|\rangle=0, \qquad \frac{\partial}{\partial x_\mu} \dot{A}_\mu(\vec{r}, t)|\rangle=0 \quad . \quad . \quad . \quad (26)$$
$$[t=t_0] \qquad\qquad [t=t_0]$$

are satisfied.

By applying the method described by C. N. Yang (1950) we may construct the S-matrix for the extended source theory. Since the ingoing and outgoing waves satisfy the same commutation relations, there should exist a unitary matrix transforming the ingoing into the outgoing waves

$$A^{out}=S^{-1}A^{in}S, \quad \psi^{out}=S^{-1}\psi^{in}S. \quad . \quad . \quad . \quad . \quad . \quad (27)$$

From (17), (19) and (27) we get

$$[A^{(0)R}_\mu S]=-\tfrac{1}{2}\{S, \int d^4x' D^{RR}(x-x')j_\mu(x')\}, \quad . \quad . \quad . \quad . \quad (28')$$

$$[\psi^{(0)}, S]=-(e/4i)\{S, \int d^4x' S(x-x')\{\gamma^\mu\psi(x'), A^R_\mu(x')\}\}, \quad . \quad . \quad (28'')$$

$$[\bar{\psi}^{(0)}, S]=(e/4i)\{S, \int d^4x'\{A^R_\mu(x'), \bar{\psi}(x')\gamma^\mu\}S(x'-x)\}. \quad . \quad (28''')$$

From (17) and (28) the S-matrix may be computed as a power series in the coupling constant e

$$S=1+\sum_{n=1}^{\infty} R^{(n)}. \quad . \quad . \quad . \quad . \quad . \quad . \quad . \quad . \quad (29)$$

The explicit computation of $R^{(1)}$ and $R^{(2)}$ shows that the equations (17) and (28) are compatible in this approximation and yield the result

$$R^{(1)}=i\int d^4x A_\mu^{(0)R} j_\mu^{(0)}, \quad \ldots\ldots\ldots \quad (30')$$

$$R^{(2)}=\tfrac{1}{2}(R^{(1)})^2+P+Q, \quad \ldots\ldots\ldots \quad (30'')$$

where

$$P=\frac{i}{2}\int\int d^4x'd^4x''\{j_\mu^{(0)}(x'),\ j_\mu^{(0)}(x'')\}\bar{D}^{RR}(x'-x''), \quad \ldots \quad (30''')$$

$$Q=(ie^2/8)\int\int d^4x'd^4x''([\bar{\psi}^{(0)}(x'')\gamma^\mu\bar{S}(x''-x'),\ \gamma^\lambda\psi^{(0)}(x')]$$
$$+[\bar{\psi}^{(0)}(x'),\ \gamma^\lambda\bar{S}(x'-x'')\gamma^\mu\psi^{(0)}(x'')])\{A_\lambda^{(0)R}(x'),\ A_\mu^{(0)R}(x'')\}.$$
$$\ldots \quad (30^{iv})$$

The S-matrix is obviously unitary in this approximation and differs from the usual one merely by the fact that every A_μ has been replaced by the averaged A_μ^R and every $\bar{D}$ has been replaced by the twice averaged $\bar{D}^{RR}$. This is exactly the same replacement which converts the traditional equations of a local theory into our new fundamental equations (17) and (28). We may easily guess the form of the S-matrix elements in all higher approximations. They will differ from the traditional ones by the same replacements which convert the usual field equations into the new equations (17) and (28). However, in the S-matrix elements appear only the unperturbed potentials $A_\mu^{(0)}$ whence (taking account of (8)) the general rule for the transcription of the traditional S-matrix elements into the new form is very simple : *we have to replace every $\bar{D}$ function by the twice averaged* $\bar{D}^{RR}$ while every $A_\mu^{(0)}$ and every $D^{(1)}$ function (which will be obtained by taking a vacuum expectation value) remain unchanged.

The very fact that it has been possible to construct a unitary S-matrix confirms the compatibility of the set of quantized equations (13) and (15).

We have to examine finally whether the extended source theory is able to improve the situation with respect to the convergence problem. The expressions of the vacuum polarization current and the photon self-energy remain unchanged (since the $\bar{D}$ function does not appear in the well-known tensor $K_{\mu\nu}$). On the other hand the expression for the self-mass of the electron derivable from the S-matrix is

$$\delta m=-\frac{e^2}{2}\int d^4x\gamma^\mu(S^{(1)}(x)\bar{D}^{RR}(x)+\bar{S}(x)D^{(1)}(x))\gamma^\mu \exp(-ip_\mu x_\mu). \quad (31)$$

If we assume a suitable function $F(x)$ the first term will converge while the second term is left unchanged and diverges.*

---

* A convergent expression for the electron self-energy could be obtained if we used the integrations of the causal function D_C of Stueckelberg and Feynman in the complex plane instead of Schwinger's $\bar{D}$ and $D^{(1)}$ functions integrated as principal values.

§ 2. Another Type of a Non-Local Interaction.

Let us investigate another type of non-local interaction derivable from the following Lagrangian

$$L=L^{(0)}+L', \quad . \quad . \quad . \quad . \quad . \quad . \quad . \quad . \quad . \quad (1)$$

where

$$L'=s_\mu A_\mu \quad . \quad . \quad . \quad . \quad . \quad . \quad . \quad . \quad . \quad (1')$$

with

$$s_\mu=(ie/2)[\bar{\psi}^R, \gamma^\mu\psi^R], \quad . \quad . \quad . \quad . \quad . \quad . \quad . \quad . \quad (2)$$

where ψ^R and $\bar{\psi}^R$ are the averaged spinor wave functions obtained with the aid of a general rule

$$a^R(x)=\int d^4x' G(x-x')a(x'). \quad . \quad . \quad . \quad . \quad . \quad . \quad (3)$$

G is again a delta-like function

$$G(x)=\frac{1}{(2\pi)^4}\int d^4k \exp(ik_\mu x_\mu) g(k_\mu^2, \lambda), \quad . \quad . \quad . \quad . \quad . \quad (4)$$

where

$$g(k_\mu^2, 0)=1. \quad . \quad . \quad . \quad . \quad . \quad . \quad . \quad . \quad . \quad (5)$$

For a spinor field *in vacuo* we have

$$\psi^{(0)R}(x)=g(-m^2, \lambda)\psi^{(0)}(x), \quad . \quad . \quad . \quad . \quad . \quad . \quad (6)$$

where m is the rest mass of the electron so that the current $s_\mu^{(0)}$ *in vacuo* differs from the usual current merely by a charge renormalization

$$e'=eg^2(-m^2, \lambda). \quad . \quad . \quad . \quad . \quad . \quad . \quad . \quad . \quad (7)$$

Thus, it will be convenient to use g-functions with the property

$$g(-m^2, \lambda)=1. \quad . \quad . \quad . \quad . \quad . \quad . \quad . \quad . \quad (8)$$

For example we may assume

$$g(k_\mu^2, \lambda)=\frac{1}{1+\lambda^4(k_\mu^2+m^2)^2} \quad \text{or} \quad g(k_\mu^2, \lambda)=\exp\{-\lambda^4(k_\mu^2+m^2)^2\}. \quad . \quad (9)$$

With such functions G the current $s_\mu^{(0)}$ will be identical with the usual $j_\mu^{(0)}$. On the other hand the property § 1 (7) is lost:

$$\int d^4x G(x)=g(0, \lambda), \quad . \quad . \quad . \quad . \quad . \quad . \quad . \quad (10)$$

where $g(0, \lambda)$ is different from unity but tends to unity for $\lambda\to 0$.

The field equations derivable from (1) are

$$\Box A_\mu=-s_\mu, \quad . \quad . \quad . \quad . \quad . \quad . \quad . \quad . \quad . \quad (11)$$

$$\gamma^\mu\frac{\partial\psi(x)}{\partial x_\mu}+m\psi(x)=ie\int d^4x' G(x-x')\gamma^\mu\psi^R(x')A_\mu(x') \quad . \quad . \quad (12)$$

with a similar equation for $\bar{\psi}$.

It should be noticed that, with this type of interaction, neither j_μ nor s_μ satisfy the continuity equations. This unusual feature of the field theory seems acceptable since it is possible to guarantee the integral conservation

laws without continuity equations. In particular, the charge conservation is secured simply by the gauge invariance of the first kind.* The non-existence of the continuity equation for the current four-vector should be interpreted as a fundamental uncertainty preventing a strict localizability of charge.

The field equations (11) and (12) violate the postulate of gauge invariance of the second kind.* The resignation of this postulate seems also acceptable since we may replace it by a less stringent requirement that the experimental rest mass of the photon should be zero. This may be achieved either by formal renormalization or by the so-called realistic compensation (Jost and Rayski 1949). In this respect the new formalism by no means constitutes any drawback in comparison with the traditional quantum electrodynamics which was gauge invariant only formally so that we were also obliged to remove the (infinite !) self-mass of the photon by means of a renormalization or compensation.

The equations (11) and (12) may be integrated by means of retarded potentials which yield

$$A_\mu(x)=A_\mu^{\text{in}}(x)+(ie/2)\int d^4x' D^{\text{ret}}(x-x')[\bar{\psi}^{\text{R}}(x'),\ \gamma^\mu\psi^{\text{R}}(x')], \quad . \quad (13)$$

$$\psi(x)=\psi^{\text{in}}(x)+(e/2i)\int d^4x' S^{\text{R ret}}(x-x')\{\gamma^\mu\psi^{\text{R}}(x'),\ A_\mu(x')\}, \quad . \quad (14)$$

where the products have been written in a symmetrized form. Similar equations hold for the advanced potentials. By adding and subtracting the equations with the retarded and advanced potentials we get

$$A_\mu(x)=A_\mu^{(0)}(x)+(ie/2)\int d^4x' \bar{D}(x-x')[\bar{\psi}^{\text{R}}(x'),\quad \gamma^\mu\psi^{\text{R}}(x')], \quad . \quad (15)$$

$$\psi(x)=\psi^{(0)}(x)+(e/2i)\int d^4x' \bar{S}^{\text{R}}(x-x')\{\gamma^\mu\psi^{\text{R}}(x'),\ A_\mu(x')\} \quad . \quad (16)$$

and

$$A_\mu^{\text{in}}(x)-A_\mu^{\text{out}}(x)=(ie/2)\int d^4x' D(x-x')[\bar{\psi}^{\text{R}}(x'),\ \gamma^\mu\psi^{\text{R}}(x'), \quad . \quad (17)$$

$$\psi^{\text{in}}(x)-\psi^{\text{out}}(x)=(e/2i)\int d^4x' S^{\text{R}}(x-x')\{\gamma^\mu\psi^{\text{R}}(x'),\ A_\mu(x')\} \quad . \quad (18)$$

where $\psi^{(0)}$ and $A_\mu^{(0)}$ mean half the sum of the ingoing and outgoing waves. From (16) and (18) we get analogous formulæ for the averaged ψ^{R}

$$\psi^{\text{R}}(x)=\psi^{(0)\text{R}}(x)+(e/2i)\int d^4x' \bar{S}^{\text{RR}}(x-x')\{\gamma^\mu\psi^{\text{R}}(x'),\ A_\mu(x')\}, \quad . \quad (16')$$

$$\psi^{\text{R in}}(x)-\psi^{\text{R out}}(x)=(e/2i)\int d^4x' S^{\text{RR}}(x-x')\{\gamma^\mu\psi^{\text{R}}(x'),\ A_\mu(x')\}. \quad . \quad (18')$$

We quantize directly the field equations by assuming again that the ingoing and outgoing waves satisfy the well-known commutation relations for the separate fields *in vacuo*. The commutation relations for the perturbed wave functions will follow automatically from the field equations.

The S-matrix may be computed from the formulæ

$$[A_\mu^{(0)},\ \mathbf{S}]=-(ie/4)[\mathbf{S},\ \int d^4x' D(x-x')[\bar{\psi}^{\text{R}}(x'),\ \gamma^\mu\psi^{\text{R}}(x')], \quad . \quad . \quad . \quad . \quad (19)$$

$$[\psi^{(0)\text{R}},\ \mathbf{S}]=-(e/4i)[\mathbf{S},\ \int d^4x' S^{\text{RR}}(x-x')\{\gamma^\mu\psi^{\text{R}}(x'),\ A_\mu(x')\}] \quad . \quad . \quad . \quad (20)$$

* For a definition of this, see Wentzel (1949), §§4, 11, 16.

with the aid of (15) and (16). There is little doubt in the compatibility of our fundamental formulæ and we may immediately guess the S-matrix elements in any approximation. They will be quite similar to the usual ones with the only difference that every $\psi^{(0)}$, $\bar{\psi}^{(0)}$ and $\bar{S}$ should be replaced by $\psi^{(0)R}$, $\bar{\psi}^{(0)R}$, and $\bar{S}^{RR}$. Due to (6) and (8) the general rule for an immediate transcription of the usual S-matrix into the new form is simply: *every* $\bar{S}$ *should be replaced by* $\bar{S}^{RR}$.

The new S-matrix elements yield non-vanishing probabilities only for processes in which energy, momentum and charge are conserved. Thus, integral conservation laws are secured in spite of the absence of the notion of densities satisfying continuity equations.

As the perturbed current s_μ does not satisfy the continuity equation, the question arises as to the form of the auxiliary condition. In order to answer this question we introduce (15) into (16) and get a new equation

$$\psi(x)=\psi^{(0)}(x)+(e/2i)\int d^4x'\bar{S}^R(x-x')\times\{\gamma^\mu\psi(x'),\ A_\mu^{(0)}(x')+\int d^4x''\bar{D}(x'-x'')s_\mu(x'')\} \quad . \ . \ . \quad (21)$$

(and a similar equation for $\bar{\psi}$) where only $A_\mu^{(0)}$, but not A_μ appear explicitly. In the same way, by substituting (15) into (20) we get new formulae for the computation of the S-matrix in which only the unperturbed potentials $A_\mu^{(0)}$ appear explicitly. Now (15) may be treated as a definition and not as one of the equations. Thus, the perturbed potentials A_μ become secondary quantities without influence upon the fundamental equations. Now we may limit ourselves to the unperturbed $A_\mu^{(0)}$ and assume the Lorentz condition as a restriction upon the state vector

$$\frac{\partial}{\partial x_\mu}A_\mu^{(0)}|\rangle=0, \quad . \ . \ . \ . \ . \ . \ . \quad (22)$$

which reduces to two well-known initial conditions, as usual, due to the fact that the unperturbed potentials obey the Laplace equation

$$\Box A_\mu^{(0)}=1. \quad . \ . \ . \ . \ . \ . \ . \ . \quad (23)$$

The computation of the vacuum polarization current yields now

$$\langle j_\mu(x)\rangle_{vac}=-4e^2\int d^4x'K_{\mu\nu}(x-x')A_\nu(x'), \quad . \ . \ . \ . \quad (24)$$

where

$$K_{\mu\nu}=\frac{\partial\bar{\Delta}^R}{\partial x_\mu}\frac{\partial\Delta^{(1)}}{\partial x_\nu}+\frac{\partial\bar{\Delta}^R}{\partial x_\nu}\frac{\partial\Delta^{(1)}}{\partial x_\mu}-\delta_{\mu\nu}\left(\frac{\partial\bar{\Delta}^R}{\partial x_\lambda}\frac{\partial\Delta^{(1)}}{\partial x_\lambda}-m^2\bar{\Delta}^R\Delta^{(1)}\right) \quad . \ . \quad (25)$$

or

$$\langle s_\mu(x)\rangle_{vac}=-4e^2\int d^4x'L_{\mu\nu}(x-x')A_\nu(x'), \quad . \ . \ . \quad (26)$$

where $L_{\mu\nu}$ differs from $K_{\mu\nu}$ merely by the fact that every $\bar{\Delta}$ is averaged twice, $\bar{\Delta}^{RR}$. The appearance of a $\bar{\Delta}^R$ or $\bar{\Delta}^{RR}$ changes essentially the situation in the problem of the induced current and secures convergence. The condition for the gauge invariance and the continuity equation for the induced current is, of course, violated as

$$\frac{\partial}{\partial x_\mu}K_{\mu\nu}=\delta^R\cdot\frac{\partial}{\partial x_\nu}\Delta^{(1)} \quad . \ . \ . \ . \ . \ . \quad (27)$$

is different from zero. However, the regularized delta function

$$\delta^{R}(x)=G(x) \quad . \quad . \quad . \quad . \quad . \quad . \quad . \quad . \quad (28)$$

is even and essentially different from zero only in the neighbourhood of zero while $\partial/\partial x_\nu \Delta^{(1)}$ is odd, so that (27) vanishes if integrated over a small region about the origin. Hence, the continuity equation and the gauge invariance are still valid in the mean. The photon self-energy and the self-charge are finite so that the procedures of mass and charge renormalization are now mathematically correct and may be applied consistently.

The electron self-energy derivable from the S-matrix is

$$\delta m=-(e^2/2)\int d^4x\gamma^\nu(S^{(1)}(x)\overline{D}(x)+\overline{S}^{RR}(x)D^{(1)}(x))\exp(-ip_\mu x_\mu), \quad . \quad (29)$$

where the second term is convergent but the first term still diverges. By comparing (29) with § I (31) we see that a full convergence may be achieved by combining both modifications discussed in this paper. The convergence will be generally secured if we assume the following Lagrangian

$$L'=(ie/4)\{[\bar{\psi}^{R}(x),\ \gamma^\mu\psi^{R}(x)],\ A^{R}_\mu(x)\}, \quad . \quad . \quad . \quad . \quad (30)$$

where ψ and $\bar{\psi}$ are averaged by means of a delta-like function $G(x)$ while A_μ is averaged by means of another delta-like function $F(x)$. The question of the definitive form of the delta-like function lies beyond the scope of the present investigation. We mention here only that other types of non-local field theories (*e. g.* the non-local field of Yukawa) may be quantized by the method of a direct quantization of field equations. An investigation of Yukawa's non-local field will be published by the author elsewhere.

Acknowledgment.

I thank Professor Rzewuski for making his paper on a related subject available to me prior to publication and for stimulating discussions.

References.

Jost, R., and Rayski, J., 1949, *Helv. Phys. Acta*, **22**, 457.
Källén, G., 1950, *Arkiv för Fysik*, **2**, 371.
Peierls, R., and McManus, H., 1948, *Proc. Roy. Soc.* A, **195**, 323.
Wentzel, G., 1949, *Quantum Theory of Fields* (Interscience Publishers).
Yang, C. N., and Feldman, D., 1950, *Phys. Rev.*, **79**, 972.

CXXVIII. *A Theoretical Derivation of the Plastic Properties of a Polycrystalline Face-Centred Metal.*

By J. F. W. Bishop and R. Hill,
H. H. Wills Physical Laboratory, University of Bristol†.

[Received June 22, 1951.]

Summary

In continuation of a previous paper (Bishop and Hill 1951) it is conjectured that the work done in plastically deforming a polycrystal is approximately equal to that which would be done if the grains were free to deform equally. In conjunction with the principle of maximum plastic work, this enables the yield function of an aggregate to be calculated. This is done for an isotropic aggregate of face-centred cubic crystals, following a determination of the stresses needed to produce multi-slip. The theoretical yield criterion lies between those of Tresca and von Mises, in good agreement with observaton for copper and aluminum. It is shown further that the work-hardening of an aggregate would be a function only of the total plastic work if the grains hardened equally; the departure from this functional relation is expressed explicitly in terms of the non-uniform hardening.

§ 1. Résumé of Previous Work.

In a recent paper (Bishop and Hill 1951, henceforward referred to as BH) some general theorems were proved for an aggregate in which the crystals individually deform by slip according to the Schmid law. The theorems depend, in essence, on a principle of maximum plastic work for a homogeneously deformed single crystal (BH, equation (9)). This principle states that if a crystal is caused to deform plastically through an increment of strain $d\epsilon_{ij}$, the work done by the required stress σ_{ij} is not less than that done by any other stress σ^*_{ij} not violating the yield condition; thus

$$(\sigma_{ij}-\sigma^*_{ij})\,d\epsilon_{ij}\geqslant 0. \quad . \quad . \quad . \quad . \quad . \quad . \quad . \quad . \quad (1)$$

The yield condition is that the component shear-stress in any of the possible slip-directions, and over the associated slip-planes, cannot exceed the corresponding critical shear-stress in the current state of hardening. The critical shear-stress may vary from one slip-direction to another, due to differential hardening, or may be different in the two opposite senses of the same slip-direction, due to a microscopic Bauschinger effect. In a statistically homogeneous aggregate, in which cohesion between crystals is maintained by multi-slip, the same principle was proved for the *macroscopic* stress S_{ij} and strain-increment dE_{ij}. (BH, equation (16)).

† Communicated by the Authors.

From this it was shown to follow immediately that, if the yield criterion for the aggregate is

$$f(S_{ij})=0 \quad . \quad . \quad . \quad . \quad . \quad . \quad . \quad . \quad . \quad (2)$$

in a certain state of hardening and anisotropy, then the relation between the ratios of the components of the stress and strain-increment tensors is

$$dE_{ij}=h\frac{\partial f}{\partial S_{ij}}\,df. \quad . \quad . \quad . \quad . \quad . \quad . \quad . \quad . \quad (3)$$

The function f is, moreover, concave to the origin when regarded as a surface in stress hyperspace, and does not involve the hydrostatic component of S_{ij}. h is a function of the stress and strain-history, controlling the *magnitude* of the strain-increment produced by a further increment of stress.

The plastic behaviour of an aggregate is thus completely determined by the functions f and h. The present paper is concerned with their calculation for an aggregate of face-centred cubic crystals.

§ 2. The Basic Theorem.

Since the actual stress distribution σ_{ij} is in equilibrium, it follows by virtual work that

$$\int(\sigma_{ij}\,dE_{ij})\,dV=S_{ij}\,dE_{ij},$$

where the integral extends over a unit cube of aggregate (see BH, equation (14) and succeeding remarks). Let σ^*_{ij} be a stress which, at each point of the aggregate, would produce the strain dE_{ij} in a free crystal having the local orientation and hardening. The distribution σ^*_{ij} is, of course, not necessarily in equilibrium. Then, by (1),

$$(\sigma^*_{ij}-\sigma_{ij})\,dE_{ij}\geqslant 0,$$

the equality holding in general only when the deviatoric parts of σ_{ij} and σ^*_{ij} are equal. Hence

$$S_{ij}\,dE_{ij}=\int(\sigma_{ij}\,dE_{ij})\,dV\leqslant dE_{ij}\int\sigma^*_{ij}\,dV. \quad . \quad . \quad . \quad . \quad . \quad (4)$$

On the other hand, by integrating (1) through a unit cube of aggregate, we obtain

$$S_{ij}\,dE_{ij}\geqslant\int(\sigma^*_{ij}\,d\epsilon_{ij})\,dV.$$

Assuming that there can be no statistical correlation between any components of σ^*_{ij} and $d\epsilon_{ij}$,

$$\int(\sigma^*_{ij}\,d\epsilon_{ij})\,dV=\int\sigma^*_{ij}\,dV\times\int(d\epsilon_{ij})\,dV=dE_{ij}\int\sigma^*_{ij}\,dV,$$

provided there is no rupture or relative sliding of the grains. Hence

$$S_{ij}\,dE_{ij}\geqslant dE_{ij}\int\sigma^*_{ij}\,dV. \quad . \quad . \quad . \quad . \quad . \quad . \quad . \quad (5)$$

On combining (4) and (5) we obtain the theorem on which the possibility of a calculation of the function f depends :

$$S_{ij}\,dE_{ij}=dE_{ij}\int\sigma^*_{ij}\,dV. \quad . \quad . \quad . \quad . \quad . \quad . \quad . \quad (6)$$

In words : the actual work done is equal to the work that would be done if the grains all underwent the same (macroscopic) strain.

In particular, when the slip-directions in any one grain all have the same critical shear-stress τ (in both senses), we may define an average value $\bar{\tau}$ for the aggregate, such that

$$\bar{\tau}=\int \tau \, dV.$$

Then, if σ^*_{ij} would produce a strain $d\mathrm{E}_{ij}$ in a grain with critical shear stress τ, $\bar{\sigma}^*_{ij}=\bar{\tau}\sigma^*_{ij}/\tau$ would produce the same strain in a grain of the same orientation but with critical shear stress $\bar{\tau}$. Hence

$$\bar{\tau}\int \sigma^*_{ij}\, dV=\int \tau \bar{\sigma}^*_{ij}\, dV=\bar{\tau}\int \bar{\sigma}^*_{ij}\, dV,$$

assuming that there is no correlation between $\bar{\sigma}^*_{ij}$ and τ. Therefore :

$$\int \sigma^*_{ij}\, dV=\int \bar{\sigma}^*_{ij}\, dV,$$

and so, from (6),

$$\mathrm{S}_{ij}\, d\mathrm{E}_{ij}=d\mathrm{E}_{ij}\int \bar{\sigma}^*_{ij}\, dV. \quad . \quad . \quad . \quad . \quad . \quad . \quad . \quad (7)$$

We can thus evaluate the work using the average value of the critical shear stress in the aggregate.

But equations (5) and (6) cannot be strictly true since (6) implies that the deviatoric part of σ_{ij} is equal to that of σ^*_{ij}, all components of which are generally discontinuous across grain boundaries or wherever else the lattice orientation changes. (It is shown later that a general strain can only be produced by some one of a *finite* set of stresses.) However, we are inclined to think (though we have not found a rigorous proof) that equation (6) is not much in error, and we assume it as an approximation.

§ 3. Method of Calculation of the Yield Function.

The way in which f can be calculated is conveniently visualized geometrically. A strain increment $d\mathrm{E}_{ij}$ can be considered as a free vector in stress hyperspace. According to (6) the scalar product $\mathrm{S}_{ij}\, d\mathrm{E}_{ij}$ is calculable in terms of the slip properties of a single crystal. The extremity of the stress vector S_{ij}, corresponding to a strain-increment $d\mathrm{E}_{ij}$, is thus known to lie on a plane which is perpendicular to $d\mathrm{E}_{ij}$ and whose distance from the origin is

$$\frac{d\mathrm{E}_{ij}\int \sigma^*_{ij}\, dV}{(d\mathrm{E}_{ij}d\mathrm{E}_{ij})^{1/2}}. \quad . \quad . \quad . \quad . \quad . \quad . \quad . \quad . \quad . \quad (8)$$

(Although the point $\int \sigma^*_{ij}\, dV$ lies on the plane, it does not, of course, necessarily coincide with S_{ij}.) Now according to (3), the normal to the yield surface at the point S_{ij} is parallel to $d\mathrm{E}_{ij}$, and so perpendicular to the plane. The plane is therefore tangential to the yield surface at S_{ij}. The surface is thereby found as the envelope of planes whose distances from the origin are given by (8). Since possible strains have zero hydrostatic part (being the result of simultaneous simple shears), the surface is cylindrical with generators parallel to the direction δ_{ij}.

When the aggregate as a whole is isotropic the principal axes of the stress and strain-increment tensors are coincident, and we only need to consider the relation between their principal values represented in three dimensional space. The aggregate will be statistically isotropic when the orientations of grains in the same state of hardening are randomly distributed ; this condition must be satisfied for each of the various states of hardening at any moment in the differentially-hardened aggregate (if not, the aggregate might be anisotropic despite the absence of a preferred orientation).

The numerical calculations in the present paper are restricted to such an isotropic aggregate in which, moreover, the slip-directions in any grain are equally hardened (so that equation (7) is applicable). The development of deformation textures and their effect on the yield surface is left to a later paper.

§ 4. Multi-Slip in a Face-Centred Cubic Crystal.

At ordinary temperatures and rates of strain, glide occurs in a face-centred cubic crystal on the octahedral planes in the directions of the octahedron edges. Each of the four distinct glide-planes contains three possible slip-directions, making twelve in all, each of which has two opposite senses. The positive senses of the slip-directions are arbitrarily chosen here according to the following Table ; letters a, b, c, d refer to the four glide-planes, and with suffixes 1, 2, or 3, denote incremental shears in the respective positive senses. The components, referred to the

Plane	(111)			($\bar{1}\bar{1}$1)			($\bar{1}$11)			(1$\bar{1}$1)		
Shear	a_1	a_2	a_3	b_1	b_2	b_3	c_1	c_2	c_3	d_1	d_2	d_3
Direction	01$\bar{1}$	$\bar{1}$01	1$\bar{1}$0	0$\bar{1}$1	101	$\bar{1}$10	01$\bar{1}$	101	$\bar{1}\bar{1}$0	0$\bar{1}$1	$\bar{1}$01	110

cubic axes, of the strain tensor $d\epsilon_{ij}$ due to simultaneous shears in the twelve directions are given by the equations (Taylor 1938 a)

$$\left.\begin{aligned}
\sqrt{6}\,d\epsilon_{11} &= -a_2+a_3-b_2+b_3-c_2+c_3-d_2+d_3,\\
\sqrt{6}\,d\epsilon_{22} &= \;\;a_1-a_3+b_1-b_3+c_1-c_3+d_1-d_3,\\
\sqrt{6}\,d\epsilon_{33} &= -a_1+a_2-b_1+b_2-c_1+c_2-d_1+d_2,\\
2\sqrt{6}\,d\epsilon_{23} &= \;\;a_2-a_3-b_2+b_3+c_2-c_3-d_2+d_3,\\
2\sqrt{6}\,d\epsilon_{31} &= -a_1+a_3+b_1-b_3+c_1-c_3-d_1+d_3,\\
2\sqrt{6}\,d\epsilon_{12} &= \;\;a_1-a_2+b_1-b_2-c_1+c_2-d_1+d_2.
\end{aligned}\right\} \quad . \; . \; . \quad (9)$$

Any possible strain has five independent components (the hydrostatic part being zero), and therefore in general can only be produced by multi-slip over a group of directions containing an independent set of five.

Of the ${}^{12}C_5=792$ sets of five shears, only 384 are independent. The remaining 408 include dependent combinations of type

$$a_1+a_2+a_3=0 \quad (144),$$
$$a_1+b_2+d_3=0 \quad (228),$$
$$a_1-b_1+c_1-d_1=0 \quad (36),$$

or their equivalents; these equations are to be interpreted as meaning that such combinations of *unit* shears produce zero resultant strain. Of the 384 independent sets of five shears, 216 have two shears on each of two planes, and 168 have two shears on one plane only (the latter were apparently thought by Taylor to be dependent sets).

If the components of a stress applied to the crystal are σ_{ij} referred to the cubic axes, the shear stress components, multiplied by $\sqrt{6}$, are equal to

$$\left.\begin{array}{lll} \text{A}-\text{G}+\text{H}\ (a_1), & \text{B}+\text{F}-\text{H}\ (a_2), & \text{C}-\text{F}+\text{G}\ (a_3), \\ \text{A}+\text{G}+\text{H}\ (b_1), & \text{B}-\text{F}-\text{H}\ (b_2), & \text{C}+\text{F}-\text{G}\ (b_3), \\ \text{A}+\text{G}-\text{H}\ (c_1), & \text{B}+\text{F}+\text{H}\ (c_2), & \text{C}-\text{F}-\text{G}\ (c_3), \\ \text{A}-\text{G}-\text{H}\ (d_1), & \text{B}-\text{F}+\text{H}\ (d_2), & \text{C}+\text{F}+\text{G}\ (d_3), \end{array}\right\} \quad . \quad (10)$$

where

$$\text{A}=\sigma_{22}-\sigma_{33}, \quad \text{B}=\sigma_{33}-\sigma_{11}, \quad \text{C}=\sigma_{11}-\sigma_{22},$$
$$\text{F}=\sigma_{23}, \quad \text{G}=\sigma_{31}, \quad \text{H}=\sigma_{12}.$$

It will be observed that the 12×6 matrix of coefficients in the relations (10) between the 12 shear stress components and the 6 applied stress components is just the transpose of the 6×12 matrix of coefficients in (9). This is a simple consequence of the virtual work equation $\sigma_{ij}\,d\epsilon_{ij}=\Sigma\tau\,d\gamma$, and does not depend on any particular lattice geometry. It follows that we can always find a stress for which the component shear stresses attain the critical values in prescribed senses in a given set of five independent slip-directions (the respective minors being identical and non-zero). The critical value would usually be exceeded in one or more of the other seven directions, but, for any given strain, it is always possible to find at least one of the independent sets for which there exists a physically possible stress to operate the constituent shears. However, in evaluating the expression (8) there is no need to determine a physically possible combination of shears which are equivalent to the strain. It is necessary merely to calculate the works done in the given strain by stresses not violating the yield condition, and to select from these works the greatest. In fact it is only necessary to make the choice from the works done by 56 particular stresses, which correspond to the "vertices" of the polyhedral surface in stress space representing the yield criterion for the crystal. Proofs of these statements are left to a subsequent paper.

The 56 stresses may be classified in five groups, in which the typical values of (A, B, C, F, G, H)/$\sqrt{6}\tau$ are as follows when the critical shear stress τ is the same in all the slip-directions:

(i.) (1, -1, 0, 0, 0, 0). Tension or compression of amount $\sqrt{6}\tau$ along a cubic axis.

(ii.) (0, 0, 0, 1, 0, 0). A pure shear of amount $\sqrt{6}\tau$ in a cubic plane and parallel to a cubic axis.

(iii.) ($\frac{1}{2}$, $\frac{1}{2}$, -1, 0, 0, $\pm\frac{1}{2}$). A pure shear of amount $\sqrt{3}\tau$ in a cubic plane and at $22\frac{1}{2}^\circ$ to the cubic axes.

(iv.) ($\frac{1}{2}$, $-\frac{1}{2}$, 0, $\pm\frac{1}{2}$, $\pm\frac{1}{2}$, 0). Principal stresses $\pm\sqrt{6}\tau(1, -\frac{1}{2}, 0)$ with the second normal to an octahedral plane and the third along a slip-direction in that plane.

(v.) (0, 0, 0, $\frac{1}{2}$, $\pm\frac{1}{2}$, $\pm\frac{1}{2}$). Tension or compression of amount $\frac{3}{2}\sqrt{6}\tau$ normal to an octahedral plane.

The 56 stresses have 6 members in each of (i.) and (ii.), 12 in (iii.), 24 in (iv.), and 8 in (v.). The critical shear-stress is attained in 8 slip-directions for (i.), (ii.), and (iii.), and in 6 slip-directions for (iv.) and (v.).

§ 5. The Numerical Method.

For a calculation of the yield function of an isotropic aggregate in which there is no Bauschinger effect, it is only necessary to consider macroscopic strains $d\mathrm{E}_{ij}$ whose principal values are $(1, -\lambda, \lambda-1)\,d\mathrm{E}$ where $\frac{1}{2}\leqslant\lambda\leqslant 1$ (Hill 1950, p. 17 *et seq.*). The work done in such a strain of a free crystal has to be computed for each orientation of the strain axes to the cubic axes. If (θ, ϕ, ψ) are the Eulerian angles of the strain axes with respect to the cubic axes, all essentially distinct orientations occur once only in the intervals

$$0\leqslant\phi\leqslant\pi/4, \qquad 0\leqslant\cot\theta\leqslant\sin\phi, \qquad 0\leqslant\psi\leqslant\pi,$$

in view of the lattice symmetry and the assumption of equally hardened slip-directions. In other words, it is sufficient to restrict the major strain axis to one of the 48 identical spherical triangles in the stereographic projection, and allow the other axes to rotate through half a revolution. If $d\mathrm{W}$ is the work done on unit volume of crystal in a strain defined by given values of λ, θ, ϕ and ψ ($\bar{\tau}$ being the average critical shear stress), then, from (7),

$$\mathrm{S}_{ij}\,d\mathrm{E}_{ij}(\lambda)=\iiint d\mathrm{W}\sin\theta\,d\theta\,d\phi\,d\psi/\iiint\sin\theta\,d\theta\,d\phi\,d\psi.$$

In the computation, net points were taken at 5° intervals of θ and ϕ, and 18° intervals in ψ. Five values of λ were taken in steps of $\frac{1}{8}$ between $\frac{1}{2}$ and 1. It was found convenient to express $d\mathrm{W}$ in terms of the principal values of the 56 stresses and the angles between the stress and strain axes. The angles were read from a stereographic net on which were marked the axes of the 56 stresses.

If p denotes the perpendicular (8) from the origin to a tangent plane of the yield surface in principal stress space, the results of the calculations are

λ	$\frac{1}{2}$	$\frac{5}{8}$	$\frac{3}{4}$	$\frac{7}{8}$	1
$\sqrt{(\frac{3}{2})}p/\bar{\tau}$	3·06	3·04	2·98	2·91	2·86

The error involved in the integration is estimated to be not more than one unit in the second decimal place.

§ 6. Discussion of Results.

Fig. 1 shows a typical 60° sector of the cross-section of the yield surface, obtained from the values of p as described in § 3. The calculated curve cuts orthogonally the radii corresponding to pure shear and to pure tension, and lies between the Tresca hexagon and the von Mises circle when all are made to coincide for tension. In particular, the ratio of the yield stress in shear to that in tension is $2{\cdot}86/(\sqrt{3}\times 3{\cdot}06)=0{\cdot}540$, compared with 0·500 and 0·577 for the Tresca and Mises criteria.

The experimental data of Taylor and Quinney (1931) for copper and aluminium are also shown in the figure, and tend to lie between the Mises circle and the theoretical curve. The small discrepancy may be due to defects in the theory such as the approximation involved in equation (6), unequal hardening of slip-directions in individual crystals, or microscopic modes of distortion other than slip in the 12 directions. On the other hand, the experimental data may not be completely reliable, due to anisotropy or to a slight uncertainty in the extrapolation used to circumvent the hysteresis loop.

Also shown in the figure are the plastic potential curves computed from Taylor and Quinney's measured relation between the directions of the stress and strain-increment vectors ; Taylor's (1947) calculations for copper have been corrected in some instances. The agreement of the plastic potential curves with the directly measured yield loci suggests the substantial validity of (3), the theoretical derivation of which does not involve the further assumptions made in the present computation of the actual form of f.

The comparison can also be made in terms of Lode's diagram, but in our opinion, this over-magnifies small variations in the stress–strain relations, and is responsible for frequent statements that the Lévy–Mises equations are merely a moderate approximation. Thus, to the uncritical eye, a typical observed pair of Lode variables (0·5, 0·4), compared with the Lévy–Mises prediction (0·5, 0·5) might suggest an error of 20 per cent. However, it can be seen from the figure that the maximum difference in direction between the normals to the Mises circle and the measured plastic potential curves for copper and aluminium is only about 4° ; without any theory at all the strain-increment vector could be anywhere in the 360° range.

Fig. 1.

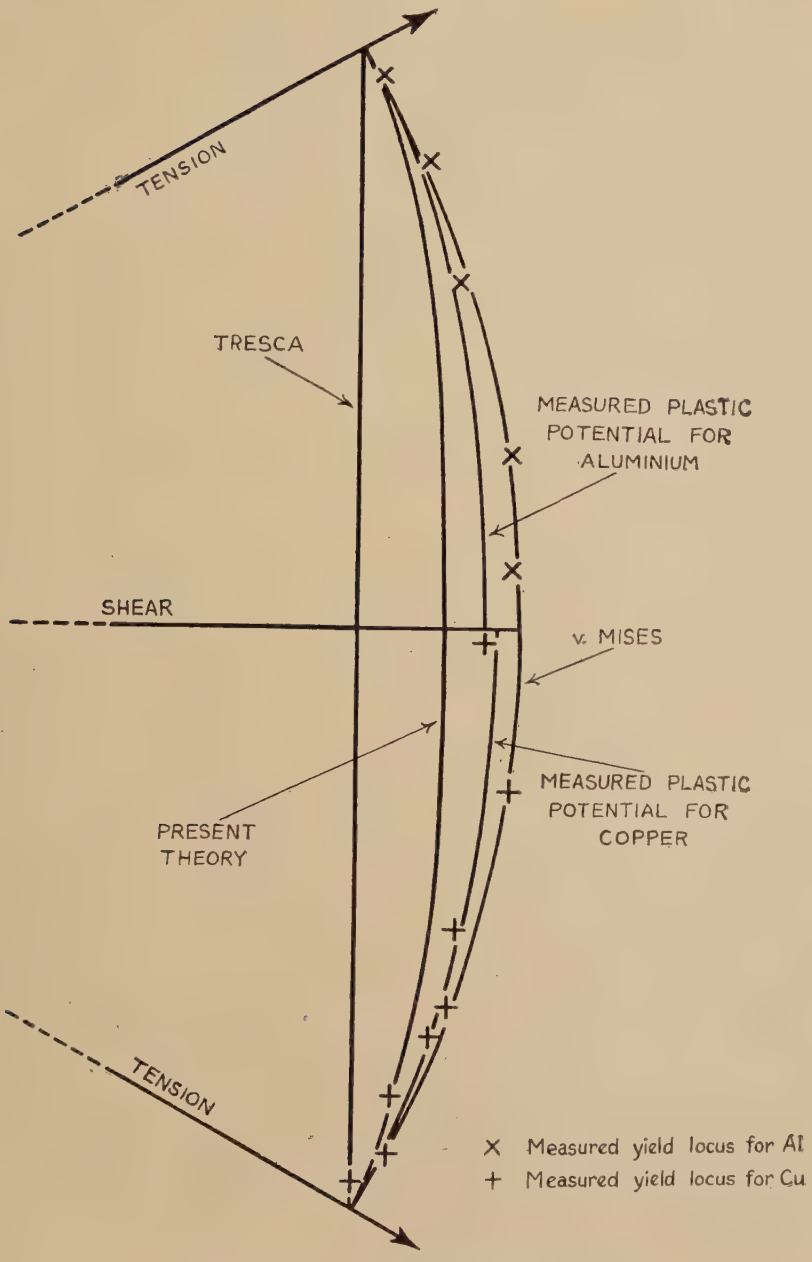

§ 7. Influence of Residual Stresses.

When the external loads are removed from a plastically-deformed aggregate, a residual distribution of internal stress remains. According to the maximum work principle for the aggregate (BH, equation (16)),

the yield function for the aggregate does not depend in any way on these internal stresses, but only upon the intrinsic hardening of the grains (as specified by the current values of the critical shear stresses in the slip directions). This conclusion is directly due to the neglect of elasticity in the present theory. In effect, the theory assumes that the elastic moduli are indefinitely large, so that a single crystal remains rigid under increasing load until it yields plastically. Similarly, an aggregate remains rigid until all grains are stressed to their individual yield points, and there is therefore no hysteresis loop. During loading, the weakest grain becomes plastically stressed under a load which may be termed the elastic limit of the aggregate. The elastic limit is generally appreciably lower than the yield-point load of the aggregate and clearly depends directly on the residual stresses. With increasing load other grains in turn are plastically stressed, but are prevented from deforming (or hardening) by the remaining non-plastic, and therefore rigid, grains. Hence, apart from the restricted possibilities of a stress adjustment within the individual yield surfaces of such plastically stressed grains, the greater part of further increments of load is borne by the non-plastic grains.

In an actual aggregate, elasticity permits plastic distortion and hardening of the weakest grains as soon as the elastic limit is reached. The immediate consequence is a hysteresis loop, greatly dependent on residual stresses (and correspondingly removable by a mild annealing), and with a breadth equivalent to a strain of elastic magnitude. When the hardening during the loop is small, it is naturally to be expected (in accord with observation) that the reloading branch of the loop will bend over fairly sharply to rejoin, virtually, the continuation of the previous stress–strain curve. Moreover, the local ordinate of the curve should be effectively identical with the yield-point stress calculated for a plastic-rigid aggregate. Many parallels might be instanced in stress analyses of structural parts on the basis of the macroscopic theory for a plastic-elastic homogeneous solid.

Similar considerations apply to the hysteresis loop during reverse loading, and to the tendency of the residual stresses to act so as to lower the elastic limit (Bauschinger effect). However, a further distinction must be made here. When the sign of dE_{ij} is reversed, the value of S_{ij} calculated from equation (6) would not be merely reversed when there is a *microscopic* Bauschinger effect ; that is, when the critical shear stress on a slip-plane depends on the sense of slip. Thus, even for the plastic-rigid model, one would expect in such circumstances a macroscopic Bauschinger effect on the *yield-point*.

§ 8. Work Hardening of an Aggregate.

The calculated value of the tensile yield stress is $3{\cdot}06\bar{7}$. This agrees closely with the value obtained by Taylor (1938 b), who assumed that an aggregate *actually* deforms uniformly (whereas we have conjectured that the work done is *as if* it did). Taylor was able to determine the yield

stress directly from the work done in a pure extension since, for an isotropic aggregate, it follows from symmetry alone that the stress is uniaxial. In general, of course, it is also necessary to know the relations between the directions of the stress and strain-increment vectors.

Taylor computed the work from the minimum shear principle. As we have proved (BH, equation (11)), this leads to the same result as the maximum work principle, but the latter is much more convenient. Taylor's values for the works done in the individual orientations agree closely with ours (even though he selected the shears from only 216 of the 384 independent sets).

As Taylor showed, the formula $S=m\tau(m\mathrm{E})$ for the tensile stress–strain curve of an aggregate, where $\tau(\gamma)$ is the shear-hardening curve for a crystal, is in fairly good agreement with observation (when $m=3{\cdot}06$, in the case of aluminium). It is assumed in the derivation that the virtual work equation $S\,d\mathrm{E}=\bar{\tau}\,d\bar{\gamma}$ can be written for an aggregate, where the averaged quantities $\bar{\tau}$ and $\bar{\gamma}$ actually *correspond* on the shear-hardening curve.

In general, however,

$$d\mathrm{W}=\mathrm{S}_{ij}\,d\mathrm{E}_{ij}=\int\tau\Sigma\,|\,d\gamma\,|\,dV \quad\text{and}\quad d\bar{\tau}=\int(d\tau)\,d\mathrm{V}=\int r(\tau)\Sigma\,|\,d\gamma\,|\,d\mathrm{V}$$

if hardening in multi-slip is a function only of the sum of the shears. Here $r(\tau)$ denotes the rate of hardening $d\tau/d\gamma$. Assuming that there is no correlation between τ and $\Sigma\,|\,d\gamma\,|$,

$$d\mathrm{W}=\bar{\tau}\int\Sigma\,|\,d\gamma\,|\,d\mathrm{V} \quad\text{and}\quad d\bar{\tau}=\overline{r(\tau)}\int\Sigma\,|\,d\gamma\,|\,d\mathrm{V}.$$

Hence

$$d\mathrm{W}=\bar{\tau}\,d\bar{\tau}/\overline{r(\tau)}. \qquad (11)$$

If all grains are equally hardened, $\overline{r(\tau)}=r(\bar{\tau})$ and $d\mathrm{W}=\bar{\tau}\,d\bar{\gamma}\,.\,\tau$ and the hardening of the aggregate (*i. e.* the scale of the yield surface) are then functions only of the total plastic work. The unequal hardening of the grains in such a way that $\overline{r(\tau)}\neq r(\bar{\tau})$ is presumably responsible for the observed departures from this functional relation and from the formula $S=m\tau(m\mathrm{E})$.

Acknowledgment.

We wish to thank the Director of the Mechanical Engineering Research Organization, Department of Scientific and Industrial Research, for permission to publish this paper, one of us (J. F. W. B.) being seconded by D.S.I.R. to the Wills Physical Laboratory.

References.

Bishop, J. F. W., and Hill, R., 1951, *Phil. Mag.*, **42**, 414.

Hill, R., 1950, *The Mathematical Theory of Plasticity* (Oxford: Clarendon Press).

Taylor, G. I., 1938 a, *Timoshenko Anniversary Volume*, 218; 1938 b, *J. Inst. Met.*, **62**, 307; 1947, *Proc. Roy. Soc.* A, **191**, 441.

Taylor, G. I., and Quinney, H., 1931, *Phil. Trans. Roy. Soc.*, **230**, 323.

CXXIX. *Note on the Boundary Layer on a Rotating Sphere* *.

By L. Howarth, F.R.S.,
Department of Mathematics, University of Bristol †.

[Received July 6, 1951.]

Summary.

The solution of the boundary layer equations for the flow associated with a rotating sphere is considered and an approximate solution is obtained. The solution on either hemisphere is thought to be valid up to the immediate vicinity of the equator where it is invalidated by the interaction with the flow from the other hemisphere.

A short appendix gives the flow due to a semi-infinite cylinder rotating in a uniform stream.

§ 1. Introduction.

The problem of the flow engendered by a sphere rotating about a diameter in otherwise undisturbed fluid has two features which are not without interest. In the first place it provides an example in which the curvature terms in the three-dimensional boundary layer equations are important. In the second place the boundary layers from the two hemispheres impinge on each other in the neighbourhood of the equator and their interaction is, in itself, of interest.

The object of this note is to discuss in some detail the first of these aspects and to place the second on record as a problem still to be solved in detail. In explanation of this second problem, it may be said at once that the boundary layers on the two hemispheres may be regarded as originating at the poles (where the flow approximates to the rotating disk solution) and developing towards the equator where they impinge on each other. The boundary layer equations can deal adequately with most of this development but must fail to represent the region of interaction between the two impinging layers if for no other reason than the parabolic character of the equations.

§ 2. The Boundary Layer Equations.

We shall use spherical polar coordinates r, θ, ϕ with r measured radially outwards from the centre of the sphere, θ measured from the axis of rotation and ϕ the azimuth. In order to preserve w for the velocity normal to the surface (*i. e.* in the direction r increasing) we shall use

* This paper forms a small part of one of the essays to which the Adams Prize was awarded in 1951.

† Communicated by the Author.

u, v for the velocities in the directions θ, ϕ increasing respectively. The boundary layer equations can then be derived directly from the full equations of flow in spherical polar coordinates or from Howarth (1951) by placing $K_1=0$, $K_2=-(1/a)\cot\theta$, where a is the radius of the sphere. They are :

$$\frac{u}{a}\frac{\partial u}{\partial \theta}+w\frac{\partial u}{\partial r}-\frac{v^2}{a}\cot\theta=\nu\frac{\partial^2 u}{\partial r^2}, \quad \ldots\ldots (1)$$

$$\frac{u}{a}\frac{\partial v}{\partial \theta}+w\frac{\partial v}{\partial r}+\frac{uv}{a}\cot\theta=\nu\frac{\partial^2 v}{\partial r^2}, \quad \ldots\ldots (2)$$

$$\frac{1}{a}\frac{\partial u}{\partial \theta}+\frac{\partial w}{\partial r}+\frac{u}{a}\cot\theta=0, \quad \ldots\ldots (3)$$

where use has been made of the fact that derivatives with respect to ϕ all vanish and that there is no imposed pressure gradient.

Apart from the curvature terms $(v^2/a)\cot\theta$ and $(uv/a)\cot\theta$, we should have the ordinary kind of two-dimensional boundary layer in u and w, with v determined by a convection equation. We may regard the $(v^2/a)\cot\theta$ term in (1) effectively as an imposed pressure gradient (whose intensity varies across the layer) essentially accelerating in character, since it is positive over the range 0 to $\pi/2$ in θ to which attention is restricted. At the surface, with Ω denoting the angular velocity of the sphere,

$$v=\Omega a\sin\theta,$$

so that

$$\frac{v^2}{a}\cot\theta=\Omega^2 a\sin\theta\cos\theta.$$

The effect of this term is therefore a maximum when $\theta=\pi/4$ and tends to zero as either the pole or the equator is approached. It is to be noted at once, in support of what has been said earlier, that it is most unlikely that forward integration of equations (1)–(3) from $\theta=0$ to $\pi/2$ will lead to a solution at $\theta=\pi/2$ in which $u=0$ throughout the layer. In other words the boundary layer equations, which present us with the prospect of the layer from the two hemispheres meeting head-on at the equator, are inadequate to deal with the flow in this vicinity. Nevertheless, it is to be expected that the interaction will be limited to the immediate vicinity of the equator and that it will lead to an outflow in the equatorial plane of the same order as the mass flows through the boundary layers. Since the solution of the rotating disk problem is known to lead to inflow along the axis, we may reasonably expect inflow at the poles, and this combined with the outflow at the equator gives us a picture similar to the one envisaged by Stokes (1845). The arguments used here must however be regarded as essentially different from Stokes's, his being based on pressure which, to the order of the approximation here, has been regarded as uniform.

§ 3. The Solution Near the Poles.

A solution of equations (1), (2), (3) in series in powers of θ is obtainable, though it is unlikely to converge sufficiently rapidly to make an approach to the equatorial conditions practicable. To obtain it we put

$$\left.\begin{aligned} Z&=\left(\frac{\Omega}{\nu}\right)^{1/2}(r-a),\\ u&=a\Omega[\theta F_1+\theta^3 F_3+\dots],\\ v&=a\Omega[\theta G_1+\theta^3 G_3+\dots],\\ w&=(\nu\Omega)^{1/2}[H_1+\theta^2 H_3+\dots], \end{aligned}\right\} \quad \dots\dots \quad (4)$$

and find the following equations for the first six functions

$$\left.\begin{aligned} &F_1^2+F_1'H_1-G_1^2=F_1'',\\ &2F_1G_1+H_1G_1'=G_1'',\\ &2F+H_1'=0. \end{aligned}\right\} \quad \dots\dots \quad (5)$$

$$4F_1F_3+F_1'H_3+F_3'H_1+\tfrac{1}{3}G_1^2-2G_1G_3=F_3'', \quad \dots\dots \quad (6)$$

$$2F_3G_1+4F_1G_3+H_3G_1'+H_1G_3'-\tfrac{1}{3}F_1G_1=G_3'', \quad \dots\dots \quad (7)$$

$$4F_3+H_3'-\tfrac{1}{3}F_1=0. \quad \dots\dots \quad (8)$$

The boundary conditions are $F_1=F_3=0$, $G_1=1$, $G_3=-\frac{1}{6}$, $H_1=0$, $H_3=0$ at $Z=0$.

$$F_1\to 0,\ F_3\to 0,\ G_1\to 0,\ G_3\to 0 \text{ as } Z\to\infty.$$

Equations (5) are, as mentioned earlier, the equations determining the flow due to a rotating disk Kármán (1921). It is to be doubted whether, since the functions defined in equations (6), (7), (8) refer to this specific problem only, the labour involved makes their integration worth while. The significance of the expansion lies in giving the form of that solution near the poles.

§ 4. The Solution by the Kármán Method.

We may look to the momentum integral equation to provide a more rapid though approximate solution. Integrating (1) through the boundary layer and making use of (3) we have, writing $z=r-a$,

$$\int_0^\delta \frac{\partial}{\partial\theta}u^2\,dz+a\Big[wu\Big]_0^\delta+\int_0^\delta (u^2-v^2)\cot\theta\,dz=-\nu a\left(\frac{\partial u}{\partial z}\right)_0,$$

that is

$$\frac{d}{d\theta}\int_0^\delta u^2\,dz+\int_0^\delta (u^2-v^2)\cot\theta\,dz=-\nu a\left(\frac{\partial u}{\partial z}\right)_0, \quad \dots \quad (9)$$

since $u=0$ when $z=0$ and $z=\delta$.

Similarly from (2)

$$\int_0^\delta \frac{\partial}{\partial\theta}(uv)\,dz+a\Big[vw\Big]_0^\delta+2\int_0^\delta uv\cot\theta\,dz=-\nu a\left(\frac{\partial v}{\partial z}\right)_0,$$

that is

$$\frac{d}{d\theta}\int_0^\delta uv\,dz+2\int_0^\delta uv\cot\theta\,dz=-\nu a\left(\frac{\partial v}{\partial z}\right)_0, \quad \ldots \quad (10)$$

since $u=v=0$ when $z=\delta$ and $w=0$ when $z=0$.

We may now follow Kármán's approximate method of solution of the rotating-disk problem by putting

$$\left.\begin{aligned} u&=\mathrm{A}[\mathrm{Z}-3\mathrm{Z}^3+2\mathrm{Z}^4]-\frac{\delta^2\Omega^2 a}{\nu}\sin\theta\cos\theta\,[\tfrac{1}{2}\mathrm{Z}^2-\mathrm{Z}^3+\tfrac{1}{2}\mathrm{Z}^4],\\ v&=\Omega a\sin\theta\,[1-\tfrac{3}{2}\mathrm{Z}+\tfrac{1}{2}\mathrm{Z}^3],\end{aligned}\right\} \quad \ldots \quad (11)$$

where $\mathrm{Z}=z/\delta$; these expressions satisfy the conditions

$$\left.\begin{aligned} &u=0,\quad \frac{\partial^2 u}{\partial \mathrm{Z}^2}=-\frac{\Omega^2\delta^2 a}{\nu}\sin\theta\cos\theta \text{ at } \mathrm{Z}=0\,; \qquad u=0,\quad \frac{\partial u}{\partial \mathrm{Z}}=0 \text{ at } \mathrm{Z}=1,\\ &v=\Omega a\sin\theta,\quad \frac{\partial^2 v}{\partial \mathrm{Z}^2}=0 \text{ at } \mathrm{Z}=0\,; \qquad v=0,\quad \frac{\partial v}{\partial \mathrm{Z}}=0 \text{ at } \mathrm{Z}=1,\end{aligned}\right\}$$

$$\ldots \quad (12)$$

the conditions on the second derivatives at $z=0$ being obtained direct from equations (1) and (2). The significance of A is that it is $\delta(\partial u/\partial z)_0$. The quantities A and δ are unknown and are to be determined by (9) and (10). Let us for convenience write $\mathrm{A}=(\chi\Omega^2\delta^2 a/\nu)\sin\theta\cos\theta$, $\delta=(\nu/\Omega)^{1/2}\lambda$, so that χ, λ are the new unknowns.

In the solution of the rotating-disk problem it is certainly true that

$$\int_0^\delta v^2\,dz \gg \int_0^\delta u^2\,dz. \quad \ldots \quad (13)$$

We may therefore make a tentative approach to the present problem by neglecting the terms containing $\int_0^\delta u^2\,dz$ on the left-hand side of (9). It then follows from (9) that

$$\chi=\int_0^1(1-\tfrac{3}{2}\mathrm{Z}+\tfrac{1}{2}\mathrm{Z}^3)^2\,d\mathrm{Z}, \quad \ldots \quad (14)$$

so that

$$\chi=0{\cdot}2357. \quad \ldots \quad (15)$$

It then follows from (10) that

$$\left(\frac{d}{d\theta}+2\cot\theta\right)(0{\cdot}00864\sin^2\theta\cos\theta\,\lambda^3)=\frac{3}{2\lambda}\sin\theta, \quad \ldots \quad (16)$$

so that

$$\tfrac{3}{4}\sin\theta\cos\theta\frac{d\lambda^4}{d\theta}+(4\cos^2\theta-\sin^2\theta)\lambda^4=173{\cdot}6, \quad \ldots \quad (17)$$

and therefore

$$\frac{d}{d\theta}[\sin^{16/3}\theta\cos^{4/3}\theta\,\lambda^4]=231{\cdot}5\sin^{13/3}\theta\cos^{1/3}\theta. \quad \ldots \quad (18)$$

Hence

$$\lambda^4=\frac{231{\cdot}5}{\sin^{16/3}\theta\cos^{4/3}\theta}\int_0^\theta\sin^{13/3}\theta\cos^{1/3}\theta\,d\theta. \quad \ldots \quad (19)$$

For small θ this solution should agree with the rotating-disk solution. From (19) we see that $\lambda^4=43{\cdot}4$ when θ is small, so that

$$\lambda=2{\cdot}57, \quad \left(\frac{\partial u}{\partial z}\right)_0=0{\cdot}61\frac{\Omega^{3/2}a\,\theta}{\nu^{1/2}}, \quad \left(\frac{\partial v}{\partial z}\right)_0=-0{\cdot}58\frac{\Omega^{3/2}a\,\theta}{\nu^{1/2}}.$$

Cochran (1934), using this type of approximate solution for the rotating disk but retaining the terms in u^2, gives the corresponding numerical coefficients as 2·79, 0·54 and −0·54 respectively. In the solution he obtained by numerical integration of the full equations the first of these coefficients is infinite, of course, and the other two are 0·51 and −0·62 respectively.

Returning now to the rotating sphere, the solution of (19) for λ is given in Table I. The value $\chi=0{\cdot}2357$ given in (13) leads to

$$\frac{u\lambda_0^2}{\lambda^2 a\Omega\sin\theta\cos\theta}=\lambda_0^2[0{\cdot}2357\mathrm{Z}-0{\cdot}5\mathrm{Z}^2+0{\cdot}2929\mathrm{Z}^3-0{\cdot}0286\mathrm{Z}^4] \quad . \quad (20)$$

and

$$\frac{v}{a\Omega\sin\theta}=1-1{\cdot}5\mathrm{Z}+0{\cdot}5\mathrm{Z}^3, \quad . \quad . \quad . \quad . \quad . \quad . \quad . \quad . \quad . \quad (21)$$

where λ_0 is the value 2·57 taken by λ when $\theta=0$.

TABLE I.

θ (degrees)	λ	$\frac{u_{\max}}{a\Omega}$	$\frac{v_{\max}}{a\Omega}$	$\frac{u_{\max}}{v_{\max}}$	$\frac{1}{(\Omega\nu)^{1/2}}\int_0^\delta u\,dz$	$\frac{-u_\delta}{(\Omega\nu)^{1/2}}$
0	2·57	0·000	0·000	0·22	0·000	0·62
10	2·58	0·039	0·174	0·22	0·054	0·62
30	2·74	0·110	0·500	0·22	0·164	0·60
50	3·12	0·127	0·766	0·21	0·276	0·56
70	4·06	0·180	0·940	0·19	0·395	0·50
80	5·28	0·161	0·985	0·16	0·459	0·44
90	∞	0	1·000	0·00	0·497	0·00

The right-hand sides of (20) and (21) are both functions of Z only and are given in Table II. It will be seen that the approximation we have obtained is such that u and v retain the same *form* throughout the range 0 to $\pi/2$ for θ, the actual scale and amplitude alone varying with θ.

TABLE II.

Z	$\frac{u\lambda_0^2}{\lambda^2 a\Omega\sin\theta\cos\theta}$	$\frac{v}{a\Omega\sin\theta}$	Z	$\frac{u\lambda_0^2}{\lambda^2 a\Omega\sin\theta\cos\theta}$	$\frac{v}{a\Omega\sin\theta}$
0·0	0·0000	1·0000	0·4	0·2133	0·4320
0·1	0·1246	0·8505	0·6	0·1386	0·2080
0·2	0·1944	0·7040	0·8	0·0450	0·0056
0·3	0·2205	0·5635	1·0	0·0000	0·0000

The maximum values of the right-hand sides of (20) and (21) considered as functions of Z are 0·22 and 1 respectively. The variation of the associated values $u_{\max}$ and $v_{\max}$ are included in Table I. The ratio $u_{\max}/v_{\max}$ is also included in Table I.

It follows from (20) that

$$\frac{1}{a(\Omega\nu)^{1/2}}\int_0^\delta u\,dz=0{\cdot}0184\lambda^3\sin\theta\cos\theta. \quad . \quad . \quad . \quad . \quad (22)$$

Furthermore, from (3)

$$w_\delta=-\frac{1}{a}\left[\frac{d}{d\theta}\int_0^\delta u\,dz+\cot\theta\int_0^\delta u\,dz\right],$$

where w_δ is the value of w at the edge of the boundary layer. Hence, from (22),

$$\left.\begin{aligned} w_\delta&=-0{\cdot}0184\,(\Omega\nu)^{1/2}\left[\frac{d}{d\theta}(\lambda^3\sin\theta\cos\theta)+\lambda^3\cos^2\theta\right]\\ &=0{\cdot}0184\,(\Omega\nu)^{1/2}\left[(2\cos^2\theta-\sin^2\theta)\lambda^3+\frac{3}{4\lambda}\sin\theta\cos\theta\frac{d\lambda^4}{d\theta}\right],\end{aligned}\right\} \quad (23)$$

so that by equation (17)

$$w_\delta=-0{\cdot}0184(\Omega\nu)^{1/2}\left[\frac{173{\cdot}6-2\cos^2\theta\,\lambda^4}{\lambda}\right]. \quad . \quad . \quad . \quad (24)$$

Values of w_δ are included in Table I. It will be noticed that the solution gives an inflow throughout the whole range.

It follows from (19) that λ (and hence δ) behaves like $c\cos^{-1/3}\theta$ (where c is constant) in the vicinity of $\theta=\pi/2$. In such circumstances, neglect of the first term in (9) is no longer justified and we must expect our solution to break down in this vicinity. However, in view of the nature of the singularity, we should expect the breakdown to be limited to the immediate vicinity of the equator where, anyway, the interaction with the flow from the other hemisphere will be important. Since this interaction is probably largely determined by the flux through the boundary layers, which our solution will give with little error, it is worth while examining our results in this neighbourhood further. It follows from (20) and (21) that, as $\theta\to\pi/2$,

$$u\to 0^* \text{ and } \frac{v}{a\Omega}\to 1$$

throughout the layer. The limiting values of both $(\partial u/\partial z)_0$ and $(\partial v/dz)_0$ are zero. It appears therefore that the solution presents us with something akin to separation at the equator.

Although $u\to 0$, $\int_0^\delta u\,dz$ remains finite and equal to $0{\cdot}497\,(\Omega\nu)^{1/2}$, so that

---

* This result appears to contradict earlier remarks but it should be remembered that the value of u is unlikely to be correct in this region although the non-zero value of $\int_0^\delta u\,dz$ (see below) may be more reliable.

there is a net flux through the equatorial plane. This is to be expected from our solution, since as we have seen there is an inflow into the boundary layer and it can readily be verified that

$$2\pi a\left[\int_0^{\delta} u\,dz\right]_{\theta=\pi/2} = -2\pi a^2\int_0^{\pi/2} w_\delta \sin\theta\,d\theta \quad . \quad . \quad . \quad (25)$$

as continuity requires.

This flux through the equatorial plane cannot of course take place from symmetrical considerations and must be annihilated by the flow from the other hemisphere. As indicated earlier on general grounds, a complete solution must take account of this interaction which one might reasonably expect to be confined to the vicinity of the equatorial plane and to give a mass outflow of the order of the total flux from the two hemispheres.

On the basis of this solution it appears likely therefore that inflow will occur over a large part of the surface, the outflow necessary to maintain continuity being confined to the vicinity of the equatorial plane.

Moreover, the general equations (1) and (2) confirm that inflow probably occurs at the edge of the boundary layer. At the outside of the layer these equations may be written approximately

$$w_\delta \frac{\partial u}{\partial r} = \nu \frac{\partial^2 u}{\partial r^2}, \quad . \quad . \quad . \quad . \quad . \quad . \quad . \quad . \quad (26)$$

$$w_\delta \frac{\partial v}{\partial r} = \nu \frac{\partial^2 v}{\partial r^2}, \quad . \quad . \quad . \quad . \quad . \quad . \quad . \quad . \quad (27)$$

where w_δ is the outflow at the edge of the layer. Now it is most unlikely that $\partial u/\partial r$ and $\partial v/\partial r$ are other than negative and that $\partial^2 u/\partial r^2$ and $\partial^2 v/\partial r^2$ are other than positive in the outer parts of the layer and hence w_δ must be negative—that is there must be inflow.

APPENDIX.

Another example of an essentially three-dimensional boundary layer is provided by the boundary layer along a thin hollow semi-infinite circular cylinder which is made to rotate with constant angular velocity ω about its axis and placed in a uniform stream moving with velocity U parallel to the axis.

It has been shown by Howarth (1951) amongst others that the curvature terms disappear from the equations of flow for the boundary layer along such a cylinder, so that we have the following equations :

$$u\frac{\partial u}{\partial x} + w\frac{\partial u}{\partial z} = \nu\frac{\partial^2 u}{\partial z^2}, \quad . \quad . \quad . \quad . \quad . \quad . \quad . \quad (28)$$

$$u\frac{\partial v}{\partial x} + w\frac{\partial v}{\partial z} = \nu\frac{\partial^2 v}{\partial z^2}, \quad . \quad . \quad . \quad . \quad . \quad . \quad . \quad (29)$$

$$\frac{\partial u}{\partial x} + \frac{\partial w}{\partial z} = 0, \quad . \quad . \quad . \quad . \quad . \quad . \quad . \quad . \quad (30)$$

where x is measured parallel to the axis from the leading edge, y around a right section and z normal to the surface.

Equation (28) is the boundary layer equation for flow along a flat plate, so that we have

$$u=\tfrac{1}{2}\mathrm{U}\mathrm{F}'(\mathrm{Z}),$$

where

$$\mathrm{Z}=\tfrac{1}{2}\left(\frac{\mathrm{U}}{\nu x}\right)^{1/2} z$$

and

$$\mathrm{F}'''+\mathrm{F}\mathrm{F}''=0,$$

with $\mathrm{F}=\mathrm{F}'=0$ at $\mathrm{Z}=0$ and $\mathrm{F}'=2$ as $\mathrm{Z}\to\infty$ *.

It follows from equation (30) that

$$w=\frac{1}{2}\left(\frac{\nu\mathrm{U}}{x}\right)^{1/2}(\mathrm{Z}\mathrm{F}'-\mathrm{F})$$

and then from (21) that

$$v=\tfrac{1}{2}\omega a(2-\mathrm{F}'),$$

since $v=\omega a$ when $z=0$.

The surface traction in this case has components

$$\tau_{zx}=0{\cdot}332\,\rho\left(\frac{\nu\mathrm{U}^3}{x}\right)^{1/2},$$

$$\tau_{zy}=-0{\cdot}332\,\rho\omega a\left(\frac{\nu\mathrm{U}}{x}\right)^{1/2}.$$

The drag on the cylinder is thus unaffected by its rotation and the frictional moment M which has to be overcome in order to maintain the rotation is $1{\cdot}3282\,\pi\rho\omega a^3(\nu l\mathrm{U})^{1/2}$ for a length l of the cylinder ; the moment coefficient $\mathrm{C_M}$ is given by

$$\mathrm{C_M}=\frac{\mathrm{M}}{\pi a^2 l\mathrm{U}^2\rho}=1{\cdot}3282\,\frac{\omega a}{\mathrm{U}}\left(\frac{\nu}{\mathrm{U}l}\right)^{1/2}.$$

As a result of this nature can clearly be applied to determine the rate at which the spin would be lost if the rotation were not artificially maintained, provided the rate of loss were sufficiently slow for the aerodynamic problem to be considered steady at all stages. In such guise it is not without interest ballistically.

References.

Cochran, 1934, *Proc. Camb. Phil. Soc.*, **30,** 365–375.
Howarth, 1951, *Phil Mag.*, **42,** 239–243.
Kármán, 1921, *Z.A.M.M.*, **1,** 244–247.
Stokes, 1845, *Trans. Camb., Phil., Soc.*, **8,** 287 ; *Collected Papers*, **1,** 75–129.

* For a table of values of $\frac{1}{2}\mathrm{F}'$ see for example *Modern Developments in Fluid Dynamics* Goldstein, Oxford Univ. Press (1938), vol. I., p. 136.

CXXX. *The Melting Curve at High Pressures.*

By C. Domb,
Clarendon Laboratory, Oxford *.

[Received July 5, 1951.]

Abstract.

An attempt is made to derive theoretically the Simon formula for the variation of the melting point of a solid with pressure. The model used is similar to that of Lennard Jones and Devonshire, but the interpretation of the results is different. A formula of the right type results, but a detailed examination shows that the melting temperatures are much too high, and the reasons for the discrepancy are discussed. The theory predicts the absence of a solid-fluid critical point, and this is in disagreement with recent general work of Münster.

§ 1. Introduction.

The form of the solid-fluid transition curve at high pressures has been the subject of considerable discussion for some time. Particular attention has been fixed on the question whether a solid-fluid critical point exists above which there is continuity of state, as in the liquid-vapour transition. There were quite lively discussions on this matter between those who favoured the existence of such a critical point and those who were convinced that it could not exist. All these discussions were, however, based on very insufficient experimental data, and on the extrapolation of interpolation formulæ. The later and more complete experimental work of Bridgman showed no indication of the existence of such a critical point, and Bridgman considers that the evidence is fairly conclusively against it (see Bridgman 1949, p. 201, for a detailed discussion). On the other hand it has been pointed out by Simon (1937) that thermodynamic reasoning alone cannot suffice to decide either way, and also that there are no obvious reasons which exclude the one or the other possibility.

Some years ago Simon proposed, on semi-empirical grounds, the following formula for the melting curve :

$$\frac{p}{p_i} = \left(\frac{T}{T_0}\right)^c - 1. \quad . \quad . \quad . \quad . \quad . \quad . \quad . \quad . \quad (1)$$

(Here T_0 is the normal melting temperature, p_i the internal pressure and c is a constant.) This formula is the first one to connect the melting curve with properties of the substance. It fits all the available experimental data with reasonable accuracy, the values of the internal pressure are

* Communicated by Professor F. Simon, F.R.S.

found to be in good agreement with those calculated by van der Waals' equation, and the value of c turns out to be round about 2 for most substances (about 4 for metals). Simon argued that if one wants to penetrate relatively to very high temperatures and pressures one has to carry out experiments on substances with low internal pressures, and he therefore used the substance with the lowest internal pressure, helium, as a model substance. Recent work on helium (Simon *et al.* 1950) has shown that the formula fits the experimental data with values of T/T_0 ranging up to 50°.* It is of interest to examine the possibility of deriving theoretically a formula which fits experimentally over such a wide range.

In 1939 Lennard Jones and Devonshire put forward a theory of melting analogous to the theory of order–disorder transitions in alloys. At sufficiently low temperatures they obtained isothermals of van der Waals shape with two stationary values, which they interpreted in the usual way as a first-order phase transition. At higher temperatures the two stationary values disappeared, thus indicating the existence of a critical point. However, Lennard Jones and Devonshire pointed out that they considered the model too crude to make any reliable predictions. This model was refined slightly by Blaisse (1946) without substantially altering the conclusions. On using an adaptation of the Born theory of melting, Blaisse was able to derive a formula of type (1), but the value of c obtained was less than 1.

In the present paper we shall adopt a model similar to that of Lennard Jones and Devonshire. Our interpretation of the consequences of this model will differ, however, and we shall derive a formula similar to (1) for the melting curve. We shall also indicate the mathematical developments required to improve the theory.

§ 2. Formulation of the Problem.

We shall throughout assume classical theory, interactions between molecules being given by central forces of limited range. Our results will therefore only be applicable to systems in which the binding forces can be regarded as central, such as the inert gases, and will not be valid for metals in which the bonding is of a different character. The partition function for an assembly of classical particles reduces to a product of two factors, a kinetic energy factor $(2\pi mkT)^{3/2}/h^3$ per particle, and a configurational factor arising from the potential energy terms. The configurational factor can be conveniently specified in the following manner. Let us take an arbitrary lattice structure whose spacing is small compared with the intermolecular distance in the solid state. Suppose that molecules are restricted to occupy positions in the centre of a lattice cell. Between any two molecules in different lattice cells there is an interaction energy ϵ_i. The intermolecular forces can be ignored outside a certain radius, and for

* The normal melting point of helium would correspond to about 1° abs. if quantum effects did not interfere.

any finite lattice spacing the ϵ_i form a finite set r. In any possible configuration of the assembly let n_i be the number of pairs of molecules with interaction energy ϵ_i. The energy of this configuration is

$$\sum_{i=1}^{r} n_i \epsilon_i.$$

Let $W(n_1, \ldots n_i, \ldots n_r)$ be the number of possible configurations of the assembly in which there are n_1 pairs of energy $\epsilon_1, \ldots\ldots n_r$ pairs of energy ϵ_r. The configurational partition function is then

$$Z_c = \sum_{n_1 \ldots n_r} W(n_1 \ldots . n_i \ldots n_r) \exp\left[-\sum_{i=1}^{r} n_i \epsilon_i / kT\right]. \qquad (2)$$

The expression (2) is only exact in the limiting case of infinitely small lattice spacing. But any finite spacing which contains a sufficient number of points to give a fair description of the intermolecular energy curve should provide a reasonable approximation.

The lattice used above is fixed and artificial and, provided that it is sufficiently fine, any given crystal structure can be fitted in to it. At lowest temperatures the system will choose the configuration of minimum energy, and if the law of force is of Lennard Jones type ($\lambda/r^m - \mu/r^n$), this corresponds to the face-centred cubic structure (Lennard Jones and Ingham 1925). An increase in pressure is represented by an increase in the density of particles, and the formula (2) also embraces the possibility of polymorphic transitions. In fact the description is too general for our purposes, since we are concerned with the disordering of a particular crystal structure, and we shall therefore modifiy the model.

We consider the number of particles as fixed, but the lattice spacing as variable, an increase in pressure corresponding to a decrease in lattice spacing ; we also confine our attention to a particular cyrstal structure (fig. 1). At constant volume our problem is now formulated as a generalized order–disorder transition in which many neighbour interactions must be taken into account ; the ratio of occupied to vacant cells is very much less than $\frac{1}{2}$. It should be observed that thermal vibrations are automatically taken into account in this formulation.

§ 3. Approximate Model

If we could solve the above problem exactly we should find that as the temperature was raised from zero a point would be reached at which the partition function had a singularity. This singularity would correspond to a first-order transition, and would be associated with the disappearance of long-range order ; it could thus be interpreted as the melting point. Unfortunately the only reliable information we have concerning order–disorder transitions is in regard to systems containing equal ratios of constituents and in which only nearest neighbour interactions are taken into account. We are therefore forced to use a drastic approximation in our model, and we must then decide whether any information provided by this approximation can be considered reliable. Following Lennard Jones

Fig. 1.

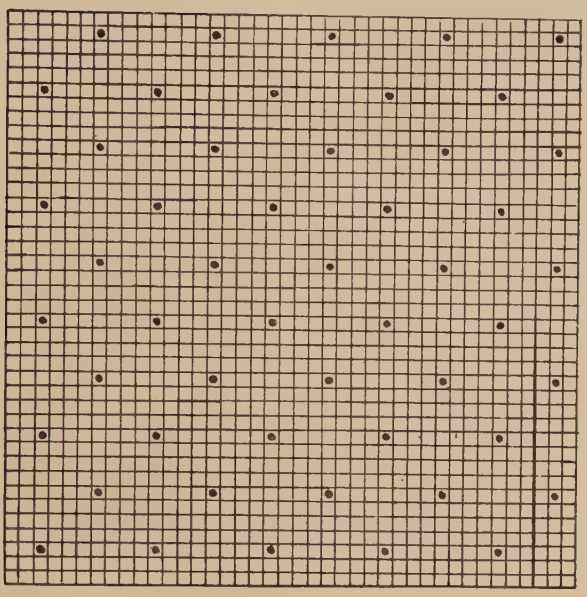

Fig. 2.

and Devonshire, we take account of small displacements from equilibrium by assuming a harmonic vibration spectrum, the kinetic energy terms now being included in the partition function ; the gradual disordering of the

crystal structure is allowed for by assuming that the molecules can jump into a single interstitial position, as shown in fig. 2. An essential physical difference between the solid and fluid states is the presence or absence of long-range order, and the model can take this into account. We can thus divide the partition function into two components,

$$F=F_{vib}+F_{or}, \quad . \quad . \quad . \quad . \quad . \quad . \quad . \quad . \quad . \quad (3)$$

F_{vib} being vibrational and F_{or} being given by order–disorder theory.

In their discussion of the problem Lennard Jones and Devonshire use a refined calculation for F_{vib}, averaging the inter-molecular energy over a cell to which a molecular is confined by its neighbours. We do not consider that the crudeness of the model warrants any such detailed calculation, and we shall use a simple Debye model, so that

$$F_{vib}=-3NkT \ln kT/h\bar{\nu}, \quad . \quad . \quad . \quad . \quad . \quad . \quad . \quad (4)$$

$\bar{\nu}$ being a mean frequency. In fact we do not consider that the present model is capable of yielding any detailed information on the nature of the singularity, and hence on matters such as the magnitude of the latent heat. Nevertheless, we do believe that it is possible to derive a reasonable idea of the position of the singularity. This assumption is based on the experience of order–disorder transitions for which an exact solution is available in two dimensions (Onsager 1944, Wannier 1945). It is there evident that crude approximations are quite incorrect in regard to the nature of the singularity, but provide a fair approximation to its position. The exact solution shows that the singularity is associated with the disappearance of long-range order, so that we can speak with precision of an ordered and a disordered phase meeting at the singularity. This is essentially different from a liquid and vapour above the critical point, where there is complete continuity, and a single analytic function for the partition function. We shall interpret the above singularity as corresponding to the melting point.

For F_{or} we shall use the Bethe approximation with a coordination number equal to 12 (Rushbrooke 1949, p. 306). Then if ϵ is the repulsive energy between a molecule in equilibrium and an interstitial molecule, the temperature of the singularity is given by

$$kT_c=a\epsilon\left[a=\frac{1}{2\ln 12/10}=2{\cdot}87\right]. \quad . \quad . \quad . \quad . \quad . \quad (5)$$

To determine the corresponding pressure we must take account of the variation of ϵ and $\bar{\nu}$ with volume, using the formula $p=-\partial F/\partial v$. For $\bar{\nu}$ we shall use Gruneisen's assumption $\bar{\nu}=K/v^{\gamma}$, so that for the vibrational term

$$p_{vib}=-\frac{\partial F_{vib}}{\partial v}=-\frac{3NkT}{\bar{\nu}}\frac{\partial\bar{\nu}}{\partial v}=\frac{3NkT\gamma}{v}. \quad . \quad . \quad . \quad . \quad (6)$$

For the intermolecular energy we shall assume a formula of Lennard Jones type, the attractive part of which can be neglected in the interstitial position. Thus

$$\epsilon=A\epsilon_0\left(\frac{r}{r_0}\right)^{-n}=A\epsilon_0\left(\frac{v}{v_0}\right)^{-n/3}, \quad . \quad . \quad . \quad . \quad . \quad . \quad (7)$$

where v_0 is the equilibrium volume of the substance and A is a constant. (If the interstitial position is at a distance from equilibrium equal to $1/\sqrt{2}$ of the spacing between atoms, the value of A is $2^{n/2}$.) Typical values of the constants for various substances are given in Fowler and Guggenheim (1939, p. 285).

Hence we have

$$p_{or}=-\frac{\partial F_{or}}{\partial v}=-Nb\frac{\partial \epsilon}{\partial v}=\frac{Nbn}{3}\frac{A\epsilon_0}{v_0}\left(\frac{v}{v_0}\right)^{-(n/3)-1} \quad . \quad . \quad . \quad . \quad (8)$$

$$\left(b=\tfrac{1}{4}.\frac{12\,.\,10}{11}=2{\cdot}73\right).$$

Combining (6) and (8), and substituting from (7) in (5), we find

$$\frac{p_c}{\varpi}=A\left(\frac{v_0}{v_c}\right)^{(n/3)+1}\left[3\gamma a+\frac{nb}{3}\right] \quad \varpi=\frac{N\epsilon_0}{v_0} \quad . \quad . \quad . \quad . \quad (9)$$

and

$$\frac{T_c}{\tau}=Aa\left(\frac{v_0}{v_c}\right)^{n/3} \quad \tau=\epsilon_0/k. \quad . \quad . \quad . \quad . \quad . \quad . \quad . \quad . \quad . \quad (10)$$

The pressure ϖ is determined by the lattice energy at the absolute zero and is related to the internal pressure, and τ is related to the ordinary melting temperature. Therefore

$$\frac{p_c}{B\varpi}=\left(\frac{T_c}{\tau}\right)^{(n+3)/n} \quad B=\frac{3\gamma+nb/3a}{(Aa)^{3/n}}. \quad . \quad . \quad . \quad . \quad . \quad (11)$$

At sufficiently high pressures this is a formula similar to (1) with $c=1+3/n$. If $n=9$, $c=1{\cdot}33$, and if $n=12$, $c=1{\cdot}25$.

§ 4. Discussion of Result.

It was pointed out by Simon (1937) that the existence of a universal formula of type (1) implied a law of corresponding states for melting. Lennard Jones and Devonshire (1939) observe that as long as the intermolecular energy curves of various substances can be adequately represented by an expression with two free parameters (such as (7) with fixed n), we will be led to a law of corresponding states. However, Bridgman is opposed to the idea of corresponding states for melting (1931, p. 207), since it is clear experimentally that latent heats and volume changes on melting cannot be fitted into such a law. Nevertheless, a law of corresponding states should only be regarded as a rough approximation; it may well be that a feature such as the melting point depends only in an average way on the shape of the intermolecular energy curve, whereas features such as latent heats and volume changes are much more sensitive to details. In this connection it is worth noting that the formula (11) is not very dependent on the coordination number used in the model.

From the experimental point of view Simon (1951) has shown in a recent article that the data for the melting curve of a number of substances fit a law of corresponding states with considerable accuracy.

When we attempt a detailed comparison between (11) and experiment we find two serious discrepancies. The value of c is too low, and the values of T_0 required to fit formula (1) are about three times too large. If we re-examine our approximate model it is not difficult to trace the source of the discrepancy. The single interstitial position we have taken corresponds to a very high energy; for $n=12$ the repulsive energy in this position is 64 times its value in equilibrium. Clearly a violent degree of thermal agitation and disorder would be required before this position would become occupied with any frequency, and this is far more than is required for melting. Interstitial positions much closer to the equilibrium position are sufficient to provide the disorder required for melting, and these would correspond to much lower temperatures. They are also situated on a flatter region of the intermolecular energy curve, and should therefore give rise to a larger value of c, since (11) indicates that the value of c varies inversely as the steepness of the curve. Confirmation of this interpretation is provided by X-ray diffraction experiments which show no very marked change in the shape of the first maximum between solid and fluid states.

It may also be noted that the Lindemann melting formula, which is well satisfied experimentally, assumes that melting occurs when the average vibration amplitude is about one-tenth of the minimum distance between atoms in the solid lattice (Grüneisen 1926). Our choice of the average interstitial position has been arbitrary, and if we were to take an interstitial position at this distance from equilibrium, our results would be in better agreement with experiment.

Unfortunately, although one can account for the disagreement qualitatively, it is difficult to see how to take adequate account of it theoretically without tackling the more complicated problem of generalized order–disorder transitions. We could start with a problem of the type indicated in fig. 3 in which nearest and second neighbours both have a repulsive energy of interaction, so that the lowest energy state is as indicated. Then we should try to introduce more intervening repulsive interactions. Our resulting critical temperature would only be expected to tend to a non-zero value as the number of interactions increased indefinitely for a three-dimensional model, since Peierls (1936) has shown that thermal vibrations on their own are sufficient to destroy long-range order in two dimensions.

§ 5. The Existence of a Critcal Point.

In a recent paper Münster (1951) attempts to show very generally that all first-order phase transitions disappear at sufficiently high temperatures, and hence that these transitions end in a critical point. This conclusion contradicts the result of the present paper, and we believe it to be incorrect. Münster's argument is rather intricate, but Mr. R. O. Davies has pointed out to the writer that an error arises in the passage from a finite canonical ensemble of N particles to a grand canonical ensemble

which provides in principle for an indefinitely large N. The finite limit to which $\partial\bar{\bar{E}}_q/\partial\Theta$ tends as $\Theta\to\infty$ may well depend on N, and its behaviour for large N must be investigated.

This point may be aptly illustrated by a particular physical example. Consider an order–disorder transition in a two-dimensional quadratic lattice with equal numbers of the two constituents. An exact solution is available (Onsager 1944), and although the transition is not first order, the specific heat is infinite at the Curie point, the fluctuations are large, and Münster's argument should apply. For any given number N the Curie point is given by

$$T_c = 1{\cdot}14\,\epsilon/k, \qquad (12)$$

where ϵ depends on the intermolecular spacing, and hence on α/N (α being the area of the assembly). As N increases so does ϵ, and hence T_c. If there is no upper bound to ϵ there is likewise no upper bound to T_c.

Fig. 3.

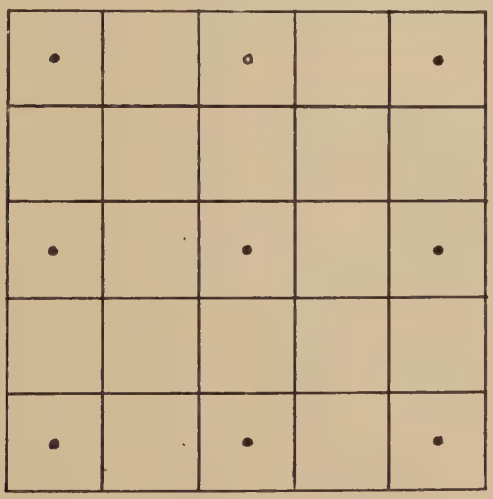

It seems clear, therefore, that a critical point could only arise in general if there were an upper limit to the intermolecular energy as the intermolecular distance decreases to zero. At the present moment there is no indication, theoretical or experimental, of the existence of such a limit. Theoretically the repulsive energy is of the form

$$R(r)\exp(-r/\rho), \qquad (13)$$

where ρ is a constant and $R(r)$ is a polynominal containing small inverse powers of r (Slater 1928). Even if $R(r)$ is replaced by a constant, P, the numerical values of P given in Fowler and Guggenheim, p. 293, would correspond, from equation (5), to melting temperatures 10^6 times the normal melting temperature.

We may sum up by saying that we have indicated the possibility of deriving, for a classical model, a formula of type (1) from the melting curve.

The parameters occurring in this formula can be related to the normal melting temperature and internal pressure. It should be emphasized, however, that the Simon formula (1) is of much greater general validity than the present theory since it applies even when quantum effects are present (Simon 1951).

Acknowledgements.

The author is indebted to Professor F. E. Simon, F.R.S., for many valuable discussions. He is also grateful to the University of Oxford for the award of an I.C.I. Fellowship.

References

Blaisse, B. S., 1946, *Thesis*, Amsterdam.
Bridgman, P. W., 1949, *The Physics of High Pressure* (London : G. Bell).
Fowler, R. H., and Guggenheim, E. A., 1939, *Statistical Thermodynamics* (Cambridge : University Press).
Grüneisen, E., 1926, *Handbuch der Physik* X (Berlin : Springer), p. 51.
Lennard Jones, J. E., and Devonshire, A. F., 1939, *Proc. Roy. Soc.* A, **170,** 464.
Lennard Jones, J. E., and Ingham, A. E., 1935, *Proc. Roy. Soy.* A, **107,** 636.
Münster, A., 1951, *Z. Naturforschg.*, **6a**, 139.
Onsager, L., 1944, *Phys. Rev.*, **65,** 117.
Peierls, R. 1936, *Helv. phys. Acta*, Suppl. (ii), 81.
Rushbrooke, G. S., 1949, *Introduction to Statistical Mechanics*, (Oxford : University Press).
Simon, F. E., Holland, F. A., Huggill, J. A. W., and Jones, G. O., 1950, *Nature, Lond.*, **165,** 147.
Simon, F. E., 1937, *Trans. Farad. Soc.*, **33,** 65.
Simon, F. E., 1951, *Farkas Memorial Volume*, in the press.
Slater, J. C., 1928, *Phys. Rev.* **32,** 349.
Wannier, G. H., 1945, *Rev. Mod. Phys.* **17,** 50.

CXXXI. CORRESPONDENCE.

The Influence of Exchange Energy on the Specific Heat of Free Electrons in Metals.

By A. B. Lidiard,
King's College, London*.

[Received August 15, 1951.]

In a recent paper Wohlfarth (1950) has published calculations of the effect of the exchange energy on the thermal properties of free electrons. His starting point is an expression (due to Koppe (1947)) for the free energy, F, in terms of the distribution function $f(k)$. (His equation (2.1) is, in fact, only $\frac{1}{2}$F and should be multiplied by 2.) The first two terms in this expression are respectively the kinetic energy and the exchange energy of the electrons; together they make up the *internal* energy, E. The third term is the entropy, S, multiplied by $-$T. As an approximation it is assumed that S is the same function of $f(k)$ as it would be in the absence of exchange interactions. We should expect this to be a good approximation when the exchange energy is small compared with the kinetic energy, simply because it is correct when the exchange energy is actually zero. An integral equation for $f(k)$ may be obtained by putting the variation $\delta F=0$, namely

$$\frac{h^2}{8\pi^2 m}k_1^2-\frac{e^2}{\pi k_1}\int_0^\infty k_2 f(k_2)\ln\left|\frac{k_1+k_2}{k_1-k_2}\right|dk_2-\zeta=\boldsymbol{k}\mathrm{T}\ln\left(\frac{1-f(k_1)}{f(k_1)}\right). \quad . \quad (1)$$

ζ is a parameter introduced by the condition that the total number of electrons, N, is a constant. It is equal to the chemical potential $\partial F/\partial N$. Owing to the difficulty of solving equation (1) its derivation by putting $\delta F=0$ is made the basis of a variation treatment. As Wohlfarth takes a rather crude variation function $f(k)$ (equation 2.3), it seems desirable to obtain some confirmation that the results of its use are not seriously in error.

Firstly we note the possibility, in principle, of solving (1) by a method of successive approximations, an nth approximation for $f(k)$ being inserted on the L.H.S. to give an $(n+1)$th approximation on the right. We could therefore consider Wohlfarth's variation function as a starting point in this iterative process. This we have done, and found that for low temperatures the next approximation was, *in its variation with k*, graphically indistinguishable from a simple Fermi–Dirac function, in which the temperature T is replaced by a parameter τ, say. τ was

* Communicated by Professor C. A. Coulson, F.R.S.

several times smaller than T, in general agreement with Wohlfarth's result that the specific heat was greatly decreased by the exchange energy.

This means that probably a very good *variational* distribution function would be

$$f(k)=\left[\exp\frac{1}{\boldsymbol{k}\tau}\left(\frac{h^2}{8\pi^2 m}k^2-\zeta\right)+1\right]^{-1}. \quad . \quad . \quad . \quad . \quad (2)$$

The parameter ζ may be found as usual by the condition that the total number of electrons is a constant, N. The second parameter τ will be determined by putting $\partial F/\partial\tau=0$: when the exchange energy is not included, this method, of course, yields $\tau=T$, as is necessary. Now Yokota (1949), in the course of a paper on the Thomas–Fermi–Dirac equation, has evaluated the exchange term in the expression for F, using the (incorrect) Fermi–Dirac distribution function. It is thus only necessary to substitute τ for T in his result (6) to obtain $F(\tau)$, since the kinetic energy and entropy expressions are well known. (There is a minor error in Yokota's equation (6) which is corrected here.) In this way we obtain

$$\frac{F}{N\epsilon_0}=\frac{3}{5}\left(1+\frac{5x^2}{12}\right)-\frac{3}{4}\frac{\epsilon_j}{\epsilon_0}\left[1+\frac{x^2}{6}\left(\ln x+\frac{\gamma}{2}-\ln\pi-1\right)\right]$$
$$-\frac{\pi\boldsymbol{k}T}{\epsilon_0}\cdot\frac{x}{2}, \qquad x\ll 1, \quad . \quad . \quad . \quad . \quad . \quad . \quad . \quad . \quad (3)$$

in which

$$x=\frac{\pi\boldsymbol{k}\tau}{\epsilon_0}, \qquad \epsilon_0=\frac{h^2}{8m}\left(\frac{3N}{\pi V}\right)^{2/3}, \qquad \epsilon_j=e^2\left(\frac{3N}{\pi V}\right)^{1/3}$$

and γ is a numerical constant. (In terms of γ_1, γ_2, and γ_3, defined in Yokota's paper,

$$\gamma=3-4\ln 2+12\gamma_1/\pi^2-\gamma_2+2\gamma_3:$$

the 3 appears incorrectly as a 2 in his paper.) We have evaluated γ numerically and found it to be 0·648. The quantity ϵ_0 is just the Fermi energy, and ϵ_j/ϵ_0 gives a convenient measure of the exchange energy. By minimizing F with respect to x (*i. e.* with respect to τ) we obtain as the equation determining x as a function of T

$$\frac{\pi\boldsymbol{k}T}{\epsilon_0}=x-\frac{\epsilon_j}{\epsilon_0}\left[\frac{x}{2}\ln x-\frac{x}{2}\left(-\frac{\gamma}{2}+\ln\pi+\frac{1}{2}\right)\right], \qquad x\ll 1. \quad . \quad (4)$$

These two equations (3) and (4) are to be compared with Wohlfarth's equations (2·6) and (2.7), namely

$$\frac{F}{N\epsilon_0}=\frac{3}{5}\left(1+\frac{5x^2}{12}\right)-\frac{3}{4}\cdot\frac{\epsilon_j}{\epsilon_0}\left[1+\frac{x^2}{6}\left(\ln x-\ln 2-\frac{13}{12}\right)\right]$$
$$-\frac{3\boldsymbol{k}T}{\epsilon_0}\cdot\frac{x}{2}, \qquad x\ll 1, \quad . \quad . \quad . \quad (5)$$

$$\frac{3\boldsymbol{k}T}{\epsilon_0}=x-\frac{\epsilon_j}{\epsilon_0}\left[\frac{x}{2}\ln x-\frac{x}{2}\left(\ln 2+\frac{7}{12}\right)\right], \qquad x\ll 1. \quad . \quad . \quad . \quad (6)$$

Apart from the substitution of 3 for π in the entropy terms, these two equations differ from (4) and (5) only in the replacement of $\left(\ln\pi+\frac{1}{2}-\frac{\gamma}{2}\right)=1{\cdot}32$ by $\left(\ln 2+\frac{7}{12}\right)=1{\cdot}28$, *i. e.* a difference of 4 per cent. Finally, Wohlfarth's equation (2·8) for the specific heat, C, is replaced by

$$C/C^0=\left\{1-\frac{1}{2}\cdot\frac{\epsilon_j}{\epsilon_0}\ln x-\frac{\epsilon_j}{\epsilon_0}\left(\frac{1}{4}+\frac{\gamma}{4}-\frac{1}{2}\ln\pi\right)\right\}^{-1}, \quad . \quad . \quad (7)$$

where C^0 is the Sommerfeld specific heat $\frac{1}{2}\pi^2 N\boldsymbol{k}(\boldsymbol{k}T/\epsilon_0)$. This again is equivalent to the replacement of $\ln 2+7/12$ by $\ln\pi+\frac{1}{2}-\gamma/2$. This reaffirms the result that the specific heat is greatly *decreased* by the inclusion of the exchange energy. For it is clear from (4) and (6) that as $T\to 0$, $x\to 0$ and from (7) that as $x\to 0$, $C/C^0\to 0$.

This close agreement between the results obtained by using the first and second order variation functions is strong evidence for the validity of the variation method. This is confirmed by a comparison of the approximate and exact values of the thermodynamic functions for a perfect Fermi-Diracgas without exchange interactions (published elsewhere, Lidiard 1951).

In conclusion I should like to thank Isaaki Yokota for supplying the derivation of his equation (6) which has been used here.

References.

Koppe, H., 1947, *Z. Naturforsch.*, **2A**, 429.
Lidiard, A. B., 1951, *Proc. Phys. Soc.* A, **64**, 814.
Wohlfarth, E. P., 1950, *Phil. Mag.*, **41**, 534.
Yokota, I., 1949, *J. Phys. Soc. Japan*, **4**, 82.

A Dislocation Reaction in the Face-Centred Cubic Lattice.

By W. M. Lomer,
Cavendish Laboratory, Cambridge*.

[Received July 15, 1951.]

The marked difference in the initial rates of strain-hardening of hexagonal and cubic crystals has often been ascribed to some form of interference between slip on non-parallel planes in the cubic material. It is shown in this paper that dislocations on two intersecting slip planes can attract one another and combine to form a " sessile " dislocation (Frank 1949), which may act as a considerable immobile nucleus of internal stress, and so cause the crystal to harden.

---

* Communicated by the Author.

Consider two dislocations on slip planes inclined at an angle θ as shown in fig. 1. (Only dislocation lines parallel to the line of intersection will interact strongly, so the problem is effectively two dimensional.) The force per unit length exerted on dislocation 2 by dislocation 1 is $b_2\tau$, where b_2 is the Burgers vector of number 2, and τ is the shear stress due

Fig. 1.

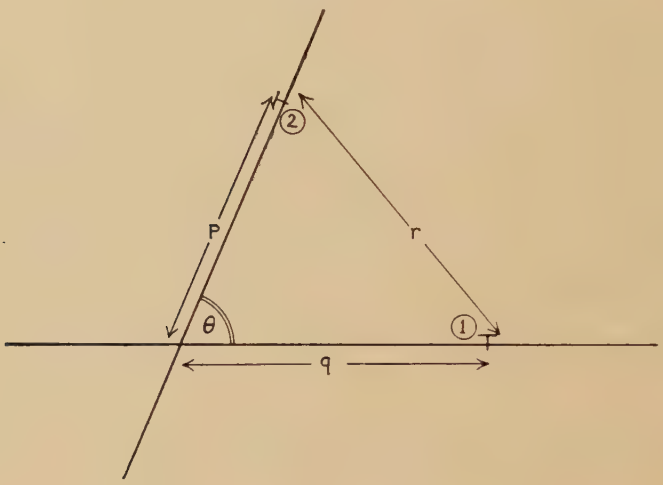

Coordinate system used for calculations.

to number 1 resolved first into the slip plane of 2, and then into the slip direction. A full analysis shows that the force can be derived from the following energy functions :—

1 and 2 both screw type $E=\frac{\mu b_1 b_2}{2\pi}\log r$.

1 and 2 both edge type $E=\frac{\mu b_1 b_2}{2\pi(1-\nu)}\left\{\cos\theta\log r+\frac{pq\sin^2\theta}{r^2}\right\}$.

1 ; edge and 2 ; screw, or *vice versa*, $E=0$.

where μ=modulus of rigidity, ν=Poisson's ratio,

b_1, b_2=Burgers vectors,

p, q, r as diagram.

In the close-packed cubic lattice the planes may be for instance (111) and (11$\bar{1}$), intersecting in [1$\bar{1}$0] and making an angle $\cos^{-1}1/3$ with each other. The only dislocation lines considered are therefore those parallel to [1$\bar{1}$0]. Possible displacement vectors (excluding " half-dislocations " (Heidenreich and Shockley 1948) for reasons explained later) are in the directions [1$\bar{1}$0] ; [101] ; [01$\bar{1}$], in the first plane, and [1$\bar{1}$0] ; [101] ; [011], in the second. The first one of each of these sets is a pure screw, and of no particular interest. The reaction to be studied in detail is

that between $[10\bar{1}]$ and $[011]$ which can add to give $[110]$, a single dislocation of the same strength as each of the two combining ones. This resulting dislocation line is parallel to $[1\bar{1}0]$ and its displacement vector is $[110]$; these two directions are not contained in the same close-packed plane, and so the dislocation is sessile.

The displacement vectors may be resolved into screw and edge components as follows, with a=length of unit cell edge :—

$$\tfrac{1}{2}{}^{*}a[10\bar{1}]=\tfrac{1}{4}a \quad ([1\bar{1}0]+[11\bar{2}])$$

$$\tfrac{1}{2}a[011]=\tfrac{1}{4}a(-[1\bar{1}0]+[112])$$

Fig. 2.

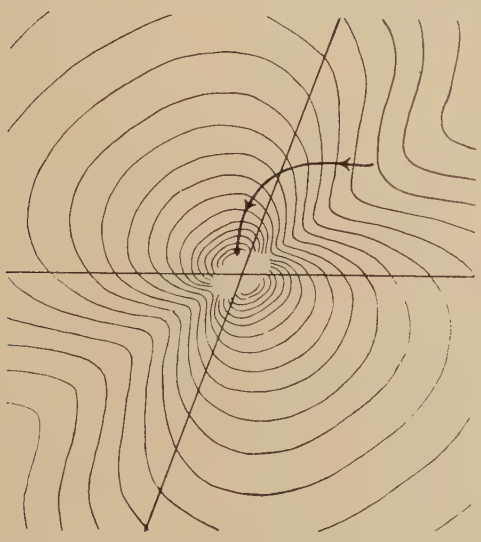

Interaction energy contour map for reaction $[10\bar{1}]+[011]\rightarrow[110]$; energy contour interval$=\dfrac{\mu a^2}{32\pi}$ ergs per cm.$=0{\cdot}85$ e.V. per atom plane in copper.

giving the screw components a magnitude $a/2\sqrt{2}$ and the edges $\sqrt{3}a/2\sqrt{2}$. With these values, and taking $\nu=1/3$ we get, adding all the energy contributions

$$\mathrm{E}=\frac{\mu a^2}{32\pi}\left\{5\log r+\frac{7pq}{r^2}\right\}.$$

It is convenient to represent the energy as a function of the oblique coordinates p and q by the contour map of fig. 2, where the energy value for dislocation 1 at q and dislocation 2 at p is plotted at the point p, q.

---

* $\dfrac{a}{2}[10\bar{1}]$ is a vector with components $\dfrac{a}{2}$, 0, $-\dfrac{a}{2}$ and so on.

It may be presumed that the representative point of the system will move down the line of greatest slope on the diagram, so that both dislocations will in practice move simultaneously. A typical " trajectory " for the system has been sketched in.

There is also an attractive force between dislocations with Burgers vectors $[10\bar{1}]$ and $[101]$. It is small and depends on the fact that the self-energy of a screw dislocation per unit length is less than that for an edge with the same displacement vector. The energy function for this pair is

$$E = \frac{\mu a^2}{32\pi}\left\{\log r + \frac{7pq}{r^2}\right\}.$$

This is mapped in fig. 3 ; the trajectory shows that at first the dislocations adjust their angular relationship, and only when p/q is approximately -1 do they both approach the centre.

Fig. 3.

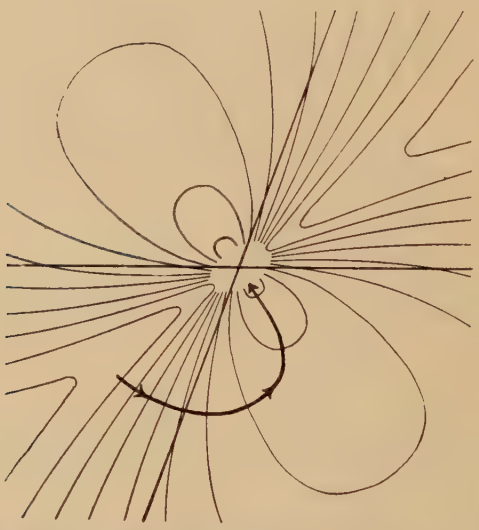

Interaction energy contour map for reaction $[10\bar{1}]+[101] \rightarrow [200]$; contour interval as fig. 2.

The details of this picture probably depend on the assumptions made, such as the infinitely long, straight dislocations, and on neglecting the effect of the dissociation into half dislocations. Since it is believed that the halves will only separate by some 10 A. this cannot have a large effect on interactions at a considerable distance, but might play some part in the details of the actual process of coalescence of the dislocations. The production of sessile dislocations by the interaction of mobile ones, and not only by stacking faults in the growth process, should almost certainly have some effect on the rate of hardening, but it is not yet

clear to what extent it will be important, or what the exact mechanism of the interaction of the sessile dislocations with those still mobile would be.

Recent experimental work has shown that hardening is very closely associated with the occurrence of deformation bands (Honeycombe, in the press), and that the latter occur more frequently in crystals with several slip planes. This may imply that the effect dealt with in this paper is not important, although it is perhaps possible that sessile dislocations produced in this way help the formation and stabilization of the deformation bands.

References.

Frank, F. C., 1949, *Proc. Phys. Soc.* A, **62**, 202.
Heidenreich, R. D., and Shockley, W., 1948, *The Strength of Solids*, (London : Physical Society), p. 57.
Honeycombe, R. W. K., *J. Inst. Met.* (in the press).

Lattice Defects in Silver Bromide at Room Temperature.

By H. D. Keith and J. W. Mitchell,
University of Bristol*.

[Received September 7, 1951.]

As a result of the experiments of Tubandt and Eggert (1920), Wagner and Beyer (1936), Berry (1951) and others, it has now been established fairly conclusively that, at temperatures above 200° C., the lattice disorder in silver bromide is predominantly of the Frenkel type. Concerning the nature of the lattice disorder in this material at lower temperatures, however, little direct experimental evidence is available, and an attempt has therefore been made to determine the " soundness " of pure silver bromide at room temperature from newly-measured values of its lattice-parameter and density.

The experiment consisted of comparing the molecular weight of silver bromide as determined by X-rays, that is, as calculated by means of the formula (Straumanis 1949)

$$M_x = k \frac{N_s a^3 d}{n},$$

(where k is a factor introduced to correct for an error in the value of the molecular weight of calcite used by Siegbahn, N_s is the effective Avogadro's number, a is the lattice-parameter in kX, n is the number of molecules in the unit cell of the ideal lattice and d is the density in gm./c.c.), with the value, M, of the molecular weight which is known from accurate

* Communicated by the Authors.

chemical data. If $D=(M_x-M)$ is negative and greater than the experimental error, then it can be concluded that the silver bromide contains vacancies which may be located either at grain or mosaic boundaries or within the lattice (Schottky disorder and/or aggregates of vacant lattice sites); the experiment does not, however, enable the presence of Frenkel disorder to be detected since interstitial ions and vacant lattice sites in *equal* concentrations do not affect the macroscopic soundness of a crystal.

The lattice-parameter of pure silver bromide was measured at 25° C. by means of the X-ray powder method, the results of two determinations carried out with a directly calibrated 19 cm. " Unicam " camera and with a 64 mm. Straumanis camera agreeing to within 1 part in 4×10^4 ($a=5{\cdot}7633$ *k*X). The densities of large well-annealed polycrystalline specimens of silver bromide were determined by the displacement of doubly-distilled water using the method of Snoek (1950) and the results obtained with three such specimens agreed to within 1 part in 2×10^4 ($d=6{\cdot}4799$ gm./c.c. at 18° C.). For the purpose of correcting the value of the lattice-parameter for temperature differences, the value of the thermal expansion coefficient given by Strelkow (1937) was used.

The averaged result of six determinations of D gave the result $(D/M)=+8{\cdot}6\times10^{-5}$ but, due to experimental errors and uncertainties in certain fundamental constants, this may be in error to the extent of $\pm1{\cdot}6\times10^{-4}$. The maximum possible number of vacant lattice sites in pure silver bromide at room temperature represents, therefore, a fraction $(1{\cdot}6-0{\cdot}86)\times10^{-4}=7{\cdot}4\times10^{-5}$ of the total number of lattice sites in the ideal crystal. This is probably an over-estimate and, as allowance has to be made for the probably not inconsiderable number of vacancies associated with mosaic and grain boundaries, it is therefore unlikely that Schottky defects are present in sufficiently large numbers to contribute significantly either to ionic conductivity or to the mechanisms of latent image formation. The situation may well be different, however, in the sensitized silver bromide grains of photographic emulsions (Mitchell 1951).

References.

Berry, C. R., 1951, *Phys. Rev.*, **82**, 422.

Mitchell, J. W., 1951, *Photographic Sensitivity* (London: Butterworths), p. 242.

Snoek, J. L., 1950, *Phil. Mag.*, [7], **41**, 1188.

Straumanis, M. E., 1949, *Acta Cryst.*, **2**, 82.

Strelkow, P. G., 1937, *Phys. Zeits. d. Sowjetunion*, **12**, 73.

Tubandt, C., and Eggert, S., 1920, *Zeits. f. Anorg. Chemie*, **110**, 196.

Wagner, C., and Beyer, J., 1936, *Zeits. f. Phys. Chem.* B, **32**, 113.

A Note on the Trace of the Product of Dirac's Matrices.

By L. M. Yang,
The University, Edinburgh*.

[Received September 7, 1951.]

It is well known that the trace of the product of any odd number of Dirac's matrix γ_μ is zero. For a product of any even number of γ_μ's, the trace can be written down simply in the following manner:

$$\chi\{\underbrace{\gamma_\mu\gamma_\nu\cdots\gamma_\eta\gamma_\zeta}_{2n\text{ factors}}\}=4\Sigma\pm\delta_{n_\mu n_\nu}\cdots\delta_{n_\eta n_\zeta}, \quad . \quad . \quad . \quad . \quad (1)$$

where $\chi\{\ldots\}$ denotes taking the trace of the matrices in the bracket, and the summation sign indicates summing over all possible pairings ($[(2n)!]/[n!\,(2!)^n]$ in number), preceded by a positive or negative sign according to whether an even or odd number of transpositions are required to bring $(n_\mu n_\nu)\ldots(n_\eta n_\zeta)$ to $(\mu,\nu)\ldots(\eta,\zeta)$, transposition within each pair not counted.

The proof of the rule consists in the repeated application of the relation $\gamma_\mu\gamma_\nu+\gamma_\nu\gamma_\mu=2\delta_{\mu\nu}$,

$$\begin{aligned}\chi\{\gamma_\mu\gamma_\nu\gamma_\lambda\cdots\gamma_\eta\gamma_\zeta\}&=2\chi\{\gamma_\lambda\cdots\gamma_\eta\gamma_\zeta\}\delta_{\mu\nu}-\chi\{\gamma_\nu\gamma_\mu\gamma_\lambda\cdots\gamma_\eta\gamma_\zeta\}\\&=2[\chi\{\gamma_\lambda\cdots\gamma_\eta\gamma_\zeta\}\delta_{\mu\nu}-\chi\{\gamma_\nu\cdots\gamma_\eta\gamma_\zeta\}\delta_{\mu\lambda}+\cdots\\&\quad+\chi\{\gamma_\nu\gamma_\lambda\cdots\gamma_\eta\}\delta_{\mu\zeta}]-\chi\{\gamma_\nu\gamma_\lambda\cdots\gamma_\eta\gamma_\zeta\gamma_\mu\}.\end{aligned}$$

Since any circular permutation of the factors inside the bracket does not alter the value of the trace, one has therefore

$$\begin{aligned}\chi\{\gamma_\mu\gamma_\nu\gamma_\lambda\cdots\gamma_\eta\gamma_\zeta\}&=\chi\{\gamma_\lambda\cdots\gamma_\eta\gamma_\zeta\}\delta_{\mu\nu}-\chi\{\gamma_\nu\cdots\gamma_\eta\gamma_\zeta\}\delta_{\mu\lambda}\\&\quad+\ldots+\chi\{\gamma_\nu\gamma_\lambda\cdots\gamma_\eta\}\delta_{\mu\zeta}. \quad . \quad . \quad . \quad (2)\end{aligned}$$

The sign preceding each term on the right-hand side of (2) is positive or negative according as the number of transpositions required to bring the array of indices to the initial order on the left-hand side of (2). The process can obviously be repeated and the argument holds for each subsequent reduction until finally each term contains $n-1$ Kronecker δ's multiplied by a factor of the typical form $\chi\{\gamma_\eta\gamma_\zeta\}=4\delta_{\eta\zeta}$. Thus (1) is proved.

For practical purposes, the possible pairings and their appropriate signs can most easily be obtained by labelling the $2n$ indices $\mu,\nu,\lambda\ldots\eta,\zeta$ on the circumference of a circle and connecting the pairs by lines drawn outside the circle. The sign is determined by counting the number of crossings of the lines in a given graph, positive for the even number of crossings and minus for odd ones.

---

* Communicated by Professor M. Born.

Three-Photon Decay of Positronium.

By J. M. Radcliffe,
University of Birmingham*.

[Received August 31, 1951.]

The two spin states of positronium in its ground state have markedly different life-times against annihilation. Positronium in the singlet state has the shorter life-time ($\tau = 1{\cdot}25 \times 10^{-10}$ sec.) since it can decay into two photons. Such a decay from the triplet state is forbidden (see *e. g.* Yang 1950), the simplest decay allowed being one into three photons. Three different results of three calculations of the life-time against the latter process have been published (Lifshits 1948, Ivanenko and Sokolov 1948, Ore and Powell 1949).

As direct experimental determination of the life-time is now possible, it was thought worthwhile to repeat the calculation. Ore and Powell's value for the mean life-time, $1{\cdot}4 \times 10^{-7}$ sec., was confirmed.

A covariant approach, using the methods developed recently by Feynman, simplified the work considerably, especially in the sum over the polarizations of the photons. The matrix element was evaluated using zero-velocity free-particle wave functions, normalized so that the density was that of the electron at the positron in the ground state of positronium. (The effect of binding is to multiply this matrix element by a factor $[1+0(\alpha)]$, $\alpha = e^2/\hbar c$). Also it has been shown that three-photon decay from the singlet state does not occur, at least in the limit of zero relative velocity of the two particles. This means that the matrix element which occurs can be conveniently summed over all spin states of the particles.

The writer is indebted to Dr. G. E. Brown for helpful advice, and to the Department of Scientific and Industrial Research for the award of a maintenance grant.

References.

Ivanenko, D., and Sokolov, A., 1948, *Doklady Akad. Nauk, S.S.S.R.*, **61**, 51.
Lifshits, E. M., 1948, *Doklady Akad. Nauk, S.S.S.R.*, **60**, 211. (See also *Science Abstracts*, 1949, 52A, abs. 1006.)
Ore, A., and Powell, J. L., 1949, *Phys. Rev.*, **75**, 1696.
Yang, C. N., 1950, *Phys. Rev.*, **77**, 242.

---

* Communicated by Professor R. E. Peierls, F.R.S.

CXXXII. *Notices of New Books and Periodicals received*

Josiah Willard Gibbs. By L. P. Wheeler. (Yale University Press. London : Geoffrey Cumberlege.) [Pp. 264.] Price 25*s.*

" In the course of the thirty-two years of his teaching somewhat less than one hundred students attended Gibbs' courses." " Only a handful of these students still survive." " In the whole period of his teaching there were but a baker's dozen of dissertations which can be said to owe their inspiration to Gibbs."

Lynde Phelps Wheeler, from whose book the above quotations are taken, is one of the few survivors of the lucky dozen. Having received three separate requests to write a biography of Gibbs, he was eventually persuaded reluctantly to undertake the difficult task. Mathematicians, physicists, chemists and all interested in the history of science will be grateful to him for carrying out this labour of love as thoroughly, honestly and conscientiously as humanly possible.

The theme of this book is in the author's own words " Gibbs' scientific work *was* Gibbs ". There is little else, that is live, to tell. In this biography, or any other biography of Gibbs, there is a tragedy for him who can read between the lines. Whereas Gibbs was honoured and recognized as at least an equal by such giants as Maxwell and Rayleigh, and at Yale he was undoubtedly well liked and respected by his immediate colleagues, when he died in 1903 his genius was inadequately appreciated in his own country. No proper care was paid at the time of his death to preserving his correspondence. Not until a score of years had passed was there any active desire to know more about the man and then it was too late. Wheeler is able to tell us something of Gibbs as a lecturer, but scarcely an anecdote of his private life.

An epitaph, similar to Wren's, would seem apposite to Gibbs : " Si momentum requiris, opera lege mea ".

E. A. G.

An Introduction to the Theory of Control in Mechanical Engineering. By R. H. MacMillan. (Cambridge : University Press, 1951.)

Fundamentals of Automatic Control. By G. H. Farrington. (Chapman and Hall, London, 1951.)

The present applications of automatic control, or as it has recently been termed " feed-back engineering " are by far too numerous and wide-spread to mention. The study of the theory of control, which is now well formulated, is of major interest in almost all branches of engineering and of more than passing interest in the fields of economics and physiology, since the recent work of Wiener, Tustin, *et al.*, have shown the dependence of many natural phenomena upon the same laws and equations applicable to mechanical systems.

The foundations of the basic control theory can be traced to a classical paper by Clerk Maxwell, " On governors " (*Proc. Roy. Soc.*, **16,** 270, 1868), but the modern development dates essentially from the application of the Nyquist method of harmonic response analysis, originally developed for use with electronic circuits. There is now a very considerable literature on the subject, but no British text-book dealing exhaustively with the subject has previously appeared. It is thus gratifying to note the almost simultaneous appearance of the above two books.

The former, by MacMillan, claims only to be an introduction to the subject, but correlates excellently the very diverse fields of application which respond to the same basic theory and to identical methods of analysis, *e.g.* regulation, position control servo-mechanisms, and process control. The early chapters are mainly descriptive, leading to the concept of transfer functions and system

equations. The human operator and non-linear effects are discussed only qualitatively, but a very full account is presented of the methods of transient and harmonic analysis by both analytical (Laplace) and graphical (Nyquist diagram) methods. An extensive bibliography is provided and the book should be intelligible to any engineer or physicist and of particular value to the student in this subject.

MacMillan uses throughout the nomenclature and notation of servo-mechanisms, and it is to be regretted that there are significant differences between this and the corresponding nomenclature of process cntrol as used by Farringdon. This may confuse the general reader who is not aware of the independent lines of development and the consequently different nomenclature used in these allied fields.

Farringdon deals solely with the theory of process control: in general the treatment is basically similar to that of MacMillan, but greater emphasis is naturally placed on the types of control and discontinuities normally encountered in process applications. There is an excellent discussion of analogous transfer stages, and the system equations utilising proportional, integral and derivative controls. Plant characteristics, and the control discontinuities and non-linearities such as are found in process regulating units are also discussed. There is a very interesting analysis of typical pneumatic controlling intruments. The mathematical treatment is generally adequate and not beyond the capabilities of the graduate in physics or engineering.

This book will be of greatest interest to those workers concerned with process control—to the designer rather than the operator or user, but it will amply repay study by those interested in the other related fields, if only to correlate the extremely wide fields of application. A. P.

ERRATA.

Total Cross-Sections of the Elements for 156 *MeV. Neutrons*, by A. E. Taylor, T. G. Pickavance, J. M. Cassels, and T. C. Randle, 1951, *Phil. Mag.*, **42**, 751.

The experimental results reported in this paper were discussed briefly in the light of the optical model of nuclei. The discussion involved the mean free paths of neutrons in nuclear matter, and these were incorrectly calculated because wrong values had been adopted for the proton–proton cross-section. The error arose from the fact that the total cross-section for proton–proton scattering is $\int_0^{\pi} 2\pi\sigma(\theta) \sin\theta \, d\theta$, and not $\int_0^{2\pi} 2\pi\sigma(\theta) \sin\theta \, d\theta$, where $\sigma(\theta)$ is the differential cross-section as conventionally defined.

Correction of this point removes most of the difficulties which were thought to follow from the assumption that the neutron–neutron and proton–proton interactions are the same at high energies. Some discrepancy still remains, as the theoretical results of Jastrow (1951) have shown.

R. Jastrow, 1951, *Phys. Rev.*, **82**, 1951.

A Theoretical Investigation of the Compression of a Ductile Material between Smooth Flat Dies, by A. P. Green, 1951, *Phil. Mag.*, **42**, 917.

Equation below fig. 13 should read:

$$\left.\begin{aligned} \bar{x}' &= -v\,; \quad u' = \bar{y}\,; \\ \bar{y}' &= u\,; \quad v' = -\bar{x}, \end{aligned}\right\} \text{1st kind.}$$

[*The Editors do not hold themselves responsible for the views expressed by their correspondents.*]